2021

NATURE-INSPIRED MATERIAL STRATEGIES TOWARDS FUNCTIONAL DEVICES

Sayantan Pradhan

NATURE-INSPIRED MATERIAL STRATEGIES TOWARDS FUNCTIONAL DEVICES

A dissertation submitted in partial fulfillment of the requirements for the degree of Doctor of Philosophy in Chemical and Life Science Engineering at Virginia Commonwealth University.

By

Sayantan Pradhan,

B. Tech., Chemical Engineering, Jawaharlal Nehru Technical University, India, 2016

Advisor: Dr. Vamsi K. Yadavalli, Ph.D.

Professor, Chemical and Life Science Engineering

Virginia Commonwealth University

Richmond, Virginia

May 2021

ACKNOWLEDGEMENT

The work presented in this dissertation would not have been successful without the contributions and support from numerous mentors, colleagues and individuals at every stage of my Ph.D.

First and foremost, I am deeply indebted to my advisor Dr. Vamsi K. Yadavalli, for his excellent mentorship. I am thankful for his constructive criticism, perpetual encouragement, timely advice, meticulous attention and unparallel wisdom. His constant support, guidance and patience towards me along with systematic planning, advice and perseverance has shaped me both professionally and personally. I thank him for training me personally and helping me develop my experimental and scientific writing skills. I will always be grateful to him for providing me the opportunity to work in his lab under his mentorship.

I would like to thank Dr. Ram B. Gupta, Dr. Ümit Özgür, Dr. Christina Tang and Dr. Ning Zhang for accepting to be a part of my graduate dissertation committee for their constant encouragement, guidance and insightful comments at various phases of my dissertation work. I would also like to thank Dr. Dimitri Pestov and Carl Mayer for training me and helping me with various instruments and experiments at the VCU Nanomaterials Core Characterization facility. Additionally, I am also thankful to Dr. Charles Cartin and Dr. Christopher Ehrhardt for providing me access to various instruments in their lab which has been crucial to the completion of this dissertation work.

I would like to extend my gratitude towards Dr. Ramendra Pal for introducing me to all the basic research and experiments done in the lab. He has been kind enough to share his knowledge, expertise and experience in our common field of research. Apart from his help and guidance professionally, I am also thankful for his support as a friend and helping me navigate through my initial days in Richmond, VA. I am thankful to my colleague Dr. Meng Xu (Max) for his thoughtful

insights towards my research. I have thoroughly enjoyed working beside him on multiple projects and have learned a great deal from him. I would like to thank my colleague Anne Kathrine Brooks for all the engaging scientific discussions, exchange of ideas and assistance during the final year of my Ph.D.

Finally, I would like to thank my family: my father, Dr. Narayan C. Pradhan, my mother Kanika Pradhan and my sister, Somantika Pradhan for their constant affection, care, and support. I am ever grateful to my parents for all the efforts and sacrifices they have made for my success. I am thankful for the dedication and patience they have shown in raising me to be a better individual. I am also thankful to my fiancé Dr. Piyusha Pagare for her endless love and support throughout this endeavor. I thank you for believing in me and standing beside me through all the tough times. Lastly, I would like to thank Dhruv Fomra and Prudhviraj Meda for their friendship and support throughout my Ph.D. years.

TABLE OF CONTENTS

LIST OF TABLES

LIST OF FIGURES

Abstract

NATURE-INSPIRED MATERIAL STRATEGIES TOWARDS FUNCTIONAL DEVICES

By Sayantan Pradhan

A dissertation submitted in partial fulfillment of the requirements for the degree of Doctor of Philosophy in Chemical and Life Science Engineering at Virginia Commonwealth University.

Advisor: Dr. Vamsi K. Yadavalli, Ph.D.

Professor, Chemical and Life Science Engineering

Research in biodevices is at a transitional point in which there is a shift from the development of rigid electronic components to the fabrication of flexible replacements. Flexible systems have attracted increasing attention due to their huge impact in healthcare, disease diagnostics and therapeutics, and even general way of life. However, the fabrication of flexible bioelectronics is limited by the selection of materials. While conventional materials have excellent electronic properties, they often exhibit limited compliance at biointerfaces, restricted biocompatibility, and poor environmental sustainability. With the increasing need for electronics in our everyday life, the disposal of abandoned devices has raised environmental concerns globally. Naturally sourced, renewable biomaterials possess outstanding advantages for a multitude of biomedical applications owing to their biodegradability, biocompatibility, and excellent mechanical properties. This dissertation focuses on the incorporation of naturally derived materials along with well-developed fabrication techniques for the realization of functional biodevices, with an emphasis on

electrochemical biosensors for the monitoring of human bioinformation.

Of interest in this dissertation are silk (protein) and chitin (polysaccharide) biopolymers. One of the major challenges restricting these materials beyond their traditional usage as passive substrate materials is the ability to combine them with high-throughput and high-resolution fabrication techniques. Initial research work is directed towards the fabrication of micropatterned, flexible 2D substrates of silk fibroin and chitin using bench-top photolithographic techniques. Methacrylate moieties were conjugated to silk proteins and chitin in order to impart them with photocrosslinkability. The versatility of silk proteins, together with their easier processing and degradability in physiological environments led to their choice over chitin for the demonstration of functional biodevices.

The non-conductive nature of silk proteins hinders their use in active components in functional electrochemical devices. Research focused on imparting electrochemical properties to silk proteins via conducting polymers (PEDOT: PSS and PANI) and a naturally occurring semiconductor, eumelanin. In return, the photocrosslinkable silk proteins provide photopatternability into micropatterns. The silk based conductive biomimetic inks possess favorable electronic properties and stability in aqueous environments. The utility of conducting biomimetic composites in device applications was demonstrated by the fabrication of fully organic silk based flexible electrochemical biosensors. The biosensors display excellent non-specific sensing of electroactive targets, dopamine and ascorbic acid with high sensitivity. The benign nature of the conductive ink composite also allows the encapsulation of glucose oxidase enzyme (GOx) which facilitates the specific detection of glucose over a physiologically relevant concentration range. Further, the temperature dependent conductivity of PEDOT: PSS was exploited to engineer a flexible silk-PEDOT: PSS based temperature sensor. The sensor displays a linear response in the physiological

temperature range with a Temperature Coefficient of Resistance (TCR) of -0.99% $^{o}C^{-1}$ with excellent stability towards humidity and mechanical flexure. The accurate detection of skin temperature was demonstrated using the silk-PEDOT: PSS based temperature sensor.

Finally, the challenge of conformability at the biological interface is addressed using structure-based design strategies. Inspiration from the Japanese art of paper cutting was taken for the formation of patterned cuts on silk fibroin films using photolithography. Such patterned defects generate remarkable "self-shielding" leading to engineered elastic behavior and deformation. Micropatterned cuts can increase the conformability of films to soft biological interfaces by enhancing their strain tolerance. By doping with polyaniline (PANI), flexible, intrinsically conductive silk kirigami sheets could be fabricated. The unique properties of silk kirigami suggest a host of applications as transient, "green", functional biointerfaces, and flexible bioelectronics. In conclusion, the nature-inspired material strategies developed in this dissertation work paves the path towards fully organic flexible biodevices with improved conformability towards soft, biological interfaces. Such systems have potential in personalized healthcare monitoring devices, improving efficient disease detection and diagnosis.

CHAPTER 1

INTRODUCTION

1.1 INTRODUCTION

Applications at biological interfaces, particularly those that interact and interface with biological systems, require materials to satisfy a number of properties. Properties such as: i. Mechanical robustness, ii. Biocompatibility, iii. Biodegradability, iv. Availability at a reasonable cost and, v. Easy processability in a sustainable manner, play an influential role in material selection.[1] It is challenging to synthetically design materials that can accommodate all the above requirements. Nature holds a myriad of materials that it employs diligently to perform a multitude of captivating, yet complex functions including bioactivity, mechanical toughness, optical or electromagnetic properties, and biocompatibility.[2, 3] Nature-derived materials have played an integral role from the beginning of human history, as a source of basic necessities such as food, clothing and shelter. It is only very recently that the scientific community has begun harnessing some of these materials and their unique properties to provide alternative solutions for problems while developing smart systems for the future. Owing to this palette of properties, there has been extensive research toward using natural biomaterials for a variety of tissue engineering and regenerative medicine applications.[4] Recently, there has been a great interest in adopting nature-derived materials for

the formation of active functional devices such as (bio)electronics, sensors, and optical systems.[5-7] These include systems capable of performing a specific function, such as transducing signals from the biological environment, controlling, or activating biological functions etc.

Concurrently, there has been a paradigm shift from traditional rigid platforms to more flexible and stretchable biodevices for applications on the human body.[8, 9] Recent biomedical applications of such platforms include electronic skins, soft-robotics, tissue engineering and wearable, or implantable biosensors for monitoring human bio-information.[10-15] These devices are expected to make a significant impact on healthcare through personalized health monitoring devices, improving efficient disease detection, and diagnostics. However, the fabrication of such devices is limited by the choice of materials. Many traditional materials show poor performance in complex, curvilinear biological interfaces, which makes their incorporation in flexible, wearable or implantable systems much more challenging.[7] On the contrary, nature-derived biomaterials being inherently soft and flexible in nature, can overcome the mechanical mismatch between the biological milieu and wearable or implanted devices.

Flexible or conformable devices include two major components- the structural component and the functional component. The structural component in these devices have been mostly confined to synthetic polymeric materials because of their low cost, design flexibility, mechanical strength and overall processability.[16] However, most polymers are derived from fossil fuels, and have been linked to environmental pollution and poor sustainability. With the increasing need for electronics in our everyday life, the disposal of abandoned electronics has raised concerns globally.[17] Natural biopolymers provide an alternative strategy as structural materials in biodegradable functional biodevices. Being of natural origin, they are usually considered renewable and sustainable. The use of inherently biodegradable natural materials can provide additional benefits

by eliminating the need to surgically remove implants, thereby reducing patient discomfort. They can minimize immune response and scar tissue formation which are particularly important when designing implants for temporary use. Currently, there are numerous examples of functional biodevices where natural biopolymers have been used as flexible and degradable substrate on which the active functional components are developed.[5]

Natural polymeric materials also have the potential of being used as the functional component in wearable and implanted devices.[18] These materials often act as a stable and benign matrix in which other active materials can be dispersed to carry out specific functions. For example, other electronically active materials such as metals, metal-oxides, carbon materials and conducting polymers can be added to the matrix of biopolymers to form the active sensing element in electrochemical sensors.[19] Being inherently biodegradable/ bioresorbable and biocompatible in nature, they can confer biodegradability to traditionally non-biodegradable active materials along with enhancing their compatibility in biological environments. Nature also provides several conductors and semiconductors such as the pigments melanin and indigo as alternatives to traditional synthetic counterparts.[5] However, there are several challenges that deter the use of natural material as active functional components. Ability to combine high-throughput and high-resolution fabrication techniques with such materials, poor performance metrics at biological interfaces and poor long-term stability are some of the challenges which restrict their use in bioelectronics and optics, beyond functioning as substrates.[20]

This research thesis focuses on natural proteins (silk fibroin and sericin) and polysaccharides (chitin) as biomaterials of choice for the fabrication of different components for use in fully organic, flexible and degradable devices. These devices are able to detect a wide range of physical and chemical physiologically relevant targets in a flexible and degradable manner. Both silk

proteins and chitin have been widely adopted in the field of biomedical research due to their distinctive intrinsic properties in addition to general properties of biomaterials noted above. Tissue engineering scaffolds, drug delivery vehicles, medical device packaging, and prosthetics have been reported.[21, 22] Recently, they have begun to be considered for the construction of biodegradable and biocompatible electronics, sensors and optical devices. However, significant challenges remain in optimizing the use of these materials in terms of function and applicability for conformable interfaces. This dissertation work also explores the use of natural semiconductors i.e., melanin, for the fabrication of the active component in electrochemical biosensor devices. Finally, this work also explores the adoption of new structural designs to existing materials for addressing the challenge of conformability to biological surfaces.

1.2 RESEARCH OBJECTIVE

The objective of this research is to explore the use of various naturally occurring biomaterials for applications at the biological interface, which is often complex and dynamic in nature, with an emphasis on biosensors which can be used for monitoring of human bioinformation. However, most of the materials found in nature are typically not available in the form of usable form factors. Hence, suitable processing strategies need to be adopted in order to facilitate their use in device fabrications. The natural biomaterials chosen in this work, i.e., silk proteins and chitin, have been extensively researched with regard to their processability for biomedical applications. In order to increase the complexity and repertoire of applications to biofunctional devices, the need to combine these materials with well developed, high throughput fabrication techniques is crucial. Photolithography is one such nano/microfabrication technique that is widely used due to its capability of patterning over a large area in a scalable process. However, a prerequisite in

photolithographic processes is that the material should have chemical groups that can undergo photo-conjugation reactions. The initial parts of this work involve using the concepts of modular design to chemically modify silk proteins and chitin to form photoactive counterparts to improve their physical properties and make them compatible with existing photolithography techniques. These photoactive variants along with a simple bench top photolithography process, allows the fabrication of various precisely patterned structures over a large area (centimeter scale) on various flexible and rigid substrates. After establishing the photolithography process to form patterns with silk and chitin, the next part of the research deals with the introduction of electrical properties to these silk/chitin microstructures so that they can be used for the fabrication of different elements in biodevices such as electrodes and circuit designs. The subsequent goal is to design devices such as electrochemical biosensors that are used for applications on curvilinear and dynamic surfaces. To this end, an emphasis was given on developing structural design concepts to address the challenge of enhanced conformability to biological interfaces. In summary, the aim of this work is to explore the use of nature derived biomaterials as an alternative route to design biodevices that are suitable for functioning at biological interfaces in degradable fashion, thus fulfilling the need of "green" electronics.

1.3 SPECIFIC AIMS

In order to achieve the goals of realizing mechanically flexible biodevices for applications on the human body, this research is guided along three key specific aims:

1. **Develop material processing strategies that can enable the use of silk and chitin with photolithographic processes.** This is achieved by chemically modifying these materials to make them UV cross linkable. This also includes developing strategies that allow easy

processing of these materials such as enhancing the solubility, solvent compatibility and ability to form microstructured films, hydrogels etc.

2. **Photolithographic patterning of conductive architectures for silk/ chitin-based devices.** This involves developments of strategies that allows the fabrication of flexible and degradable sensors for chemical and physical biomarkers of physiological importance.
3. **Development of strategies that can improve the flexibility and conformability of devices on soft surfaces.** This involves adopting structural design strategies such as engineered "cuts" or "defects" can provide functional conformability with biological tissues as well as unique mechanical properties.

1.3.1 Micropatterning of nature derived materials using photolithography

Precise patterning of microstructures on flexible substrates using bio-derived materials is a key step towards the development of functional devices. The initial part of this dissertation work focuses on the development of a platform that allows the micropatterning of biopolymers silk and chitin on flexible and rigid substrates using photolithography. This includes the chemical modification of these materials to impart UV photocrosslinkability.

1.3.2 Imparting electrical properties to nature derived materials

This will allow their usage beyond traditional structural materials and substrates to active functional components in flexible biodevices. In the first part, the use of well-developed conducting polymers is explored due to their prevalence in modern flexible electronics to form photo-patternable biomimetic conducting inks. Subsequent studies are aimed at exploring the use of a natural semi-conductor melanin to induce electronic activity in biopolymers.

1.3.3 Development of biosensors for physiologically relevant biomarkers

In this part of the study, the application of the techniques developed above was explored for the realization of flexible biosensors for the real time monitoring of various physiologically important chemical and physical biomarkers. A part of the investigation also includes development of strategies that allow easy connection of devices eliminating the need of electrical wires. The final goal of this work is to develop fully organic, flexible functional biodevices that can be easily interfaced with biological systems.

1.3.4 Structure based design strategies towards stretchability and conformability

The final part of this study aims at addressing the issue of conformability at soft curvilinear surfaces by incorporating new structural design strategies. This is achieved by introducing precisely designed cuts on thin polymeric films of natural origin. Inspired by "Kirigami", the Japanese art of paper cutting, photolithography can be used to make selective cuts to improve flexibility and mechanical conformability of 2D substrates. The cuts also allow the fine tuning of mechanical properties of such films. The results obtained from these studies can address the development of substrates or active sensing regions in flexible and conformable biodevices.

1.4 BACKGROUND AND SIGNIFICANCE

The work outlined in this dissertation focuses on the use of naturally derived biomaterials for the fabrication of flexible devices for human health monitoring and disease diagnostics. This section discusses some of the background fundamental and applied studies on materials, fabrication techniques and design strategies that have been employed for the realization of such devices and its significance.

1.4.1 Significance of flexible devices

Flexible devices including wearable and implantable devices have revolutionized the field of bioelectronics due to their capability of integrating and interacting naturally with the human body to stimulate or to provide valuable information from the physiological environment.[23] These devices are able to maintain stability in functionality and performance even under strain.[24] Among them, flexible and stretchable bioelectronics have generated interest for the development of biological sensing platforms and point-of-care diagnostic devices.[25-27] While rigid devices provide a snapshot of the physiological environment at a particular time in a clinical setting, flexible devices have the provision of being integrated with the human body to provide continuous, real time information *in situ*.[28, 29] They can mimic the dynamic nature of biological surfaces such as the skin to minimize any hindrance or discomfort in performing common day to day activities. These devices are able to achieve this by the virtue of their light weight, high flexibility and enhanced conformability with the soft human body.

To achieve these properties, it is important to render flexibility in various components of devices such as substrates, circuits, power sources etc. Flexible substrates ensure conformal contact between the human body and the active component. The availability of a wide range of synthetic polymers has played a pivotal role in extending the frontier of wearable and implantable biosensors.[30] Commercially available silicone elastomers such as PDMS and Ecoflex have been extensively investigated as substrates for wearable devices due to their stretchability and easy processing.[31] Synthetic biodegradable polymers such as polyvinyl alcohol, polylactic acid, polycaprolactone, polyurethane, polyethylene glycol and polylactic-co-glycolic acid have also been studied to confer the added benefit of degradability in flexible devices.[32-35] Flexibility and

stretchability have been imparted to functional components using strategies such as mixing liquid metals with elastomers, reducing the lateral and vertical scale of metal electrodes, and introducing new structural designs such as serpentine, buckled and island bridge geometries.[36, 37] Carbon based materials such as rGO and CNTs have also been explored extensively.[38] However, the use of nature derived materials such as cellulose, silk proteins, collagen, gelatin and hard shellac provide alternatives for the development of fully organic flexible biodevices.[5] Concurrently, conducting polymers such as PEDOT: PSS, polyaniline and polypyrrole may be used as active components in flexible devices.[39] Combining natural biopolymers with conducting polymers can expand the repertoire of potential applications, while rendering interesting biological, mechanical and electrochemical properties. The following sections discuss some materials and strategies adopted in this dissertation work for the realization of fully organic flexible biodevices.

1.4.2 Nature derived biomaterials

Naturally-derived biomaterials is a term commonly used to describe materials primarily obtained from renewable sources such as animals and plants.[40] These materials are usually composites of polymers and minerals. They have evolved over millions of years, and have hierarchical architectures that display and wide range of fundamental structural and bioactive properties.[3] They often possess a multitude of structural and functional properties in combination with one another, including bioactivity, mechanical toughness, optical or electromagnetic properties.[2] Nature derived materials have been an integral part of human life in various forms of applications over thousands of years. In recent times, they have gained popularity in material science research due to their incomparable advantages in terms of their renewable, biocompatible, biodegradable and excellent mechanical properties. Of interest is the presence of reactive sites via which their

biological activity, porosity, and mechanical properties can be tuned by changing polymerization conditions or chemical functionalization.[40]

Recently, there has been an interest in the application of naturally derived materials in flexible electronic devices.[5] Many natural polymers are soft, which is exploited to mimic soft tissues for conformable and tactile devices.[41] These devices are designed for function on or inside the human body. To this end, the use of naturally derived materials stems from the hypothesis that most of these materials can be directly contacted with tissue or skin or implanted inside the human body without causing significant adverse side effects. Most of these materials can be degraded or resorbed in biological environments in a controllable fashion, enabling their use in transient electronics.[42-44] It is also because of their degradable/ bioresorbable property that they are chosen to replace conventional materials such as polymers derived from fossil fuels, metals, and carbon-based materials etc., due to environmental concerns associated with them.[45]

With regards to biodevice applications, nature derived materials can be used in two ways- they can either serve as the active functional component or as the structural component.[5] However, there are a few examples where they can be adopted in both structural and functional components. The properties that make them attractive for regenerative medicine, such as tunable mechanical strength and flexibility, lend the materials for adoption in flexible and wearable devices. As structural components, they have the potential to replace traditional rigid substrates as more flexible and sustainable counterparts. They have also been used as encapsulating layer in implantable devices interacting and interfacing with biological systems to enhance biocompatibility and device stability. As functional components they have been used singularly or combined with other functional materials to form the active sensing element in devices such as electrochemical sensors.

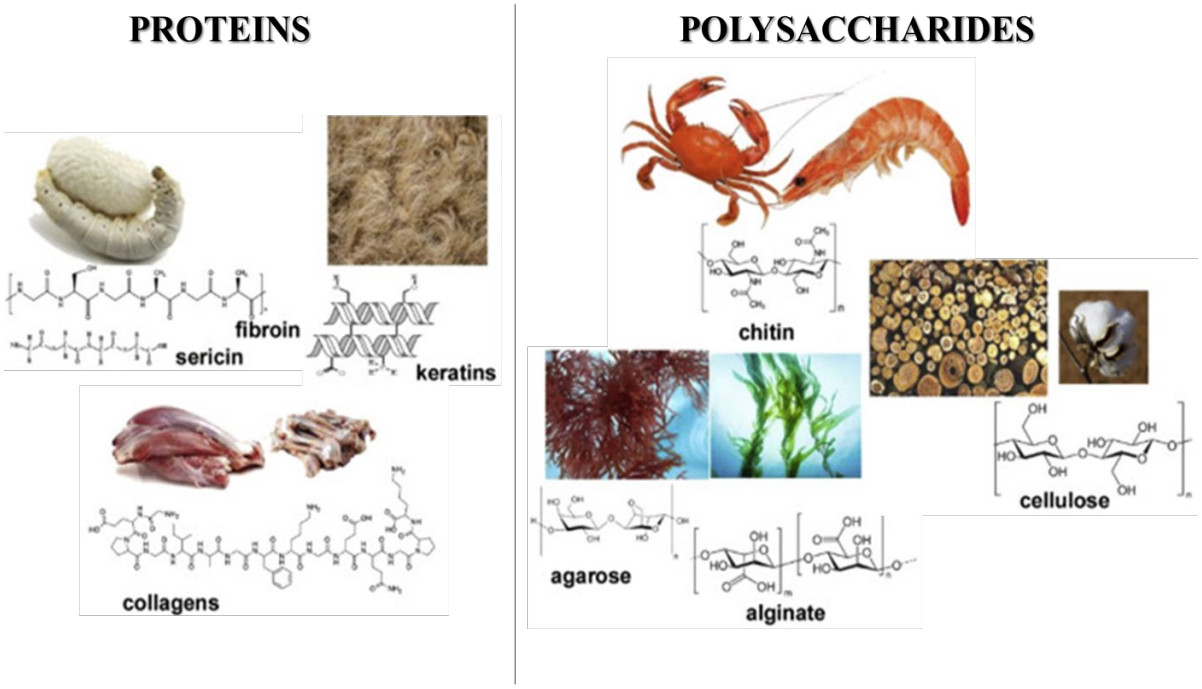

Figure 1.1 *Some common proteins and polysaccharides found in nature.[5]*

The selection of naturally derived biopolymers for degradable biodevices can be primarily divided into two categories- polysaccharides and proteins. Most of the nature derived materials that have been investigated for bio-applications, including bioelectronics, fall under one of these two categories. Polysaccharides are biopolymers that are formed through glycosidic linkages whereas proteins are made of amino acids linked through peptide bonds.[5, 46] Some examples of proteins that have been used in a wide range of biomedical applications are silk proteins, collagen and keratin.[44, 47-49] On the other hand, some commonly used polysaccharides are cellulose, chitin/ chitosan, alginate, agarose and gellan gum among many others.[7, 50-53] The work in this dissertation explores the potential use of these classes of materials in functional biodevices. The material of choice from proteins includes silk proteins- fibroin and sericin. Chitin was chosen from polysaccharides for its potential in functional biodevices and “green” electronics.

1.4.3 Silk proteins

The history of silk dates back to 4th millennium BCE by the Yangshao culture in China.[54] Ever since its discovery, silk has played a pivotal role in human life with diverse applications and social importance. Traditionally, silk fiber is typically used in the textile industry because of its durability, mechanical strength and luster. There also historical evidences of the use of silk in medical applications in the form of sutures in antient Greece.[55] These properties along with its abundance in nature, low cost, easy processing and attractive biological properties make them attractive candidates in today's biomedical research.

Silk from domesticated *Bombyx mori* mulberry silkworms is the most abundant and widely used variety of silk.[56] However, the silk obtained from orb-weaving spiders, *Nephila clavipes,* are known to be superior to silkworm silk in terms of mechanical properties.[57] Nevertheless, it is difficult to obtain large quantities of silk from these spiders due to their predatory and territorial nature. Hence, silk obtained *Bombyx mori* silkworms are widely adopted and well characterized. Silk fibers are produced by these insects in specialized epithelial cells that line glands. [58] The *Bombyx mori* silk contains two types of proteins- fibroin and sericin. Silk fibroin is present in the form of 10-25 μm diameter fibers as the core hydrophobic protein which makes up 70% of the fiber and imparts silk its mechanical properties. These proteins are coated by another class of water-soluble glue-like protein known as sericin (20–310 kDa), which makes up the remaining 30% of the silk fiber.[59]

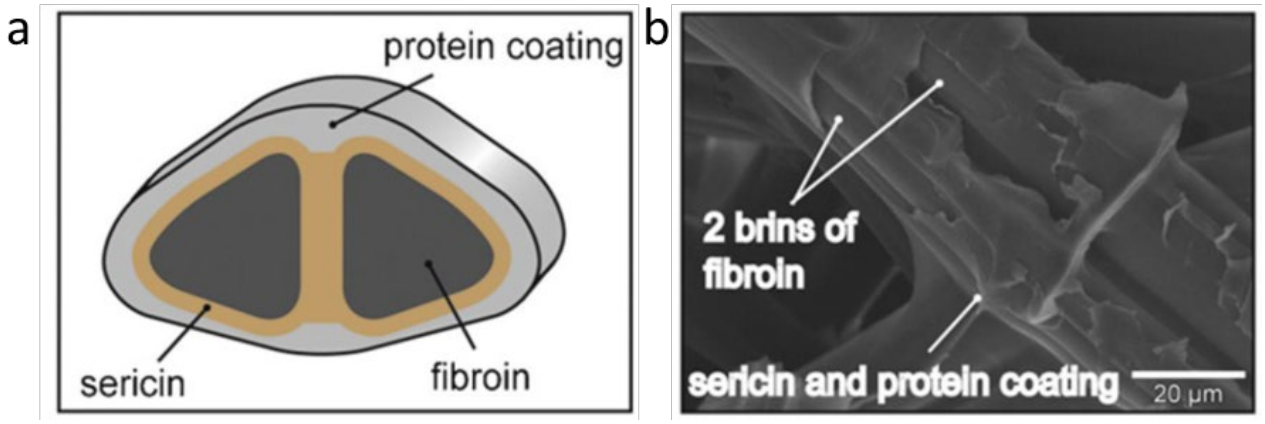

Figure 1.2 *a) Schematic showing the assembly of silk protein with fibroin comprising the hydrophobic core and the outer sericin cover and b) SEM image of silk fiber.[23]*

1.4.3.1 Silk fibroin

Fibroin from *B. mori* is obtained via a degumming process which comprises of boiling the silk worm cocoons in an alkaline solution.[60] The consensus on silk fibroin in remarkably positive among the material science community due to its exceptional mechanical and optical properties along with its inherent biocompatibility. The acceptance of fibroin as biomaterial for biomedical applications was further fortified by its approval by the US Food and Drug Administration (FDA) in 1993.[61] Silk fibroin is the main structural protein and consists of two proteins: a light chain (~26 kDa) and heavy chain (~390 kDa) which are present in a 1:1 ratio and linked by a single disulfide bond. [62] The heavy chain consists of 12 domains that form the crystalline regions in silk fibers which are interspersed with small non-repetitive hydrophilic linkers. Each domain consists of sub-domain hexapeptides such as GAGAGS, GAGAGY, GAGAGA or GAGYGA where G is Glycine, A is Alanine, S is Serine and Y is Tyrosine. Overall, the amino acid composition of silk fibroin is primarily 43% glycine, 30% alanine and 12% serine.[63]

The repetitive hydrophobic amino acid domains of the heavy chain fold and bond together via hydrogen bonds, Van der Waals forces, and hydrophobic interactions, to form anti-parallel β-sheet crystalline structures.[64] Due to strong β-sheet interactions, high degree of ordering, and high density of β-crystallites are believed to absorb impact pressure and distribute it throughout the entire fibroin network, thus giving silk fibers its excellent mechanical properties.[65] The mechanical strength and elasticity of silk is superior in comparison to other nature derived materials commonly used in biomedical applications such as collagen, poly(L-lactic acid), and chemically-crosslinked collagen, and is comparable to nylon and mild steel.[66] Silk obtained from *B. mori* possess an ultimate tensile strength of ~500 MPa and an elastic modulus of 5-12 GPa. For these reasons silk fibroin is an excellent candidate for flexible and wearable biodevices that can withstand multiple mechanical deformations.[67]

Owed to its structure and chemical composition, silk fibroin invokes minimal inflammatory potential and low immunogenic reactions.[68] Silk fibers are known to produce immunogenic reactions which can be attributed to the synergistic effect of fibroin and sericin present together.[69] However, when purified and separated from sericin, it demonstrates excellent biocompatibility. Further, minimal inflammatory potential and a favorable degree of biocompatibility was demonstrated by *in vitro* studies using silk fibroin films where absence of significant macrophage spreading along with favorable infiltration of fibroblasts was observed.[70]

Silk fibroin is intrinsically biodegradable in nature. The degradation of fibroin takes place by enzymatic hydrolysis of the peptide bonds in the presence of protease which results in the metabolization of the remaining peptide fragments. This degradation is evident from the loss in mass and mechanical integrity of silk fibroin. There have been concerns regarding the safe

biodegradation of fibroin since the degradation product, amyloid β-fibrils, have been linked to Alzheimer's.[22, 71] However, studies indicate that the degradations of fibroin do not show cytotoxicity towards neural cells.[72] The secondary structures of silk- silk I (water soluble) and silk II (water insoluble) are responsible for the biodegradation properties of fibroin.[73] During the process of spinning silk by silk worms, the conformation of silk changes from dissolved, less-ordered silk I to solidified, highly ordered silk II.[74] This suggests that changing the internal secondary structure of silk can allow us to tune its external properties such as mechanical strength, solubility and even biodegradability. All these studies indicate that silk fibroin is a favorable candidate for the realization of flexible, mechanically robust, biocompatible and biodegradable devices with tunable properties. The challenge is to combine silk fibroin with a suitable fabrication technique that can facilitate its usage beyond passive structural materials in biodevices.

Table 1.1 *Amino acid composition of silk fibroin and sericin.[69]*

Amino Acid	**Sericin**	**Fibroin**
Alanine	6.7	30.23
Arginine	3.12	0.48
Aspartic acid	18.38	1.66
Glutamic acid	5.74	1.57
Glycine	17.85	43.29
Histidine	1.32	0.2
Isoleucine	1.02	0.57
Leucine	1.49	0.36
Lysine	2.08	0.21
Phenylalanine	0.67	0.69
Serine	25.5	10.58
Threonine	7.47	0.88
Tyrosine	3.1	1.88
Valine	4.05	4.76
Cysteine	0.38	0.01
Proline	0.81	0.17
Methionine	0.31	--

1.4.3.2 Silk Sericin

Sericin constitutes approximately 25-30% of the silk cocoon. It is the outer adhesive protein that envelopes the fibroin fibers.[75] It is because of this adhesive protein that silk worms are able to form cocoons. Typically, silk sericin is considered as an undesirable side product that is generated during the fibroin extraction process.[76] However, this protein also has desirable properties along with being readily water soluble.[77] Although silk sericin and fibroin exists together in nature, they differ from each other distinctly in terms of chemical and structural properties. Silk sericin is hydrophilic with a molecular weight that ranges from 20 to 400 kDa and consists of 18 amino acid with strong polar groups such as hydroxyl, carboxyl, and amino groups.[78] Structurally, sericin is a globular protein consisting of amorphous random coil and β-sheets. The enhanced solubility of sericin in water can be attributed to the amorphous random coils.[79] It is also because of this attribute, silk sericin behaves like an amorphous material and therefore fragile in its dry state.[80] However, treatment with ethanol can induce aggregation of the protein and a transition from random coils to β-sheets by dehydration and fractionation which in turn increase its crystallinity and physical stability.[81]

The biocompatibility of sericin has been a controversial topic in biomaterials research. Even though silk fibers have been used as sutures since their biocompatibility has been established, there are concerns regarding the activation of immune system due to silk This hypersensitivity reaction has been attributed to silk sericin. However, recent studies have shown that this immune response is primarily caused by the native fibroin-sericin structure, but neither fibroin nor sericin show this behavior alone.[58, 82] Studies such as *in vitro* analysis of sericin in soluble form and intravenous injections silk sericin injections given to rabbits confirm that sericin is immunologically inter and does not produce any anti-bodies.[83] Studies have also shown the use of water based sericin cream

to treat skin wounds in rats, where there was a significant decrease in the release of cytokines within a week. Silk sericin is also known to promote cell proliferation with proteins with low molecular weight showing greater effect that high molecular weight.[84] Consequently, it is now concluded that sericin is biocompatible with very low immunogenic.

1.4.4 Chitin

Chitin, an amino polysaccharide found mostly in the exoskeleton of marine crustaceans and arthropods, is the second most abundant natural biopolymer in nature after cellulose. A copolymer of glucosamine and *N*-acetyl glucosamine, chitin has a linear chain composed of (1–4)-linked 2-acetamido-2-deoxy-β-d-glucopyranose units, with a structure very similar to that of cellulose.[85] Chitosan, which is an N-deacetylated derivative of chitin obtained by transforming the acetamide groups into primary amino groups.[86] The high percentage of nitrogen present in chitin and chitosan makes them commercially important as chelating agents.[87] One of the unique characteristics of chitin and its derivatives is that they are alkaline in nature unlike most polysaccharides such as cellulose, dextran, pectin, carrageenan etc., which are mostly neutral or acidic.[88] Both chitin and chitosan are very highly regarded as functional materials due to excellent properties mechanical and biological properties.

In terms of sustainability, the advantage of chitin and chitosan is that they are primarily obtained from crab and shrimp shell wastes which are recycled from marine food processing industries.[89] However, the extraction process of chitin involves a series of steps using chemical methods after grinding them into smaller sizes which includes demineralization, decalcification and dilute HCl treatment.[90] The low reactivity and solubility make it difficult to process chitin in forms suitable for biodevice application. This is mainly due to strong intra- and intermolecular H-bonds resulting

in a highly aggregated 3D network. Dimethylacetamide and *N*-methyl-2-pyrrolidone (NMP) containing 5-7% LiCl, NaOH/Urea and ionic liquids are some of the solvents commonly used for the dissolution of chitin.[91] Chitosan, obtained via a deacetylation process of chitin in 40–45 % sodium hydroxide at 160°Cfor 1–3 h in order to remove the acetyl groups, is more readily soluble in dilute acids.[92] When the degree of deacetylation in chitin is above 56%, it is termed as chitosan. Due to the presence of primary amino groups, chitosan is a strong base and becomes a polyelectrolyte when such amino groups get protonated. As a result, chitosan dissolves in acid aqueous mixtures such as dilute acetic acid.

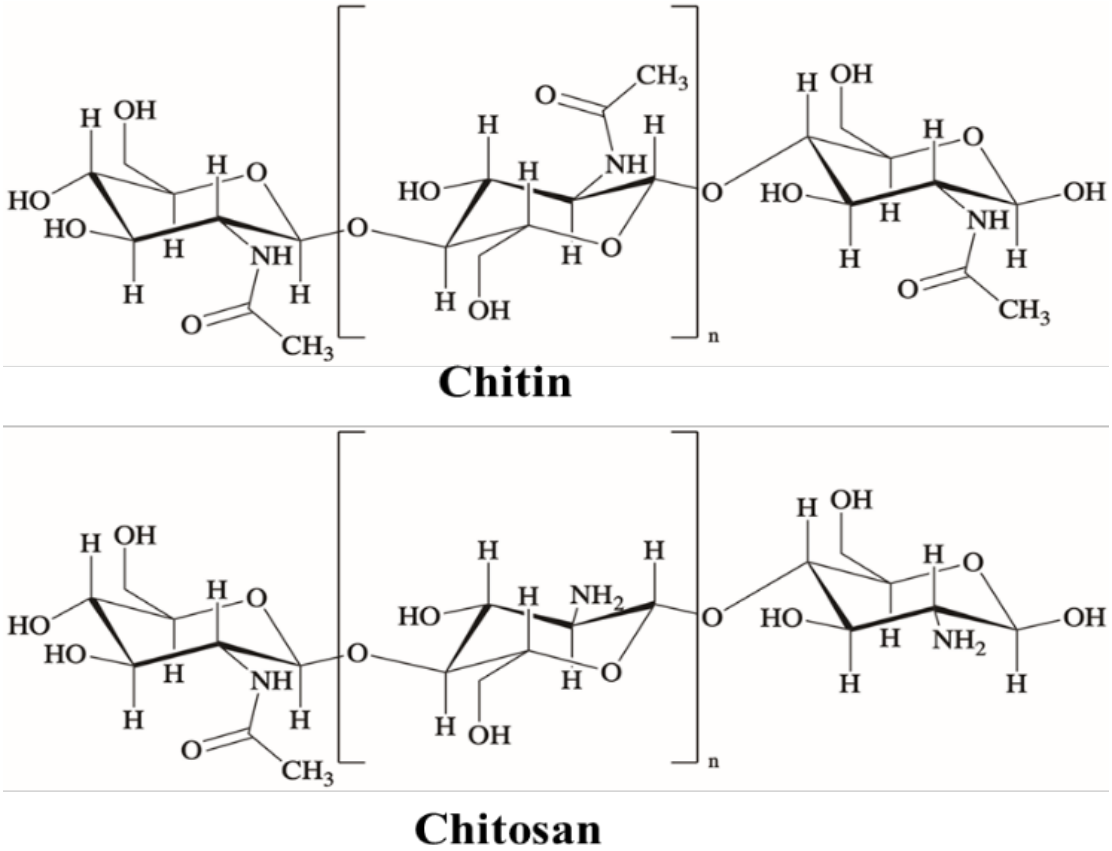

Figure 1.3 *Chemical structure of chitin and chitosan (Drawn in ChemDraw).*

Numerous studies over the years have shown the inherent biocompatible, biodegradable and non-cytotoxic nature of chitin and its derivatives.[88] Chitin and its derivative chitosan are one of the

most commonly used biomaterials for biomedical applications.[93] They have been extensively used in tissue engineering, wound healing, excipients for drug delivery and also gene delivery.[94-96] They have been processed into membranes, gels, beads, micro and nanoparticles, scaffolds and sponges in order to support a wide range of applications. Studies have also reported the antimicrobial activities of chitin against *S. aureus* and *E. coli*, along with good blood clotting properties.[97] Chitin is degraded by the chitinase family of enzymes which are found in many organisms such as bacterial, eukaryote and viruses. The biodegradation of chitin takes place via the breakdown of the β-1,4 linkages between the N-acetyl glucosamine units.[98]

Chitin also boasts exceptional mechanical properties such as mechanical properties, such as high strength, high toughness and being lightweight.[99] The elucidation of all these properties makes a compelling argument towards the use of chitin in flexible biodevices. However, to date, strategies to form chitin into precise 2D and 3D micropatterned structures with high resolution have been limited, especially using scalable techniques such as photolithography. Chitin micropatterning is limited to rigid substrates, with no reports on flexible substrates. The ability to form precise high-resolution microstructures of chitin, while using scalable techniques in different formats (2D, 3D, and on flexible substrates) can provide a new strategy to form bioelectronic devices that are biofriendly and degradable. The development of high-resolution patterning techniques using chitin is a requirement for its application as nature inspired structural and functional components in flexible and green electronics.

1.4.5 Functionalization of biopolymers

Functionalization is often carried out on present biopolymers to endow them with specific and desirable functions or to control the interactions between biomaterials and living tissues. A number

of functionalization techniques have been employed on silk proteins and chitin including physical blending/doping (non-covalent) and chemical (covalent). In this section, a discussion on some of the techniques and materials used for the functionalization of silk and chitin in order to increase their repertoire of applications.

1.4.5.1 Functionalization of silk proteins:

Although native silk has a host of attractive properties that could be used in various applications, it is often desired to modify silk proteins in order to enhance these properties or imbue them with new properties. The strategies adopted for the functionalization of silk proteins can be classified as either physical or chemical strategies. Often, a combination of chemical and physical strategies maybe employed to engineer specific properties. Physical modification strategies of silk common involves blending them with other materials to form composites with interesting properties. For example, conducting materials such as carbon nanotubes (CNTs), reduced graphene oxide (rGO), conducting polymers such as poly(3,4-ethylenedioxythiophene) polystyrene sulfonate (PEDOT: PSS), polyaniline (PANi) and polypyrrole (PPy), metals and metal oxides have been combined with silk in order to impart electrical properties.[100-103] The strategies for imparting electrochemical activities to biopolymers will be discussed in detail in further sections. Silk fibroin was combined with metal nanoparticles such as silver and gold to develop anti-microbial surfaces, enhanced Raman scattering substrates and temperature sensitive photonic sensors.[104-107] Silk fiber, membrane and scaffolds have been blended or coated with Fe_3O_4 and ferrofluid to impart magnetic properties.[108, 109] Silk proteins have also been modified with materials such as poly(-caprolactone) (PCL) and graphene to increase the mechanical strength of silk.[110]

The presence of multiple pendent reactive groups on silk proteins provides an avenue to conjugate

various chemical moieties and chemically modify silk. Numerous bioconjugation reactions can alter its chemical, physical and mechanical properties. The benefit of these methods is that they can be used to impart new properties without affecting the physiochemical or biological properties of native silk significantly. Taking advantage of the reactive side groups, silk has been grafted with threonine, tyrosine, glutamic acid, and serine to immobilize peptides, enzymes, drugs and polymers.[21] On the other hand, modifying silk with chemicals like polycarboxylic acids and acid anhydrides can impart properties such as fire retardancy, water repellency, and thermal stability.[111-113] Similarly, modification of silk fibroin with poly (ethylene glycol) chains was also found to increase the hydrophilicity significantly. Silk is often modified with materials like poly(D, L-lactic acid), integrin-binding laminin peptide motifs, GYIGSR hexapeptide (CL2-SFF) etc., to enhance attachment, proliferation and differentiation of cells such as osteoblasts, mesenchymal stem cells and neuron like cells.[114-116] By applying similar chemical modification principles, photoreactive methacrylate groups can be introduced in the silk chain in order to impart photocrosslinkability to native silk. This will be discussed in later sections.

1.4.5.2 Functionalization of chitin

Similar to silk proteins, chitin is often modified using various chemical and physical methods to form derivatives that has new and improved properties. Native chitin and its derivative chitosan are non-conductive in nature and are typically combined with conductive materials such as metal oxides, conducting polymers and carbon materials to make conducting hybrids.[117-120] For example, chitin was blended with PANi in LiCl/DMA to form a conductive chitin-PANi composite to form sensors. Chitin has been often combined with glucose oxidase via electrostatic immobilization to form thin films or dispersed in carbon/metal pastes to form glucose

sensors.[121-123] There are reports where the mechanical properties of chitosan was improved by thermomechanical processing and enhanced by carbon nanostructures to form mechanically tunable composites.[124] Chitin is often modified through other physical modification methods such as radiation, ultrasonic treatment, plasma liquid and heat treatment which has been shown to alter its inherent properties like solubility and surface wettability.[125]

The presence of reactive functional groups as well as the polysaccharide nature of chitin allow the chemical modification of chitin and chitosan. To this end, chitosan is often chosen over chitin because of its easy solubility and processing. These polysaccharides have been subjected to various chemical modifications including acylation, quaternization, alkylation, hydroxylation, phosphorylation, thiolation, and graft copolymerization.[126-129] Among various methods, graft copolymerization is the most popular chemical modification technique used with chitin and chitosan. For example, chitin grafted with D,L-lactic acid onto amino groups showed sensitivity towards pH aggregation of the hydrophobic side chains.[130] Chitin grafted with Methyl methacrylate (MMA) was found to have moisture absorption and lysozyme susceptibility greater than native chitin.[131] Chitin is frequently grafted with other natural biopolymers such as silk to form hybrid biocomposites with enhanced functionalities.[42] Similar to silk, the pendent hydroxyl groups are important to this work since they can be specifically targeted to chemically conjugate photoactive group in order to form photocrosslinkable chitin.

1.4.6 Synthesis of photocrosslinkable silk proteins

Silk proteins fibroin and sericin possess abundant pendant functional groups that allow the modification of these proteins via chemical conjugation. Therefore, the realization of photocrosslinkable silk proteins is achieved by introducing photoactive methacrylate groups in the

main chains of both fibroin and sericin.[132, 133] The synthesis of photocrosslinkable silk proteins (i.e., photosericin and photofibroin) takes place in a 5 hr hydrolysis reaction wherein the isocyanate groups (-N=C=O) in 2-isocyanatoethyl methacrylate (IEM, MW= 155.15) specifically react with nucleophilic amine-, hydroxyl-, sulfhydryl-, and carboxylic acid groups. Due to the highly reactive nature of hydroxyl groups, the reaction is optimized on the basis of the time taken to chemically conjugate these groups. The isocyanate is reactive with carboxylic acid and amide-terminated amino acids to a lesser extent. The silk proteins are dissolved in 1M Lithium chloride (LiCl) in Dimethyl sulfoxide (DMSO) solvent system. Due to the possible reaction of the isocyanate groups with water to form CO_2, the reaction is carried out in an inert nitrogen purged condition. The reaction is terminated by precipitating the reaction mixture in cold ethanol. The precipitation product - methacrylate conjugated silk proteins (photofibroin and photosericin) is washed three times with 1:1 cold ethanol acetone mixture followed by lyophilization to obtain the final product. The photocrosslinkable silk protein are then coupled with a 365 nm UV commercial photoinitiator to induce crosslinking in the bulk biopolymer.

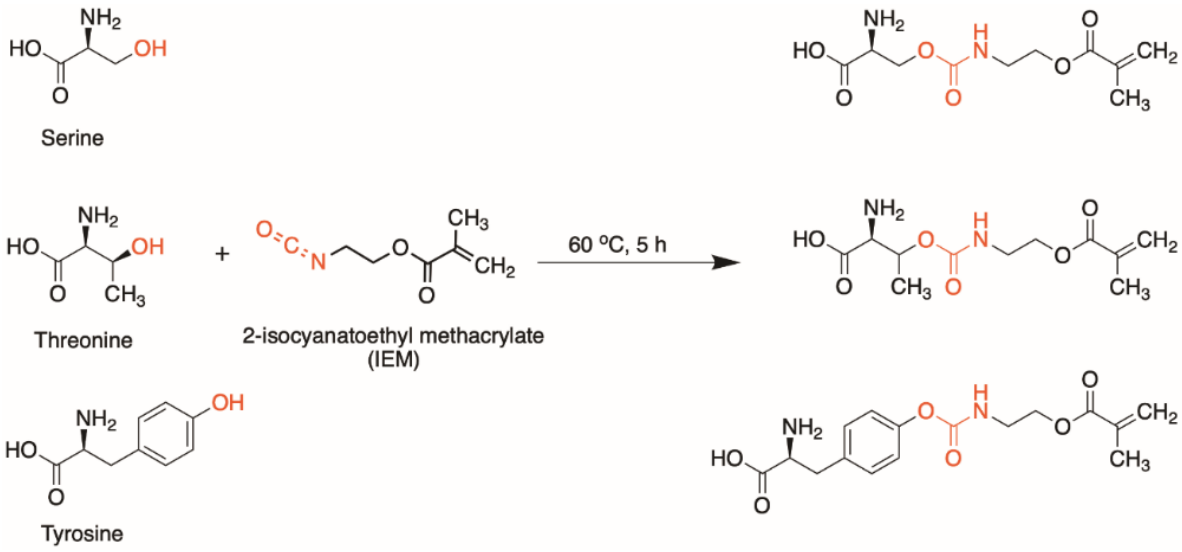

Figure 1.4 *Reaction of hydroxyl group containing amino acids in silk proteins with IEM to form methacrylate conjugated counterparts (Drawn in ChemDraw).*

1.4.7 Microfabrication techniques for biopolymers

Microfabrication techniques are used for the construction of structures with dimensions in the range of micrometers to a few millimeters. Microfabrication often involves a substrate material and structures are built either in the bulk or on the surface of the substrate material. They are commonly employed in the fabrication of microelectromechanical systems (MEMS). Most of these techniques were largely developed for applications in the semiconductor industry and hence are not specific to the development of biological systems. However, at present micro/ nanofabrication techniques have become quite common in the development of smart devices, cell culture substrates, and scaffolds that have facilitated the study of various processes at cellular and molecular scales. In this section, some of the common microfabrication techniques used with natural biopolymers are discussed.

1.4.7.1 Soft lithography

Soft lithography is a common technique used to generate micro- or even nanostructures of biopolymers onto various flexible and rigid surfaces.[134, 135] It involves the formation of a master patterns using other microfabrication techniques such as photolithography over which a microstructure replica is produced by molding a polymer, such as poly(dimethyl siloxane) (PDMS). One major advantage of this process is once the PDMS replica mold is prepared, it can be used multiple times. Techniques such as micro-stamping, stencil patterning, and microfluidic patterning comes under soft lithography where a replica mold is used.[136] This technique is widely adopted for patterning biopolymers due to its benign nature and does not require any additional modification of the biopolymer.

1.4.7.2 Etching

This technique utilizes liquid chemicals (wet etching) or gaseous physicochemical (dry etching) processes to create topographical features on a surface by selective removal of material.[137] This technique has been shown in the formation of silk microstructures.[138] Often either a metal mask or a photoresist patterned via photolithography is used to define the etching area. The advantage of dry etching over wet ones is that the structures are more well defined and flat in the former when compared to more inclined and rounded features in the latter. However, the process of etching is rather complex and often results in rough surfaces. Reactive ion etching, which utilizes oxygen or fluorine plasma, has also been extensively used.

1.4.7.3 E-beam lithography

This technique utilizes an electron beam to directly write on a material, and form the desired pattern. Although this process is commonly used for the fabrication of nanoscale structures, it can also be used to form structures in the scale of a few microns. However, there two major drawbacks to e-beam lithography. The first one is associated with the cost of purchasing and maintaining e-beam lithography machines which can be quite expensive. The second drawback is that due to the high energy dosage requirement used in e-beam lithography processes, they can damage biomolecules that are present as a whole or entrapped in other biopolymers. E-beam lithography has been demonstrated on silk proteins for the fabrication of nano-scale structures.[139, 140]

1.4.7.4. Photolithography

Photolithography is one of the most well developed and extensively used micro/ nanofabrication techniques because of the high resolution and variety of pattern attributes that are possible to

obtain.[141] Photolithography involves a series of steps that allow the generation of a desired pattern on the surface of a substrate by selectively exposing areas of a light sensitive material to ultraviolet light.[142] In the first step, a substrate material (such as silicon or glass) is coated with a layer of photoresist or any photosensitive polymer. Following this, a photomask with made of an opaque material with desired patterns that are transparent is placed on top of the substrate with photoresist. The entire setup is irradiated under UV light, thus exposing the transparent light. The patterns are formed either by formation of new bonds via chemical crosslinking (negative photolithography) or by the breaking of polymer bonds (positive photolithography). In the final step, the patterns are developed in a suitable photoresist where either the uncrosslinked or the crosslinked regions are removed depending on the type of photoresist. Usually, photoresists commonly used are synthetic photoreactive polymers. However, previous reports have described the synthesis of photoactive silk proteins suitable for photolithographic processes which will be discussed in following sections. This concept can also be translated to other biopolymers such as chitin in this dissertation work to combine them with photolithography.

1.4.8 Electroactive materials for biodevices

Naturally derived biopolymers, being intrinsically non-conductive in nature, requires them to be doped with conductive materials in order to imbibe electrochemical properties to facilitate their use as the functional sensing component in electrochemical biosensors. Electroactive biomaterials can respond to physicochemical cues which influence their optical and conductive properties, and redox state.[143] With respect to flexible bioelectronics, other than stable electrical conductivity, the material selection largely depends on properties such as biocompatibility, flexibility and chemical stability in biological environments. This section discusses some

intrinsically conducting materials that have been commonly employed for the fabrication of flexible biodevices.

1.4.8.1 Inorganic conductors

The two major classes of materials that are commonly exploited in bioelectronics are metals and carbon-based materials. A large number of current biodevices employ pure metals, metal oxides, metallic alloys, and their composites for biosensing and modulation. Some classic examples of metals used as electrodes for recording electrical signals or current stimulations are Platinum (Pt), gold (Au), and Pt–iridium alloys (Pt–Ir).[144-147] This is largely due to their high chemical stability and low cytotoxicity. Metals such as Au and Pt are often considered as good candidates because of their excellent electrical conductivity, ductility, biocompatibility, chemical stability, and various fabrication and surface modification methods that allows them to be fabricated into a variety of geometries for bioelectronic applications.[19] However, one drawback of these metals is that they are not bioresorbable in nature. Nevertheless, some of the few metals currently being studied as electrodes and interconnects in transient electronics are- Magnesium (Mg), zinc (Zn), iron (Fe), tungsten (W), and molybdenum (Mo).[148] As an alternative to conventional electrodes, intrinsically soft, low melting temperature liquid metals, such as gallium-based liquid metal (e.g., EGaIn), are promising for the further convergence of biology and epidermal electronics.[149] Other metals such as nano-silver structures (e.g. Ag nano-wires and 2D Ag flakes) have become popular as conductive fillers for stretchable biodevices.[19]

Graphene and carbon nanotubes (CNTs) have also gained much reputation in the field of bioelectronics owing to their chemical stability, biocompatibility, high mechanical flexibility, large surface area, a wide electrochemical window for doping and modification, and a variety of

fabrication methods.[150] The flexibility of carbon-based materials allows for conformal integration on human body and within dynamic tissue environments, and hence CNTs have been broadly examined in many intrinsically stretchable transistor-based bioelectronics, self-healable electronic skins, and implantable biodevices.[151-154] Other advantages include broadband optical transparency of more than 90% of graphene, exploited in imaging, optogenetic stimulation and optically transparent devices.[42, 155] For example, transparent graphene contact lenses have also been applied for electromagnetic interference shielding, glucose level measurement, and intraocular pressure sensing.

1.4.8.2 Conducting polymers

Conducting polymers describe polymeric materials that are extrinsically and intrinsically conducting. Extrinsically conducting polymers are composites of insulating polymer matrices loaded with conductive fillers such as graphene, carbon nanotubes and metallic nanoparticles.[156] Despite their prevalence in biomaterial research, there are concerns regarding the long-term effect of such fillers. Hence, this dissertation work focuses on intrinsically conducting polymeric materials and therefore be referred to as 'Conducting Polymers' (CPs). CPs owe their electrical conduction to their uninterrupted and ordered π-conjugated backbone characterized by alternating double and single bonds and conjugated π-electrons that can be delocalized, thereby facilitating electron flow along and within their polymer chains to form an electrical pathway for mobile charge carriers.[157] The use of CPs in bioelectronic devices has been limited to bulk phase dispersions to form hydrogels, films, sponges and scaffolds.[158] They have been used to coat biopolymers (such as silk fibers) to form conductive threads, which are however, temporary in nature and dissolve in aqueous environments. Although conducting

polymers have been shown in some patterning techniques such as inkjet printing and screen printing, they often lack high resolution, fidelity and precision.[159] To facilitate their use in rapid, large scale and high-resolution fabrication techniques such as photolithography, earlier reports have demonstrated the use of conducting polymers with photoactive silk fibroin to form conducting architectures and biodevices. Current research is primarily based on three CPs- poly(3,4-ethylenedioxythiophene): poly (styrene sulfonate) (PEDOT:PSS), polypyrrole (PPy), and polyaniline (PANi).[160] The conducting polymers chosen for the fabrication of biodevices in this dissertation work are PEDOT: PSS and PANi.

Poly(3,4-ethylenedioxythiophene):poly(styrene sulfonate) (PEDOT: PSS)

PEDOT: PSS is one of the most promising materials in modern flexible bioelectronics research. It consists of two ionomers- positively charged conjugated PEDOT and negatively charged insulating PSS. PEDOT is synthesized via oxidative polymerization of EDOT and is insoluble in water whereas the PSS counterion is a surfactant added to increase its dispersion. The presence of PSS allows the dispersion of PEDOT in water and increases its stability via Columbic interactions.[161] Currently, there are numerous commercially available aqueous dispersions of PEDOT: PSS with Baytron by Bayer AG, Clevios by Heraeus, and Orgacon by Agfa being some of the common ones used for preparing highly conductive and stretchable electrodes.[162, 163] The conductivity of PEDOT: PSS polymer composite largely depends on the PEDOT crystallinity since PSS in an insulator. Untreated PEDOT: PSS films have an electrical conductivity (σ) of no more than 1.0 S cm^{-1}, but are often modified with various dopants to increase conductivity by 2-3 orders of magnitude.[164, 165] The PEDOT: PSS dispersion used in this dissertation work was doped with dimethyl-sulfoxide (DMSO) in order to enhance its electrical conductivity.

PEDOT: PSS has a very well-established biocompatibility when compared to other conducting polymers. PSS and tosylate anion-doped PEDOT films have been shown to support fibroblast adhesion and proliferation.[166] They have also been successfully interfaced with neural cells where they have been shown to support a healthy morphology of neuroblastoma cells and used for chronic neural recording.[167, 168] Although some studies reported slight cytotoxicity of PEDOT, they have been shown to have good inflammatory in vivo.[169, 170] Studies have also shown the long term biocompatibility of PEDOT by implanting them in rats for 6 weeks where the tissue response was found to lower than well-established biomaterials such as platinum.[171]

Highly quality, uniform and smooth (roughness < 5 nm) films of PEDOT: PSS can be formed using the PEDOT: PSS aqueous dispersion through conventional solution-processing techniques, such as spin coating, spray deposition, screen printing and inkjet printing. Lastly, an important quality in flexible and conformable biodevices is their ability to withstand mechanical stress and maintain their useful properties under deformation. However, PEDOT: PSS can only sustain near 2% stretching and is often brittle in dry state.[19] Hence, integrating PEDOT: PSS with biopolymers which are inherently flexible in nature, can increase its stretchability, stability in dry and wet environments, ability to form stable films and biocompatibility, while conferring electrical conductivity to biopolymers.

Polyaniline (PANi)

Polyaniline (PANI) is another conductive polymer that has been extensively studied for its applications in flexible and wearable bioelectronics.[160] Chemical polymerization of polyaniline is carried out in acidic medium by using a common initiator such as ammonium persulfate and potassium persulfate, while the electropolymerization of polyaniline is carried out in the electrolyte

solution of aniline and acid through application of a potential difference between the working and counter electrodes.[172, 173] It has advantages such their relatively easy preparation, low cost, high electrical conductivity, biocompatibility, low toxicity, and environmental stability.[172] Initial studies indicated poor biocompatibility of PANi which was attributed to the presence of residual monomers and acid catalysts.[174] However, there are several reports where optimized synthetic protocols have shown that pristine aniline, especially in a base form, is biocompatible and free of embryotoxicity.

In comparison to other conducting polymers, PANi has some disadvantages such as extremely low solubility in the most common solvents, infusibility, and weak processability along with decrease in electrical conductivity over a long cycle time.[175] PANi is also known to show reduced conductivity in higher pH environments. To this end, biopolymers such as cellulose and gelatin have been known to stabilize the PANi structure (due to the presence of hydroxyl groups) and well as allowing it to be conductive in nearly neutral pH environments typically found in biological systems. Biopolymers such as chitosan, gelatin, heparin and collagen are also added to PANi to degradable scaffolds for tissue engineering.[5] The current work involves the preparation of PANi dispersion in formic acid which is then mixed with biopolymers such as silk fibroin and chitin to form highly stable, mechanically robust and electrically conducting PANI films suitable for flexible biodevices and green electronics.

1.4.8.3 Natural semiconductors

Nature also provides a host of active materials that can provide electrochemical or optoelectronic behavior, similar to that of synthetic conducting polymer. There are abundant organic dyes and pigments such as melanin, indigo and beta-carotene that behave as natural semiconductors.[5]

Although most of the research is focused on understanding the exact mechanism of electrical conductivity, there are a few examples of functional biodevices that exploit these natural semiconductors. A small part of this dissertation work also explores the possible utilization of melanin to impart electronic activity to other naturally derived materials such as silk to form active functional component in biodevices.

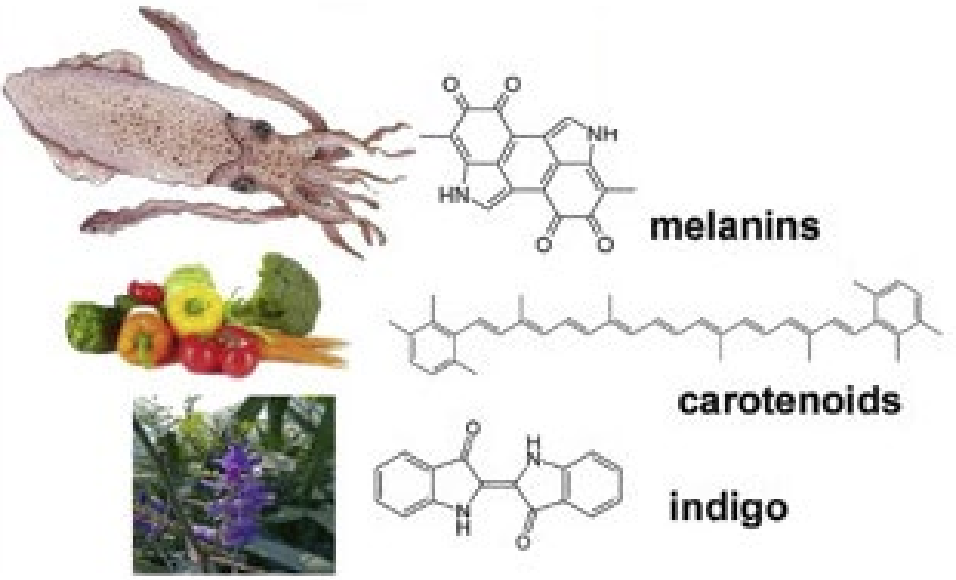

Figure 1.5 *Sources of some common semiconductors found in nature and their structures.[5]*

Melanin is a term given to a broad class of pigments found in a number of organisms. The human body contains three types of melanin- eumelanin, pheomelanin and neuromelanin. The first two act as a photoprotectant whereas neuromelanin is produced in the brain whose deficiency is associated with numerous neurological disorders. Eumelanin has been of primary interest ever due to its unique physical and chemical properties such as broad band absorbance, free radical scavenging, condensed phase photo and electrical conductivity.[176] Numerous attempts have been made in understanding the exact mechanism of conduction in melanin.[177-179] It was established recently, that hydration mediated proton transport in the main process that imparts

conductivity to melanin. [180] Integration of melanin with biopolymers can facilitate the fabrication of fully bioderived functional biodevices. Moreover, combining melanin with photoactive silk fibroin can confer photopatternability to natural melanin, thus expanding its application range.

1.4.9 Strategies for improving conformability to soft interfaces

Substrates with enhanced flexibility and conformability are of great interest for application in flexible electronics and tissue engineering substrates. To this end, it is highly desirable that devices are capable of tolerating strain levels of >> 1% without any loss in physical or chemical properties.[181] For thin films (or sheets) to be successfully applied to soft-biological samples, it is very important to reduce the Young's modulus.[37] Reducing the modulus results in a decrease of the stress induced in the device due to strain generated during mechanical deformation. The use of conventional elastomers such as polydimethylsiloxane (PDMS) was previously used to address this issue (due to low Young's modulus of 0.73 MPa).[182] Numerous electronic devices have been successfully developed such as sensor skins,[183] sheet scanner[184], circuits suitable for radio frequencies[185], and photovoltaics[186], based on flexible elastomeric materials. It is much more challenging to engineer a device that can be conformably wrapped around complex shapes which are quite common when they are integrated with biological tissues. In such cases, substrates that offer simple bending are not adequate. Hence, there is a demand for devices that can undergo out of plane bending and can be exposed to high strain levels without generating significant stress in the device. Advances made in this field primarily focus on developing strategies on improving the materials or through realizing new materials.

Another strategy by which the problem of flexibility and conformability can be tackled involves

improvement of mechanical properties by implementing structural configurations.[181] Recently, flexible and conformable structures are being explored with inspiration from “Kirigami”- the Japanese art of paper cutting[187-192]. When selective cuts are made on a sheet, the flexibility of the sheet increases as the cuts open up to accommodate strain induced stress in the material due to mechanical deformation. Further, the cuts facilitate the out-of-plane bending of the sheet which allows better conformability for curvilinear interfaces. This can be helpful for the realization of sensors for instance, that can efficiently wrap around tissues or other non-planar sensing surfaces. In spite of the frequent attempts made in the engineering of flexible devices through the creation of kirigami inspired patterned defects, very little work has been shown using such strategies for organic biomaterials. Successful application of kirigami design techniques to biomaterials can increase the conformability of biodegradable and biocompatible electronics to soft biological interfaces. In this research primarily focuses on applying such patterned defects to increase the flexibility of bio-derived thin films (chitin and silk).

[This chapter contains results that have been previously published: Sayantan Pradhan, Anne Kathrine Brooks, Vamsi K. Yadavalli, “Nature-derived materials for the fabrication of functional biodevices”, Mat. Today Bio, 7, 100065.]

CHAPTER 2

PHOTOLITHOGRAPHIC MICROPATTERNING ON FLEXIBLE SILK FILMS

2.1 INTRODUCTION

As discussed in Chapter 1, nature derived materials such as silk proteins are of great interest in the design and development of biomedical devices. Of special interest is the application of nature derived biodegradable materials for the realization of fully organic, intrinsically flexible, thin film devices. However, a challenge has often been the ability to combine high-throughput and high-resolution fabrication techniques with such materials, often restricting their use in bioelectronics and optics, beyond functioning as substrates. This chapter explores the development of a facile, scalable and simple bench top photolithographic technique that allows the fabrication of silk fibroin microarchitectures on flexible silk fibroin films.

Thin polymeric films have long been used in industry for semiconductor applications, electronics packaging, as optical coatings, diffusion barriers, friction reduction, etc.[193, 194] Recently, such films and sheets have been explored for biomedical uses such as drug delivery, biofiltration, wound healing, tissue regeneration and biosensors.[195-197] Of specific interest are flexible, free-standing sheets, which can be formed with controllable thickness (ultrathin - 10s of nanometers, to thin –few to 10s of micrometers). They can be used as substrates for soft robotics, smart skins

and wearable devices.[198, 199] At the nanoscale thickness, such films can directly conform to the underlying surface, whereas at the microscale, adhesive layers may be needed for attachment to tissue.[200, 201]

Flexible sheets may be formed using various techniques including casting elastomeric or intrinsically flexible materials, electrospinning, or by using spin coating or layer-by-layer assembly.[197] Paper has also recently attracted attention due to its porosity and flexibility, while permitting modifications of physical and chemical properties.[202] Electrospinning to form micro- and nano-fibrous architectures can form sheets (e.g. fiber mats) from a variety of synthetic and natural materials.[203-205] However, imparting the additional property of patterned architectures (micro/nano-textured surface) is limited, particularly over large areas (e.g. cm).[206, 207] Elastomers such as polydimethylsiloxane (PDMS) and polyurethanes have been used with favorable properties including high optical transparency, ability to form micropatterns, and control of important mechanical properties such as rigidity.[208-210] Despite good biomimetic characteristics and tunable mechanical properties, these materials have high surface hydrophobicity, limited aqueous processing, and importantly, a lack of degradability, which precludes their application in intrinsically biodegradable and flexible devices.

Silk proteins, fibroin and sericin as natural biomaterials have been recognized as a very appealing biocompatible and regeneratable resource and fostered various applications in tissue engineering and regenerative medicine.[211] Micropatterned thin films developed using nature-derived materials is an essential step in the realization of biodegradable flexible devices for applications at the biological milieu. Fabrication techniques using printing, molding, imprinting, and photolithography have shown silk proteins for the construction of flexible optical, photonic, optoelectronic, and electronic devices.[75, 212, 213] However, there remain several technical

challenges that need to be addressed. For instance, a direct patterning with high fidelity and complex silk-based functional features for the integration of electronic systems is an ongoing challenge. In this chapter, an approach is suggested that allows the fabrication of high-resolution microarchitectures of silk fibroin on a flexible silk fibroin films using photolithography process.

2.2 EXPERIMENTAL

2.2.1 Synthesis of photocrosslinkable silk fibroin films

Silk fibroin was extracted from silk cocoons using a standard protocol.[60] Fibroin protein photoresist (variously referred to as FPP or photofibroin) was prepared by the incorporation of photo reactive moieties to the fibroin structure as reported earlier in Chapter 1. Briefly, pure fibroin was dissolved in 1 M LiCl/DMSO and reacted with 2-Isocyanatoethyl methacrylate (IEM) in stoichiometric amounts for 5 hours at 60ºC, while maintaining inert conditions using a constant flow of nitrogen. After the completion of the reaction, the product mixture was added to cold ethanol, and the methacrylated protein was obtained as the precipitate. The product was washed with a 1:1 ratio of cold ethanol and acetone followed by centrifugation and lyophilization for 24 hours to obtain the fibroin protein photoresist (photofibroin) powder.

2.2.2 Fabrication of flexible micropatterned fibroin films

The flexible micropatterned substrate was fabricated by dissolving 7.5% (w/v) of photofibroin in formic acid (Acros Organics 98%). 2.5% (w/v) photo initiator (Irgacure 2959, BASF) was added. The solution was drop cast on plain glass slides and air dried for 15 to 20 minutes in order to evaporate the excess solvent. The samples were exposed under a 365 nm UV lamp (Lumen Dynamics OmniCure 1000 system) for 3 seconds at 20 mW cm^{-2} for cross-linking. To create

fibroin films, the samples were dipped in DI water which facilitated the delamination from the glass. Micropatterns of silk fibroin were fabricated on these films using contact photolithography. Films prepared as discussed above were used as the substrates. A 5% (w/v) solution of photofibroin in 1,1,1,3,3,3-hexafluoro-2-propanol (HFIP, Sigma-Aldrich, St. Louis, MO) was drop casted on fibroin films. The samples were air dried for 5 minutes, allowing the HFIP to evaporate. Micropatterned structures were formed by placing a photolithographic mask with the desired array of patterns on the substrates and exposing it under UV irradiation for 1.6 seconds. Patterns were developed by immersing the samples in 1 M LiCl/DMSO solution for approximately 2 hours. The patterns were then rigorously cleaned with DI water to wash off any un-crosslinked material and excess LiCl/DMSO solution.

2.2.3 Proteolytic degradation in vitro

Micropatterned fibroin films can be proteolytically degraded over time in the presence of enzymes. In the present work, the degradation of fibroin microstructures on films in the presence of protease (Protease XIV from *Streptomyces griseus,* ≥3.5 U mg^{-1}, Sigma Aldrich) was studied. Films (containing ~2.5 mg fibroin) were incubated in 5 mL protease (1 U mg^{-1} of protein) at 37 °C and the degradation was studied over 2 weeks. Another set of samples were incubated in PBS buffer under the same environment, which served as the negative control (NC). The enzyme solution was replaced every 3 days to maintain the activity of protease. Samples from each set were taken out on different days, rinsed with DI water, dried under N_2, and weighed to record their degradation over time. Degradation over time was characterized as a function of mass loss of the films.

2.2.4 Tensile tests

Tensile tests were performed on native fibroin and photofibroin films using MTS 300 series tensile testing machine (MTS Systems Corporation, Eden Prairie, MN) equipped with a 50 N load cell. The tensile measurements were taken under ambient conditions on complete dry films. A strain rate of 0.01 mm s^{-1} was applied on the films and data was collected at a rate of 10 Hz. The tensile strengths of native fibroin and photofibroin films were compared.

2.3 RESULTS AND DISCUSSION

2.3.1 Fabrication of flexible, micropatterned fibroin films

Mechanically flexible, biocompatible sheets present platforms for applications as surface for soft robotics, drug delivery vehicles, sealing of wounds, tissue scaffolds and biosensors.[195, 214] The ability to form micropatterns on these sheets can further provide opportunities to fabricate electrical circuits and other bioelectrical components in fully organic, flexible, and biodegradable devices. To date, micropatterned films have been shown on rigid or supported formats (for instance, with an underlying glass or polystyrene substrate) or using flexible materials that are not degradable (e.g., PDMS). The development of flexible, and micropatterned films and membranes using degradable biopolymers is limited. In this work, the microfabrication of flexible, silk fibroin films was realized using light-reactive conjugates and facile photolithographic techniques. These conjugates can be used as stable, biodegradable and biocompatible substrates on which patterns are formed. Previously, patterns of sericin were shown on flexible fibroin substrates, which could be accomplished since the two are soluble in different solvents (viz. sericin in water, fibroin in formic acid or HFIP). Here, we utilize fibroin as the material for both the substrate and the pattern. The use of photolithography provides a rapid route to form complex patterns that are not easily

prepared used using microcontact printing or molding.

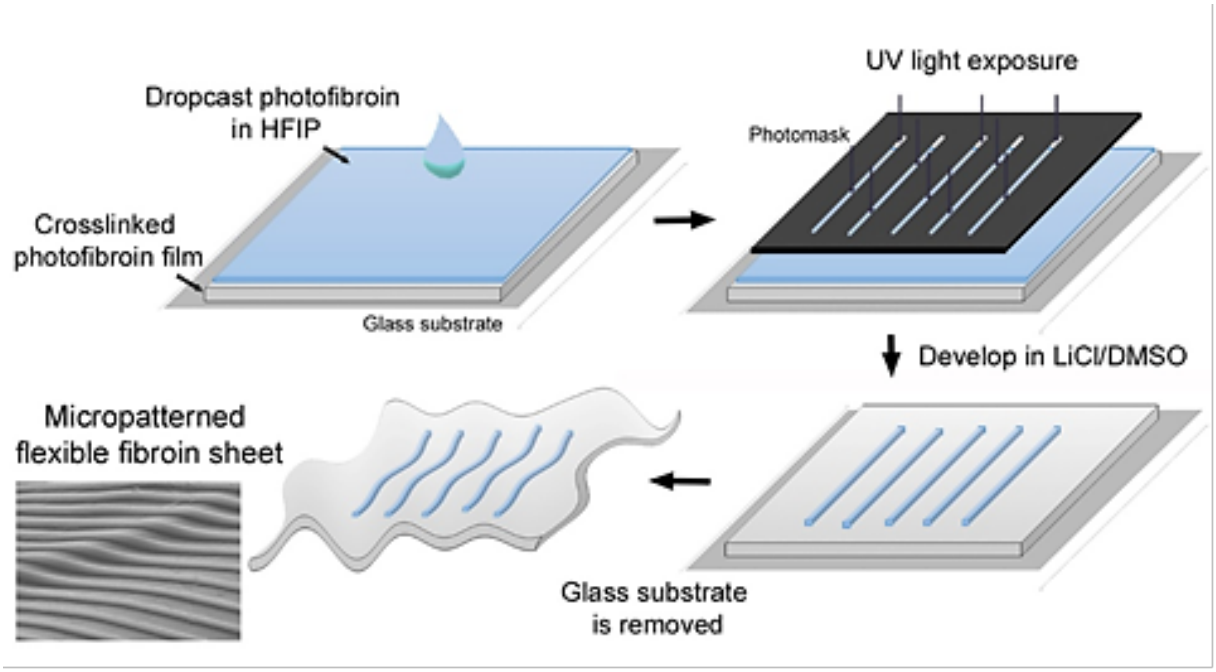

Figure 2.1 *Fabrication of micropatterned flexible fibroin films via photolithography.*

Initially, a solution of photocrosslinkable silk fibroin in formic acid with a suitable photo initiator was cast on a plain glass slide (1 cm^2 area) and crosslinked by exposure under 365 nm UV light (**Figure 2.1**). The use of formic acid as a solvent allows us to form large scale, thin, flat and stable fibroin films in an environmentally friendly process. These films are formed by crosslinking of the protein and not by a change in β-sheet conformation as shown in other works.[215] The UV crosslinked fibroin sheets formed are water insoluble and are stable in a wide range of solvents. Due to the absence of chemical linkage between the film and the glass support, the crosslinked fibroin sheet can be easily peeled off when immersed in water. The thickness of the film plays a defining role in its flexibility, and films ranging from hundreds of nm to tens of μm are easily formed by controlling the amount of fibroin/formic acid solution cast and the spin coating speed.

For example, 60 μL of fibroin solution cast on a plain glass slide of area 1 cm^2 produces films with a thickness ~10 μm at a spin speed of 800 rpm.

To fabricate micro-architectures of silk fibroin photoresist on fibroin films, a 5% (w/v) solution in HFIP was cast on silk fibroin sheets prepared as described above. The presence of residual acrylate functional groups on the surface of the films enables the covalent attachment of patterns on them. This implies that the patterns do not delaminate when the film is subjected to mechanical deformation. Patterns are formed by exposure to 365 nm UV through a photomask (Figure 1). The area exposed by the UV light is crosslinked while, the unexposed areas dissolve when immersed in 1 M of LiCl in DMSO. A wide range of patterns with different shape, size and complexity can be obtained depending on the nature of the photolithographic mask used. The use of a single material for the fabrication of the substrate and the patterns allows us to form microarchitectures of high stability due to the presence of the same chemistry. Due to the volatility of HFIP, a solution of photofibroin in HFIP can be cast on the fibroin films without disrupting the underlying film. This demands precise control over the amount of solution drop cast on the fibroin films and drying time prior to UV exposure for patterning. 30 μL of photofibroin/ HFIP solution for a fibroin film of area 1 cm^2 and a drying time of approximately 5 minutes was found to be optimum for the results shown here. Once they are immersed for development, the entire structure can be delaminated from the glass support to form mechanically flexible films (**Figure 2.2a**). The images obtained from an optical microscope shows the ability form ordered patterns of various complexities over a large area (cm scale) of flexible fibroin sheet (**Figure 2.2b, c**). Thin, moist films can be applied to and readily conform to irregular surfaces (e.g., skin) without the need for any adhesive (**Figure 2d**).

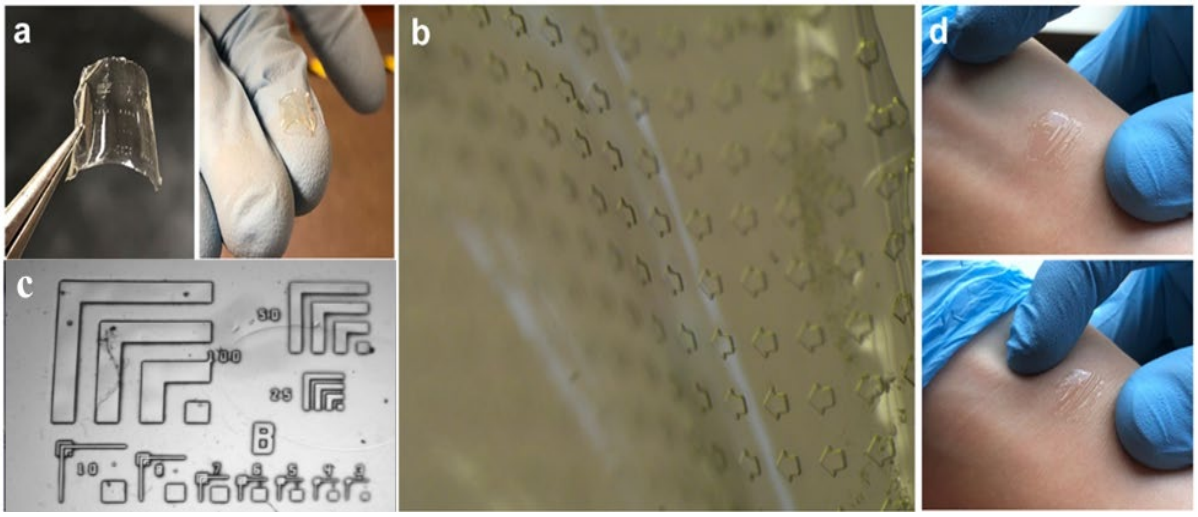

Figure 2.2 *a) Mechanically stable micropatterned films formed by photolithography. Large area films can be patterned with microscale architectures b). c) Optical image of micropatterned films showing the high resolution of patterns formed by photolithography d) Ultrathin micropatterned films (< 1 µm) can be easily applied to soft surfaces (e.g., skin) without any adhesive – shown in stretched and squeezed forms.*

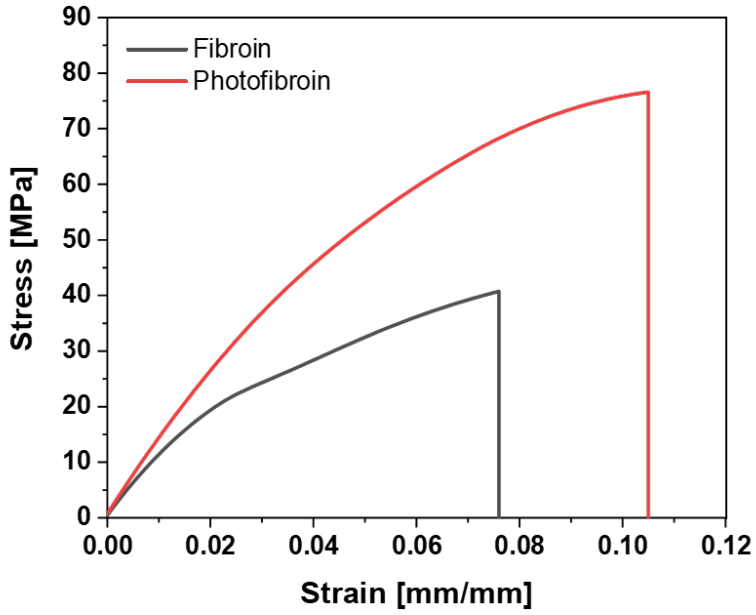

Figure 2.3 *Evaluation of mechanical properties of silk fibroin - Comparison of Stress vs strain curves of photofibroin and native fibroin.*

The photofibroin films are mechanically robust and can be rolled or bent and can be held, rolled or bent into various conformations numerous times without any loss in their chemical and physical properties. Tensile tests were performed to compare the mechanical properties of photofibroin with native fibroin (**Figure 2.3 a**). The tensile response of silk fibroin extracted using 9.6 M LiBr (the degumming of silk fiber process used in the work) was similar to earlier reports with a tensile strength of ~40 MPa.[216] In comparison the tensile strength of photofibroin films were found to be ~80 MPa, which is 2 times the value of native fibroin. The solvent used for the dissolution of photofibroin plays a crucial role on the mechanical properties of the films. It was found that the films prepared using formic acid as the solvent have a higher strength in comparison to photofibroin films prepared using HFIP as the solvent. The HFIP processed films are softer and more flexible, with a lower Young's modulus. To demonstrate the structural integrity and scalability at the microscale, optical and SEM images were taken. The SEM images (**Figure 2.3)** depict the high fidelity and spatial and structural resolution of the micropatterns as lines or dots. Due to the vinyl linkage between the patterns and the substrate, a strong adhesion is observed at the interface and the structures are intact even in bent conditions. In **Figure 2.3d**, the film was examined after conducting several (~10 times) extreme 180^{o} bends. While some minor cracks may be seen on the film at the bend junction, the patterns themselves do not delaminate, demonstrating the high robustness of this system. This can be correlated to the differences in terms of Young modulus between the softer pattern and the stiffer substrate (**Figure 2.4a-c**) which are observed under nanoindentation. Under mechanical deformation, the former is thus more flexible with respect the latter, adapting itself to the deformation of the substrate. This is critical to the designing of fully organic flexible biodevices wherein the circuits, electrodes and other active components are also highly flexible and do not lose their electrochemical properties under mechanical flexure.

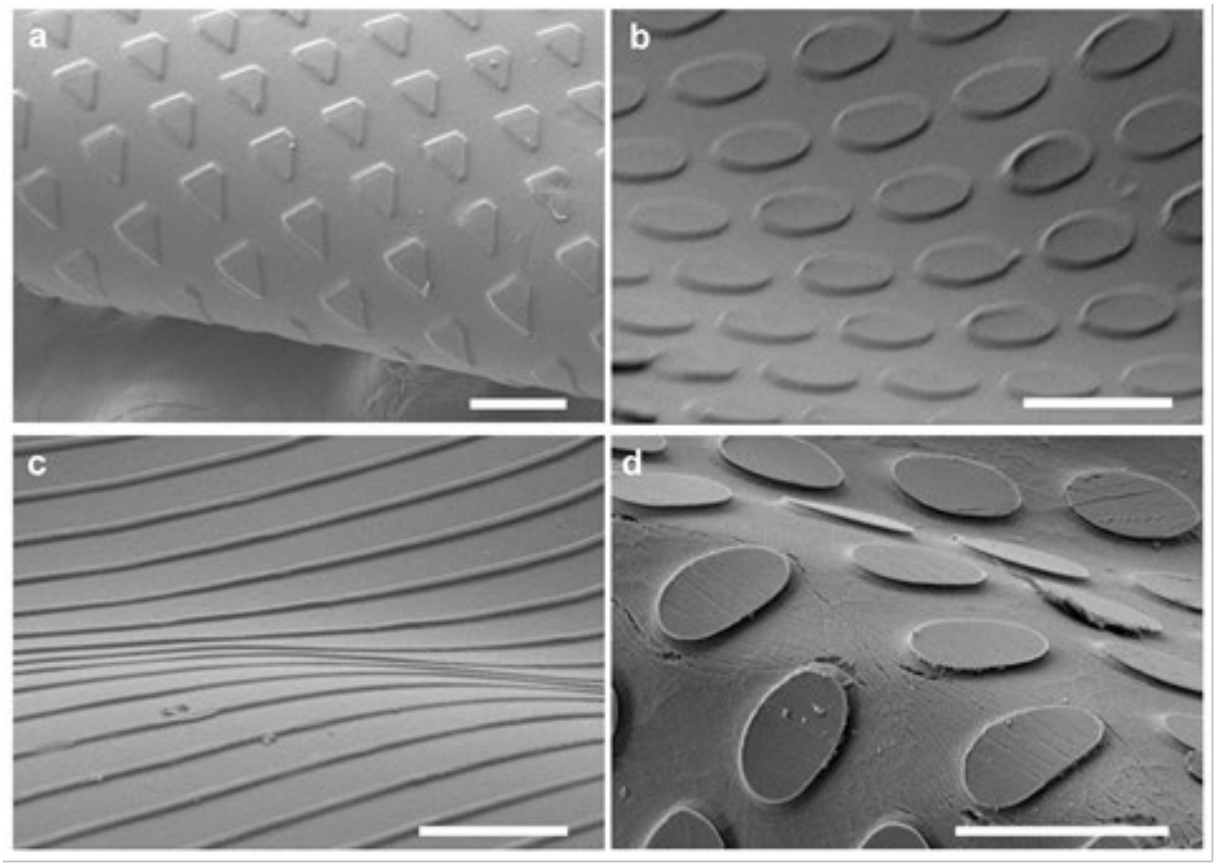

Figure 2.4 *SEM images of the different forms of flexible microstructured films of silk fibroin fabricated by photolithography a) films can be fully rolled, b, c) different kinds of surface architectures are easily patterned using different photomasks, d) image taken after repeated 180^{o} bends shows nanoscale cracks but the film integrity is preserved, and no delamination of features observed. Scale bar on all images = 100 µm.*

AFM imaging of the films (**Figure 2.4d, e**) show that they are smooth at the nanoscale (both on the film and on the surface of the patterns) with a root mean square (RMS) roughness ~ 5 nm over a 5 µm area. In these films, the patterns were around 500 nm in height, fabricated via spin coating. The lines have a high structural fidelity and resolution demonstrating the accuracy of this

photolithographic process to form micro patterns over large areas. Patterns down to ~3 µm using benchtop lithography are easily formed. However, formation of nanoscale structures with photofibroin using electron beam lithography have been demonstrated in earlier reports. Due to the optical transparency of the entire structure, they can also find application in optics for the fabrication of soft and flexible optical systems.

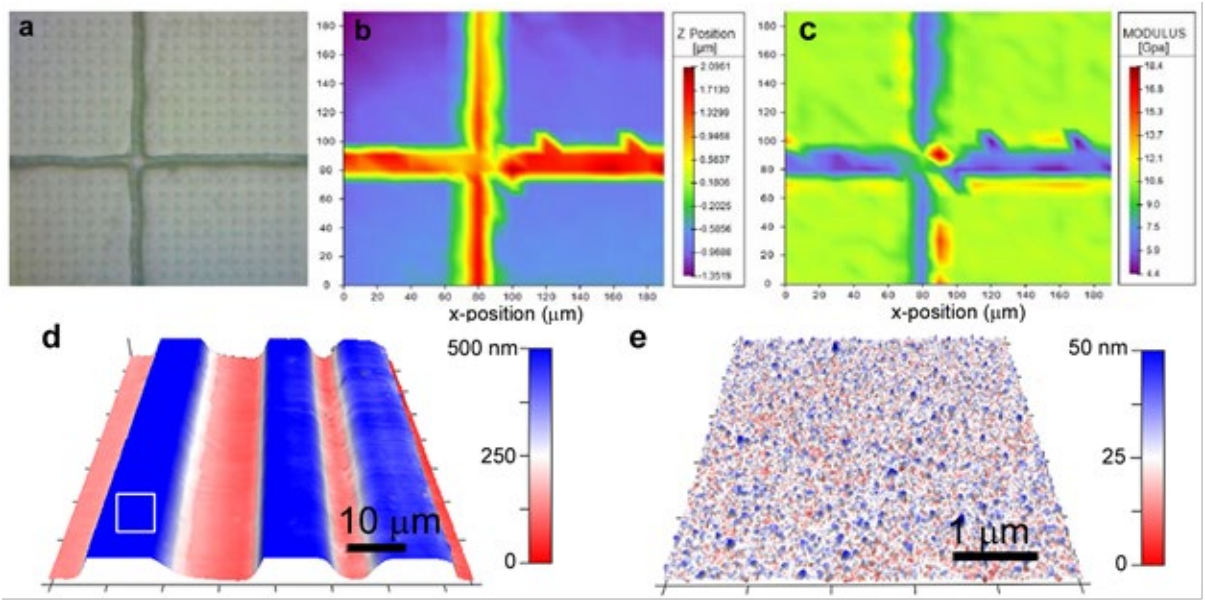

Figure 2.5 *a, b, c) Spatial distribution of the patterned surface and the localized Young's modulus of the surface, showing the softer pattern on the stiffer underlying substrate (scales on all panels are same). d) AFM imaging of the fibroin micropatterns on fibroin 75 µm scan of 10 µm lines separated by 25 µm and 5 µm gaps. The patterns are 500 nm in height. e) Scan of a 5 x 5 µm area from the flat region of the line shows the flat surface of the films (RMS roughness ~ 5 nm over this area).*

2.3.2 Proteolytic degradation of fibroin substrates *in vitro*

An advantage in using natural biopolymers is that devices fabricated based entirely on these

materials can be degraded in physiological environments. The silk fibroin biomaterial used in this study enables controllable biodegradability of the flexible devices. Under the reaction of protease, the micropatterned sheets are degraded, ultimately leading to the loss of mass and structural integrity. An enzymatic biodegradation experiment was conducted on micropatterned films incubated in PBS solution with or without protease (control) at 37ºC. The percentage of mass weight remaining (obtained as W_t/W_0) was recorded to observe the overall decomposition of the films ($n=3$) over time (**Figure 2.5**). No significant mass loss was observed when incubated in PBS over the 2-week period. Due to proteolytic biodegradation, a gradual loss of weight was observed and <40% of the weight remained after 14 days of incubation. After 14 days, the films incubated in the enzyme broke down, whereas the control samples maintained their integrity and flexibility. This was consistent with previously reported observations in which the biodegradability of fibroin based flexible devices can be tuned by controlling the degree of crosslinking and film thickness. Therefore, devices with precisely engineered lifetimes can be fabricated using these micropatterned films, which can be useful as tissue scaffolds and implantable bioelectronics.

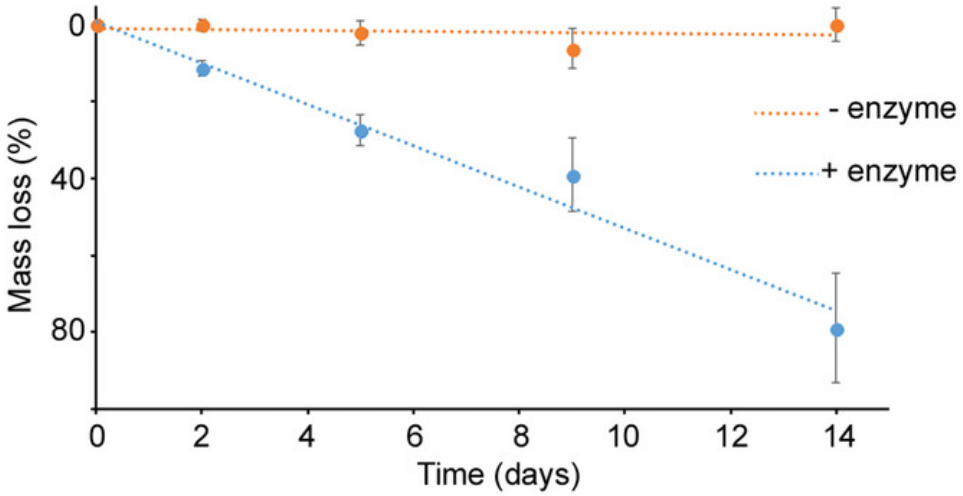

Figure 2.6 *Proteolytic degradation of micropatterned fibroin films. The films are stable in buffers but show significant mass loss in the presence of protease, ultimately breaking down completely within 3 weeks. (Sample size n=3 films for each experiment)*

2.4 CONCLUSION

In this chapter, the development of a platform that allows facile micropatterning of biopolymer silk fibroin protein is discussed. The silk fibroin has been functionalized with photoactive methacrylate groups that allows UV assisted photocrosslinking. Therefore, an easy, low cost and high throughput photolithography process is demonstrated that allows the micropatterning of high resolution and high-fidelity structures over a large area on a variety of rigid and flexible substrates. By dissolving photofibroin in two different solvents, fabrication of fibroin micropatterns on flexible fibroin sheets have been demonstrated. Due to the presence of similar methacrylate chemistry, the patterns are chemically attached to the substrate and do not come off under mechanical deformations. In addition to the patterns, it is also possible to modulate the mechanical characteristics of the patterns. Importantly, the controlled biodegradation of micropatterns silk fibroin sheets is shown under proteolytic conditions. These results suggest that micropatterned silk sheets can provide a bioinspired and biodegradable structure towards the flexible cell culture platforms and devices.

[This chapter contains results that have been previously published: Meng Xu, Sayantan Pradhan, Francesca Agostinacchio, Ramendra K. Pal, Gabriele Greco, Barbara Mazzolai, Nicola M. Pugno, Antonella Motta, Vamsi K. Yadavalli, "Easy, Scalable, Robust, Micropatterned Silk Fibroin Cell Substrates", Adv. Mater. Interfaces 2019, 6, 1801822.]

CHAPTER 3

FABRICATION OF MICROPATTERNED CHITIN FILMS USING PHOTOLITHOGRAPHY

3.1 INTRODUCTION

As discussed in Chapter 1, among the polysaccharide class of nature derived degradable biopolymers, Chitin and its derivative chitosan have gained much attention in the field of biomedical research due to attractive properties such as biocompatibility, non-toxicity, biodegradability, low immunogenicity, and ease of availability.[88, 217] Excellent biological properties and novel intrinsic antimicrobial properties have favored the use of chitin and its derivatives in tissue engineering, wound healing, and drug delivery applications.[218, 219] To develop functional architectures from chitin and chitosan, the polymers are frequently dissolved acidic solutions.[220] Using this approach, there have been reports on the use of chitinous biomaterials for porous biodegradable scaffolds, with the polymers alone, or in combination with other materials such as gelatin, collagen, poly-L-lactic acid, alginate, and silk.[221-226] While work has been done on the use of chitin and chitosan as functional biomaterials by imparting specific properties, the potential of chitin as a biomaterial is somewhat limited owing to its intractable processing.

To date, only a few strategies to form chitin into precise 2D and 3D micropatterned structures with high resolution have been reported. Micro and nanopatterned biomaterial surfaces are increasingly

important both as cell culture substrates as well as components of biosensors and organic electronics.[227, 228] Some of the techniques reported in literature for the realization of chitin/ chitosan microstructures include nanosphere lithography (NSL), micromolding, inkjet printing, macro scale molding and micro-contact patterning with a chitin nanofiber ink.[229-233] As yet, creating structures of high resolution using scalable techniques such as photolithography has not been demonstrated with chitin. Though there has been some work on micro-patterning, primarily on rigid substrates, chitin micropatterning on flexible surfaces can open new avenues for its use as bioelectronics devices that are biofriendly and degradable. Optically transparent, flexible, micropatterned chitin sheets can be used for green electronics, tissue engineering, or to achieve conformal contact for wound healing applications.

This chapter focuses on a facile reaction to modify the chitin chain with photoactive moieties for the realization of photocrosslinkable chitin. The presence of labile functional groups on the main chains of chitin and chitosan provides an opportunity to improve the material properties and function by ligating different chemical moieties. The photocrosslinkable chitin can then be easily combined with the simple bench top photolithographic reported in Chapter 2 to form micropatterned chitin films.

3.2 EXPERIMENTAL

3.2.1 Synthesis of low molecular weight chitin

In order to synthesize photocrosslinkable chitin, it was necessary to convert the raw chitin flakes into low molecular weight chitin (LMW chitin). LMW chitin was prepared using a well-established method. 60 mL of 37% HCl was added to 2 g chitin (Alfa Aesar, Haverhill, MA) in a round bottom flask. The mixture was heated at 40 ^{o}C using a water batch and continuously stirred

for 20 minutes. The contents of the flask were cooled using an ice-bath, and then carefully neutralized to a pH 7 using NaOH solution. The mixture was then centrifuged at 4000 rpm for 20 minutes and the supernatant was collected. This solution was then dialyzed against tap water using 12 kDa dialysis membrane for 2 days, with periodic replacement of the tap water. The solution within the dialysis tubing was collected and lyophilized for 2 days to obtain low molecular weight chitin powder.

3.2.2 Synthesis and characterization of photocrosslinkable chitin

Photocrosslinkable chitin (which refer to as photochitin (PC)) was prepared by adding photoactive moieties to the chitin backbone. All glassware was cleaned using deionized water and ethanol, and oven dried at 150 ^{o}C overnight. All the chemicals were dried to ensure they were free from any moisture. Low molecular weight chitin was dissolved in 5% LiCl/dimethylacetamide (DMAc) in a 3neck round bottom flask and 2-isocyanatoethyl methacrylate (IEM) was added to the reaction mixture in excess. The reaction was carried out at 65 ^{o}C for 24 hours while maintaining inert conditions using a continuous flow of nitrogen. The product obtained was precipitated overnight in cold ethanol, followed by 3 cycles of washing using 1:1 ratio of cold ethanol and acetone. The product was lyophilized to obtain PC powder. The yield of the product was ~54%.

3.2.3 Determination of degree of deacetylation

The degree of deacetylation (DD), which determines the content of free amino groups in the polysaccharides was then used to determine the chemical nature of the photochitin (PC) synthesized. The DD was determined using infrared spectroscopy (IR) and first derivative UV-spectrophotometry for confirmation of the results.

3.2.4 Fabrication of flexible films

Films were fabricated by casting a solution of photochitin in formic acid (Acros Organics 98%) with composition - 40 mL of FA, 0.1 mL of PEG-DA (Sigma-Aldrich, St. Louis, MO) and 1 mg of photo initiator (2-hydroxy-40-(2-hydroxyethoxy)-2-methylpropiophenone, Sigma-Aldrich) per 3 mg of PC. The solution was dried under ambient conditions and crosslinked under 365 nm UV lamp (Lumen Dynamics OmniCure 1000 system) for 2 seconds at 20 mM cm^{-2}. Pure chitin films were made using a suspension of 1 gm chitin powder in ~15 mL of formic acid was prepared and then frozen at -20 ^{o}C for 20 hours. The frozen suspension was thawed at room temperature, stirred and frozen again. The process was carried out for several times till a clear gel was obtained. The obtained clear chitin gel was added to small amount of trichloroacetic acid, mixed thoroughly was cast on a clean glass slide. The solvents were evaporated under ambient conditions and a chitin film was obtained. Films of chitosan was obtained by casting a 7.5% (w/v) solution of chitosan in formic acid on a clean glass slide and drying it under atmospheric conditions to obtain a film.

3.2.5 Characterization of films

IR was conducted on films of chitin and photochitin to verify the presence of the methacrylate moiety as well as determine the degree of deacetylation as discussed above. Films were cast from a solution in formic acid onto a germanium crystal for analysis. Fourier-transform infrared (FTIR) spectra were obtained at a resolution of 1 cm^{-1} and 32 scans, via a Nicolet iS10 FTIR spectrometer, equipped with a Smart iTR attachment for attenuated total reflectance (ATR) studies. Contact angles of chitin, photochitin, and chitosan films were measured using a Rame´-Hart goniometer (Succasunna, NJ) by placing a 5 mL drop of DI water on the films and taking images with the attached camera. Tensile tests were performed on PC, chitin and chitosan films prepared using

methods described above using MTS 300 series tensile testing machine (MTS Systems Corporation, Eden Prairie, MN) equipped with a 50 N load cell. The tensile measurements were taken under ambient conditions on complete dry films. A strain rate of 0.1 mm s^{-1} was applied on the films and data was collected at a rate of 10 Hz. The tensile strengths of chitin, photochitin, and chitosan films were compared.

3.2.6 Fabrication of micropatterns

Flexible chitin substrate was created using a solution of 2.5% (w/v) photochitin and 0.75% (w/v) PEG-DA in formic acid (Acros Organics 98%). 0.83% (w/v) photo initiator (2-hydroxy-40-(2-hydroxyethoxy)-2-methylpropiophenone, Sigma-Aldrich, St. Louis, MO) was added to the solution and the solution was casted on a clean glass slide. The solution was air dried under ambient conditions and then crosslinked under a 365 nm UV lamp (Lumen Dynamics OmniCure 1000 system) for 2 seconds at 20 mW cm^{-2}. The films were soaked in DI water to obtain freestanding chitin films. In order to create micropatterns on flexible chitin substrates, a solution of 2% (w/v) photochitin + 0.75% (w/v) PEG-DA with 0.66% photo initiator in 1,1,1,3,3,3- hexafluoro-2-propanol (HFIP, Sigma-Aldrich) was drop cast on the chitin films prepared as above. The samples were air dried for ~5 minutes and then exposed under the UV lamp for 1 second through a negative tone photomask with desired patterns. The patterns were developed by soaking in a 1 M LiCl/DMSO solution for 1 hour. The micropatterned films and substrates were cleaned using generous amounts of DI water.

3.2.7 Imaging

Scanning electron microscopy (SEM) images of the patterns were taken on a Hitachi SU-70 FE-

SEM to observe the fidelity of the patterned structures. The patterns were sputtered coated in a 20 A platinum Denton vacuum cold sputtering system (Moorestown NJ) prior to imaging. Optical images were taken using a Nikon Eclipse microscope.

3.3 RESULTS AND DISCUSSION

3.3.1 Synthesis and characterization of photocrosslinkable chitin

Similar to silk proteins as discussed in previous chapter, chitin main chain has of multiple pendant functional groups which provides an opportunity to introduce photo-reactive groups. This can impart photocrosslinkability to native chitin. Using the concepts of modular design, photoreactive methacrylate groups were targeted for conjugation due to their prevalence in existing photolithography techniques, ease of use, and possibility for high-resolution, microscale features. However, the extensive hydrogen bonding between adjacent polymer chains of the predominantly b-(1 - 4)-linked 2-acetamido-2-deoxy-D-glucose have contributed to high rigidity and poor solubility and processability of chitin. Hence, initial trails that were made for the dissolution of native chitin in solvent systems such as 5% LiCl in DMSO, DMF and DMAc have all resulted in failure. After repeated failures, it was found that hydrolysis into lower molecular weight chitin can increase the solubility of chitin in 5% LiCl/DMAc, which is one of the few solvent systems that can dissolve chitin.

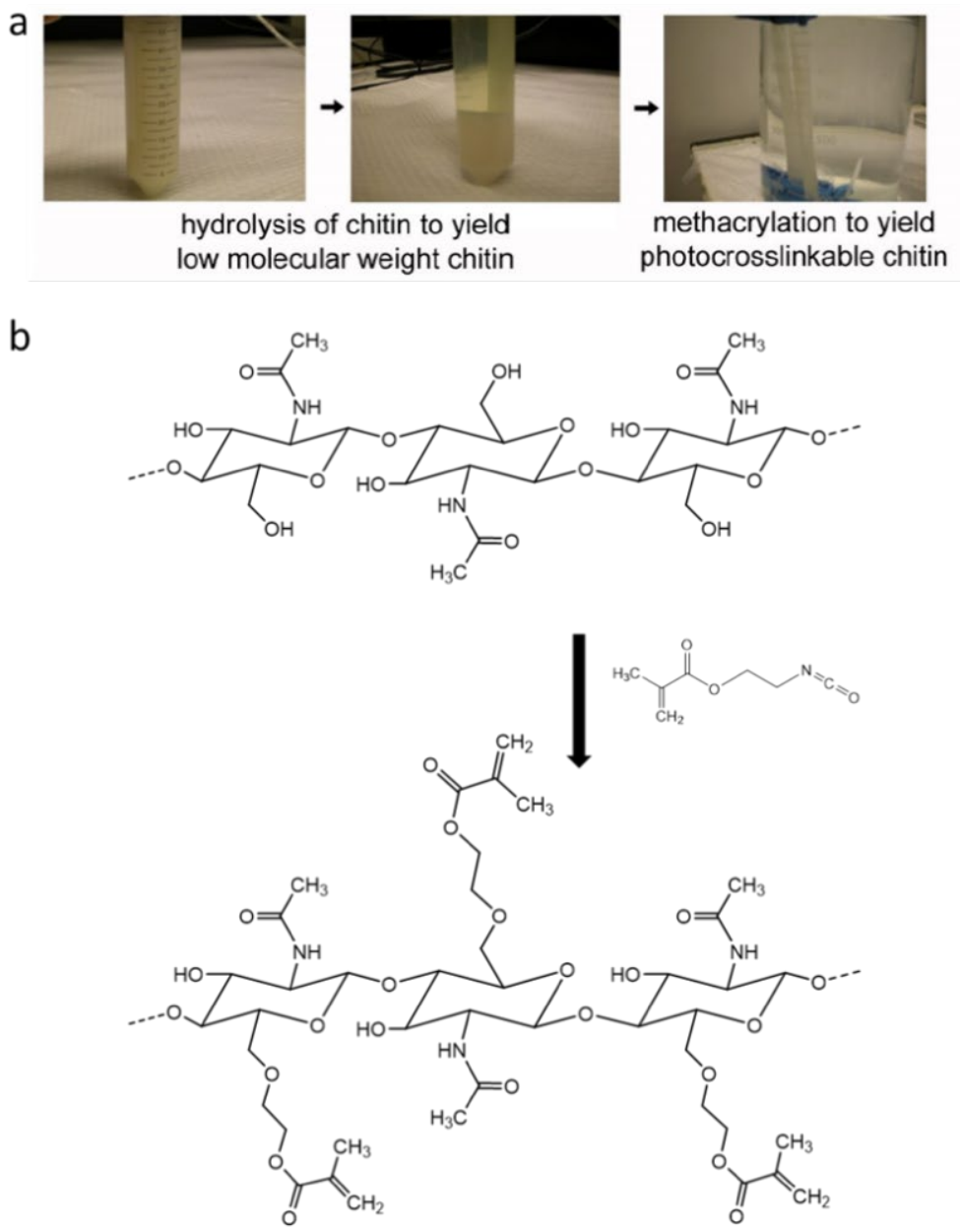

Figure 3.1 *a) Steps showing the synthesis of photocrosslinkable chitin and b) Reaction scheme of chitin with 2-isocyanatoethylmethacrylate to form photoreactive chitin.*

The polymeric chain of chitin can be broken down into smaller oligomeric or monomeric groups either by enzymatic or by acid hydrolysis. However, concentrated hydrochloric acid (37%) was used in this work since it is known to hydrolyze chitin without deacetylation or formation of side

products. The acid catalyzed hydrolysis of chitin into low-molecular weight chitin takes place via cleavage of glycosidic linkages. The LMW chitin obtained via acid hydrolysis was found to dissolve in 5% LiCl/DMAc easily. Once the solubility issue was addressed, in the next step LMW chitin was then modified to photocrosslinkable chitin (PC) using 2-isocyanatoethyl methacrylate (IEM) with LiCl/DMAc as the solvent. The product obtained was precipitated, purified to separate the water-miscible components (DMAc and IEM) and subsequently lyophilized to give PC powder. In another trial, it was found that the methacrylation of hydrolyzed low molecular weight chitin reaction can be also be carried out in 5% LiCl in *N*-Methyl-2-pyrrolidone solvent system.

3.3.1.1 Verification of conjugation

The PC powder obtained was found to be soluble in formic acid and in polar fluorinated solvents such as 1,1,1,3,3,3-hexafluoro-2- propanol (HFIP). However, formic acid was used for the dissolution of PC in order to form films since it is more benign and less toxic when compared to HFIP. PC films were prepared by casting an 11% (w/v) solution of the PC in formic acid with 2% photo initiator (w/v) and crosslinking using 365 nm UV light. The crosslinked films were found to stable in water as well as solvent systems such as 1 M LiCl in DMSO and 5% LiCl in DMAc. On the other hand, native chitin films (prepared using the protocol described in experimental section) and uncrosslinked PC films were found to be soluble in 1 M LiCl in DMSO and 5% LiCl in DMAc. From this result, it was concluded that the successful incorporation of acrylate moieties in the native chitin chain which are responsible for the crosslinking in the presence of UV light prevented the PC films from dissolving in the aforementioned solvent systems.

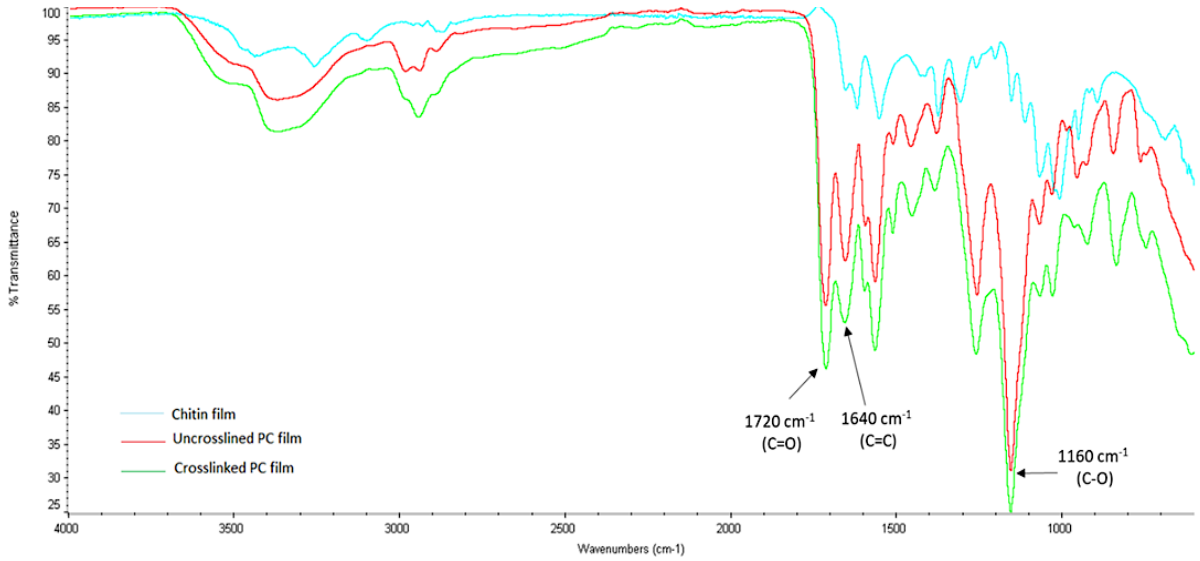

Figure 3.2 *FTIR analysis to confirm the conjugation of photoreactive groups on the chitin.*

The conjugation of the acrylate moiety on the chitin chain was further verified using FT-IR measurements. FT-IR spectra of chitin, uncrosslinked PC film and crosslinked PC film were taken and analyzed (**Figure 3.2**). The spectra of uncrosslinked PC film and crosslinked PC film showed peaks at 1720 cm^{-1}, which can be attributed to the methacrylate carbonyl group (C=O stretch) and vinyl group (C=C stretch which imparts photoreactivity) peaks at 1640 cm^{-1}, both of which are absent in the spectrum of native chitin. There is an increase in the peak intensity of C–O stretch at ~1160 cm^{-1} in PC films when compared to native chitin. On comparison of the uncrosslinked PC and crosslinked PC spectra, it was found that there is a decrease in intensity at 1640 cm^{-1} which can be attributed to the consumption of vinyl C=C groups upon crosslinking.

3.3.1.2 Determination of Degree of Deacetylation

The degree of deacetylation (DD), which determines the content of free amino groups in the polysaccharides is used to differentiate between chitin and chitosan, as well as determine the

chemical nature of the photochitin synthesized. Typically, chitin with a high degree of deacetylation is classified as chitosan. A common concern during the chemical processing and modification of chitin is that during the process it might undergo deacetylation and convert into chitosan. Hence, it is important to check the DD of PC. Various methods have been proposed for the determination of the DD. Several methods are tedious and expensive (e.g., NMR) or destructive to the sample (ninhydrin test). Therefore, we used two analytical procedures for the DD determination – viz. infrared spectroscopy and UV-spectrophotometry for confirmation of the results.[13]

Determination of degree of deacetylation using infrared spectroscopy (IR)

The degree of deacetylation (DD) of the starting chitin, a commercially available chitosan as reference and the synthesized photocrosslinkable chitin (PC) were evaluated by FTIR using a technique proposed by Moore and Roberts. Baseline corrections were made using the improved method suggested by Sabnis and Block. Films of PC, chitin and chitosan were obtained using the protocols described above and dried to ensure no moisture. The ratio of the absorbance at 1655 cm^{-1} to that of the absorbance at 3450 cm^{-1} was recorded and the DD was established using the equation:

$DD = A_{1655}/A_{3450} \times 100/1.33$ [14]

The absorbance peak at 1655 cm^{-1} corresponding to the amide I band was used as the probe and the absorbance at 3450 cm^{-1} corresponding to the *hydroxyl* stretch was used as the reference band. The *hydroxyl* band was used as an internal reference for the correction of variables such as film thickness and concentration. The "1.33" in the equation is the ratio of A_{1655}/A_{3450} for fully acetylated chitosan. The DD of commercially available chitin (Alfa Aesar) and chitosan (Sigma

Aldrich) was evaluated using FTIR and compared with the values reported by the manufacturer in order to validate the results.

Table 3.1 *DD values comparison of commercial chitin and chitosan with PC using FT-IR analysis.*

Sample	Reported DD %	Calculated DD % (FTIR)
Chitin (Alfa Aesar)	20-30	27
Chitosan (Sigma- Aldrich)	75-85	74
PC	N/A	35

Determination of degree of deacetylation using infrared spectroscopy (IR)

This method uses First Derivative UV Spectrophotometric Analysis to obtain the DD. Initially, a standard curve was formed using solutions of N-acetyl glucosamine (GlcNAc) of concentrations 0, 10, 20, 30, 40 and 50 µg/ml were made in 0.85% phosphoric acid. A calibration curve was obtained using the first derivative UV values at 203 nm as a function of GlcNAc concentration. A linear regression fit to the data was obtained (**Figure 3.3**).

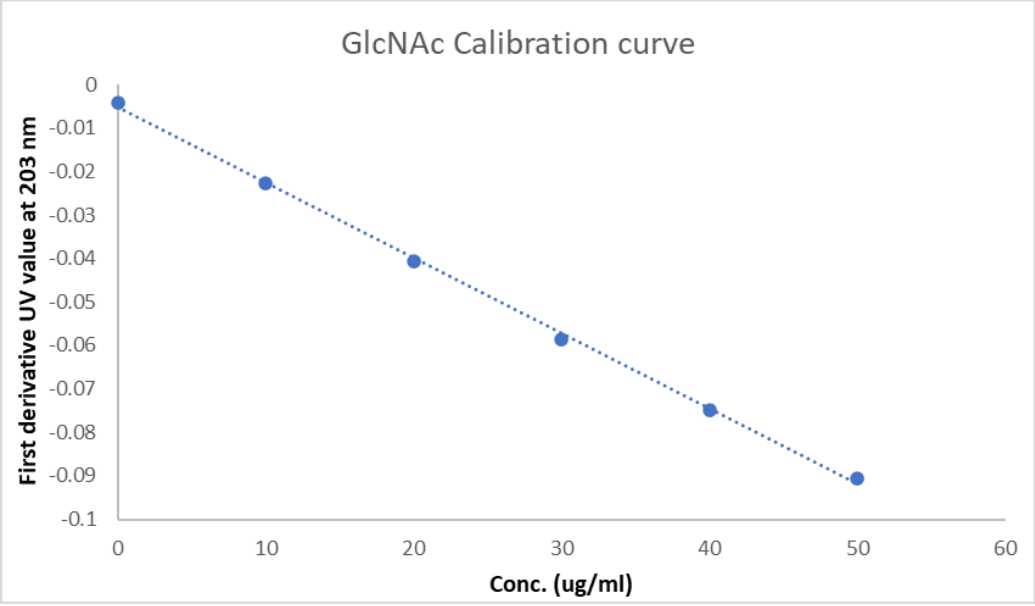

Figure 3.3 *Calibration curve of GlcNAc.*

Solutions in concentrated phosphoric acid at concentration 5 mg/ml was prepared by mixing chitin and photochitin (PC) in 85% phosphoric acid at 60 °C for 40 mins. The solution was then diluted 100 times using DI water and placed in the oven at 60 °C for 40 mins. The first derivative values at 203 nm of the samples were obtained. The amount of GlcNAc was determined using the calibration graph.

Table 3.2 *DD values comparison of commercial chitin and chitosan with PC obtained using infrared spectroscopy (IR)*

Sample	First derivative (203 nm)	Amount of GlcNAc (µg/ml)	Calculated DD %
Chitin (Alfa Aesar)	-0.076	41.59	21.9
Chitosan (Sigma- Aldrich)	-0.0245	11.29	82.2
PC	-0.0443	23.05	40.2

It was found that both methods give a very close estimate to each other as well as the validation from the manufacturer's data.

3.3.2 Fabrication and characterization of optically transparent, mechanically robust chitin films

Once the synthesis and characterization of PC to confirm the successful incorporation of methacrylate groups and the DD, the next steps focused on the formation of films using PC. There has been a great interest in the formation of thin and strong films of chitin, which is challenged by its general incompatibility with many solvents. However, in this work, the issue of solubility is addressed by converting chitin to LMW chitin, and further by converting it into a methacrylated derivative (PC). As mentioned in the previous section, films of PC were formed using formic acid which makes the entire process facile, benign and sustainable. The films are optically transparent

and mechanically robust, and can be formed with varying thicknesses by casting different concentrations of the PC in formic acid. The films were formed on substrates such as glass and silicon by spin-coating followed by UV crosslinking.

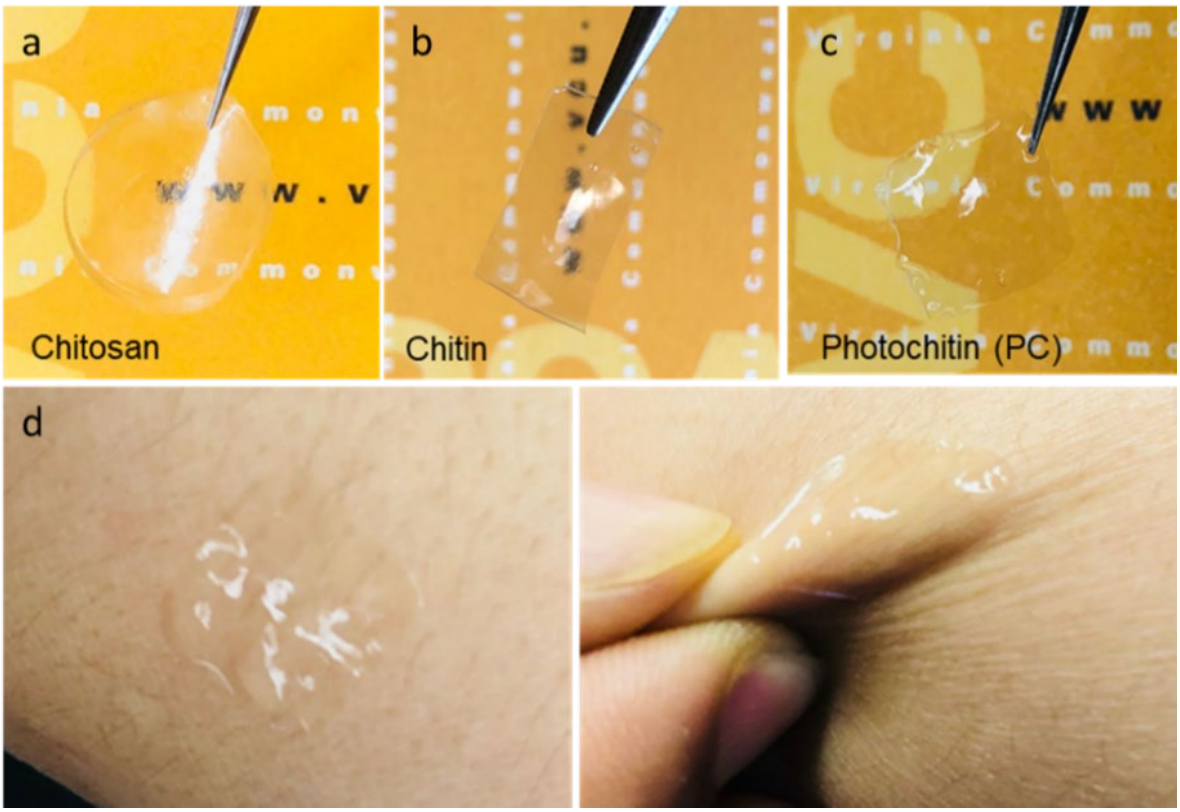

Figure 3.4 *Mechanically robust and flexible films ~60 mm thickness. a) pure chitosan, b) pure chitin, c) photochitin films, all prepared using the same solvent (formic acid). All these films can be easily handled and are optically transparent (photochitin forms the clearest films). d) At ~10–20 nm in thickness can conform to soft interfaces such as skin, where they can be mechanically deformed without breaking.*

Initial attempts at forming freestanding films of PC were hindered because of the structural characteristics of chitin. It was observed that films of 100% PC were brittle when dry, but malleable when fully hydrated. This issue was resolved by the addition of a minute amount (0.1%)

of polyethylene glycol diacrylate (PEG-DA) to the PC/formic acid solution. It was found that addition of PEG-DA enhances the mechanical properties of the films, even when dry. Additionally, the films could be peeled from the substrates to be free-standing. These films can be easily held and bent without any damage. At each point, films of native chitin and chitosan were also prepared for the purpose of comparison of properties. Upon visual inspection, pure chitin and chitosan films are somewhat cloudy whereas the PC films were optically transparent (**Figure 3.4 a, b and c**). Thin films ~10–20 mm thick can be formed that are conformable on dynamic surfaces (e.g., skin) without tearing (**Figure 3.4 d**).

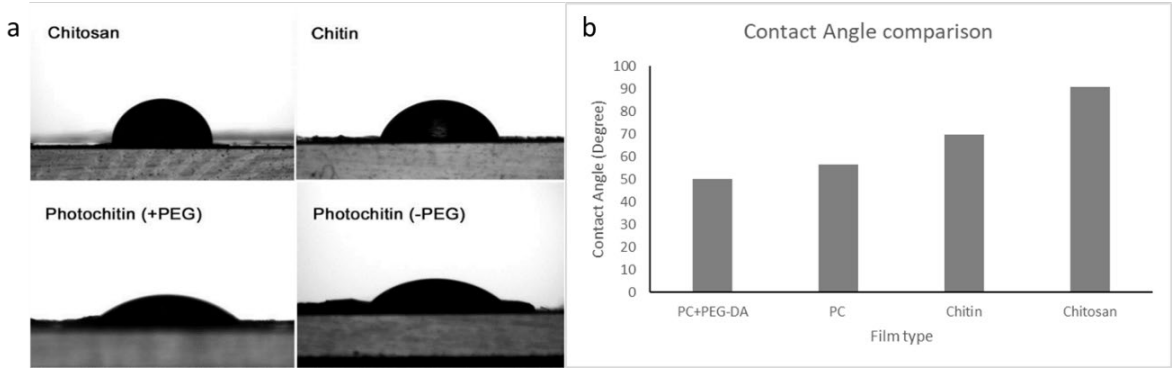

Figure 3.5 *a) Contact angle measurements showing droplet on top: chitosan and chitin films. Bottom: photochitin (with 0.1% PEG-DA) films and photochitin (with no PEG-DA), (b) comparison of contact angles of chitin, chitosan and PC with and without PEG-DA.*

Contact angles of photochitin, chitin and chitosan films were measured using a Rame´-Hart contact angle goniometer by placing a 5 mL drop of DI water on the films. The advancing contact angle of chitin and chitosan were measured to be around 68.9^{O} and 90.6^{O} respectively which is similar to the values reported in literature.[234-236] Interestingly, the contact angle of photochitin films were measured to be 56.3^{O} which is hydrophilic in comparison to chitin and chitosan films, and

hence showing better surface wettability. On addition of a small amount (0.1%) PEG to improve mechanical stability, the contact angle is even more hydrophilic at 49.9^{O}. The slight increase in the surface wettability was attributed to the addition of PEG in the composite. In order to compare their mechanical properties, tensile strength of the PC, chitin and chitosan films, all prepared using a common solvent – formic acid, was tested. The use of a common solvent for the preparation of films allows easy comparison since the properties of chitin and chitosan films are known to be dependent on the preparation conditions and solvents. The experiment was performed using a 50 N load cell by applying a strain rate of 0.1 mm s^{-1}. The tensile strengths of chitin films were found to be ~66 MPa which is similar to earlier reports. The tensile strength of PC films (with 0.1% PEG-DA) was measured to be ~90 MPa which indicates that the crosslinking induces a strength higher than the pure chitin films. As a comparison, both films were tested against chitosan and it was found that both photochitin and pure chitin films showed a lower tensile strength and elongation in comparison, which can be attributed to their higher structural rigidity.[237]

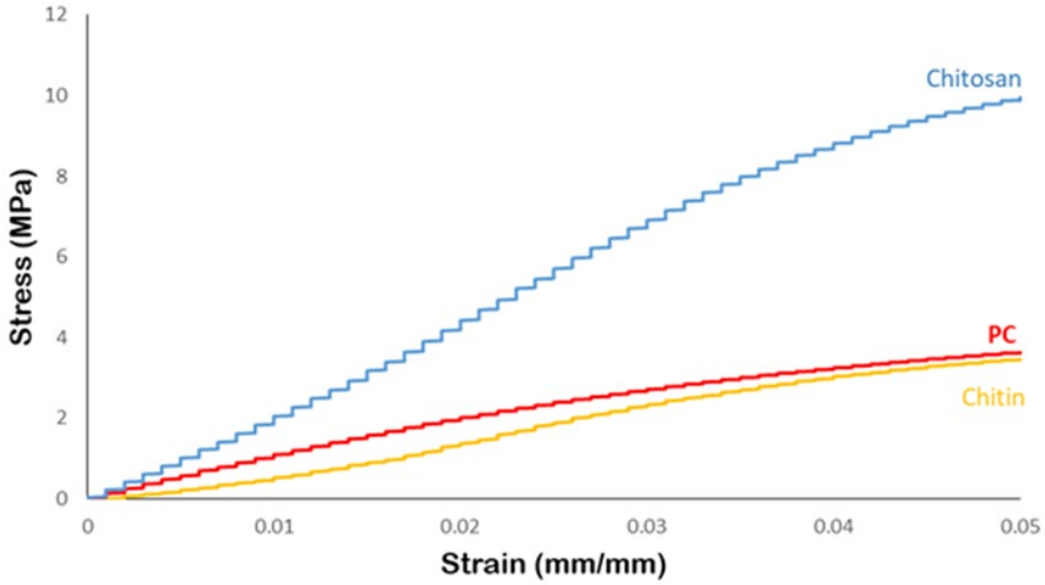

Figure 3.6 *Tensile testing of the films shows that photochitin films are of comparable, if slightly higher strength than films of pure chitin.*

3.3.3 Micropatterning of photochitin to form high resolution structures

The chemical modification of chitin using photoreactive moieties to form photocrosslinkable chitin provides a versatile biomaterial that can be micropatterned using photolithography, wherein the material acts as a "negative photoresist" crosslinked in the presence of UV light. The removal of uncrosslinked regions were achieved in the development process wherein the patterns were immersed 1M LiCl/DMSO (developing solution) followed by rigorous washing using DI water. Initially, trials were made on forming PC patterns on rigid silicon substrates using photolithography. Prior to the lithography process, the silicon substrates were functionalized with TPM in order to facilitate the attachment of PC structures to the substrate via covalent linkage. The process of micropatterning high resolution structures of PC on silicon initially required significant optimization of multiple parameters such as spin coating parameters, UV-exposure time and development time. The spin coating parameters were narrowed down to 800 rpm, 40 seconds and 30 rpm/sec ramp up. Similarly, the optimum UV exposure and development time was found to be 0.8 seconds and ~2 hours respectively.

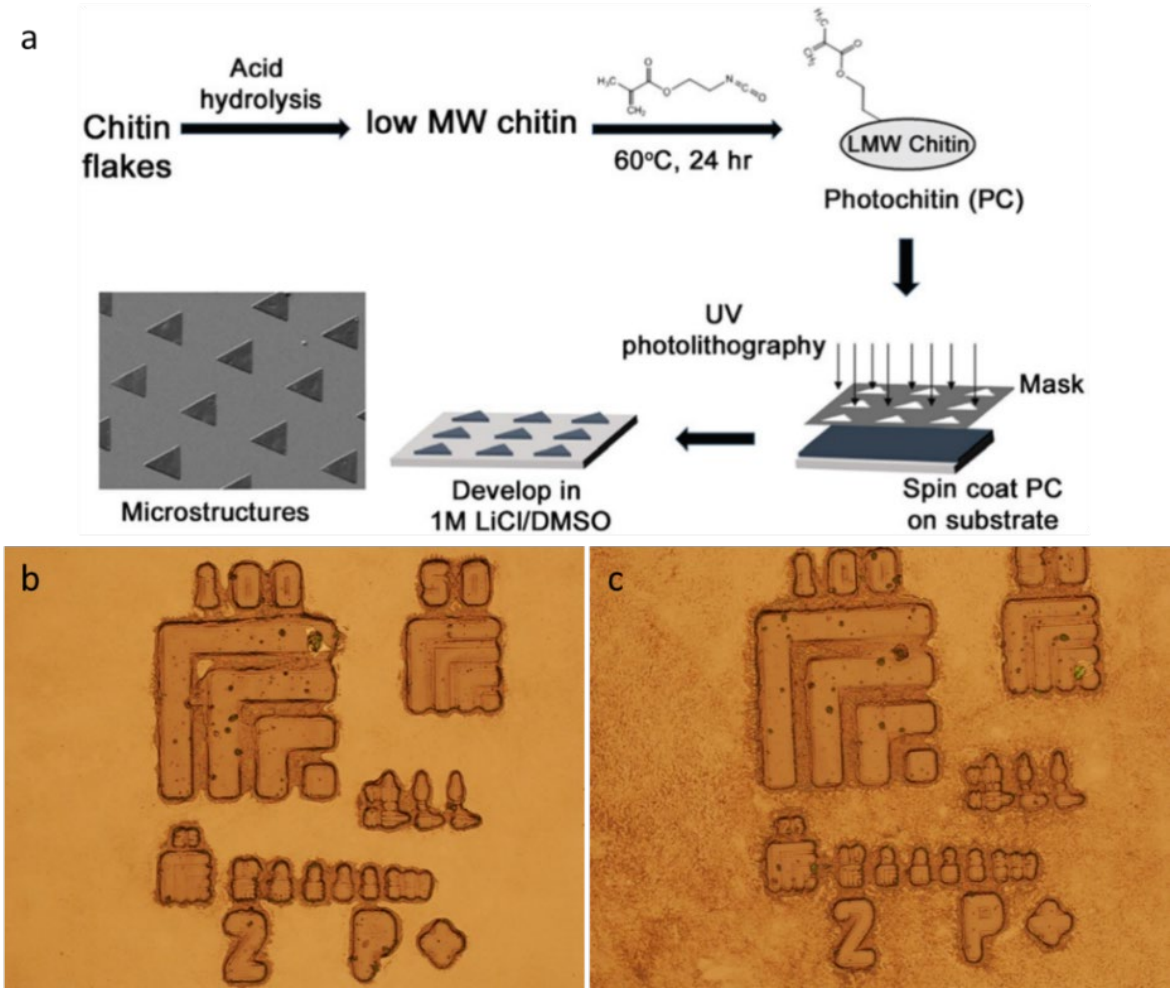

Figure 3.7 *a) Schematic showing the fabrication of microstructures of chitin. Improper formation of micropatterns due to b) over exposure of PC and c) insufficient development time.*

Following the successful optimization of the photolithography process, precise microarchitectures ranging from 10–100 mm could be easily formed on silicon and glass substrates. The scalability of photolithography allows the easy fabrication of microstructural topology over large areas (several cm), which is difficult using molding or imprinting. SEM imaging was used to characterize surface morphology and fidelity of architectures formed. Expanded views of the topography show the surface at the microscale and the ability to form features of controllable height. Various patterns of different geometry can be easily formed using different photomasks

(**Figure 3.8a and b**). More importantly, microstructures can also be fabricated on flexible films in order to form micropatterned chitin sheets using the photolithography technique developed in this work. This could be achieved due to the solubility of PC in two different solvents, i.e., formic acid and HFIP, similar to silk fibroin reported in Chapter 2. Following the fabrication of PC sheeting by casting PC/ formic acid solution on a substrate and crosslinking, a second layer of PC/ HFIP solution was casted on the first and exposed to UV light through a photomask. After developing in 1M LiCl/ DMSO solution, micropatterned PC sheets were obtained (**Figure 3.8 c–e**). Owing to the chemical crosslinking between the patterns and the underlying film, these features do not delaminate on mechanical flexure, which is not possible with pure chitin or with micromolding. As above, virtually any kinds of microscale patterns can be formed by simply changing the photomasks.

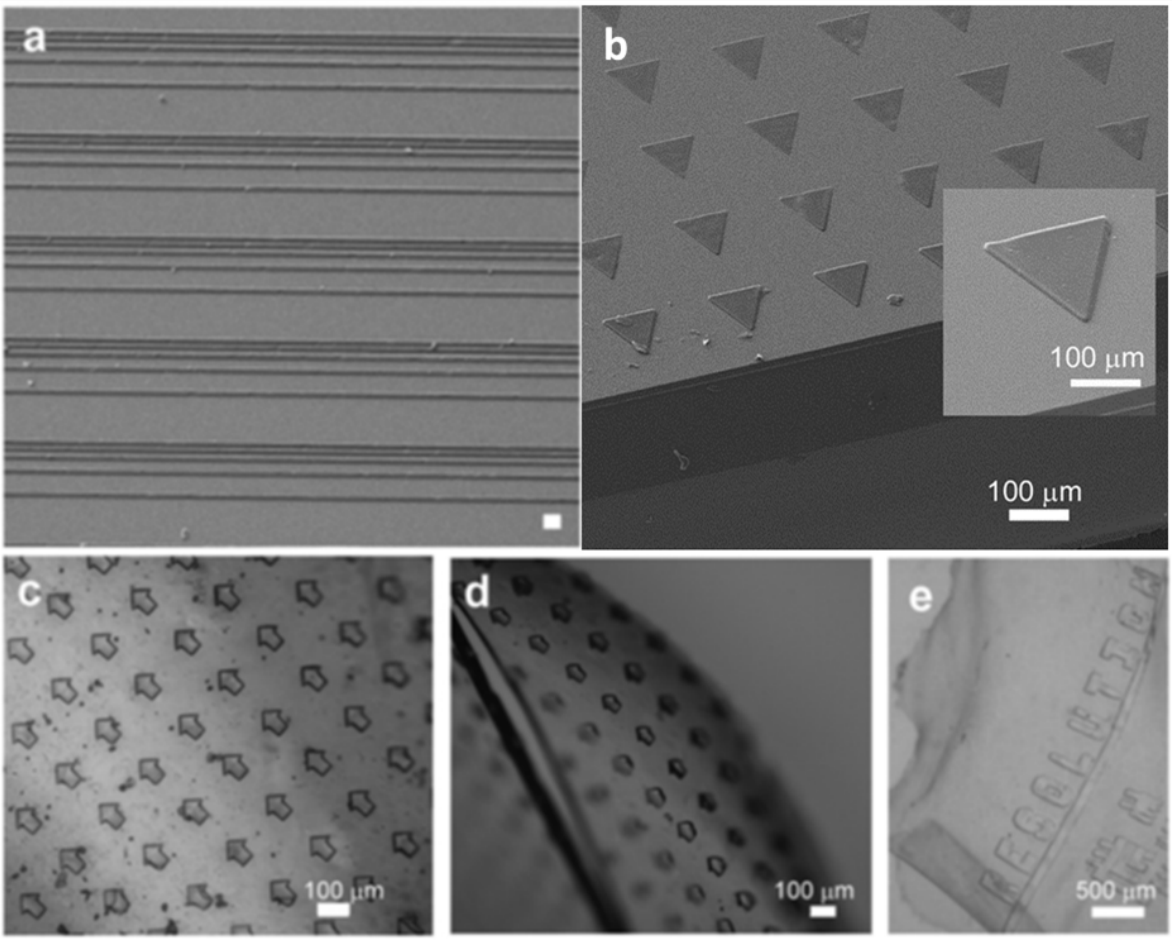

Figure 3.8 *Images of the microstructures of chitin formed using photolithography (a) and (b) SEM images of high-resolution structures (scale bars =100 mm) formed on glass substrates. (c) and (d) The patterns (50 mm arrows) can also be formed directly on chitin sheets, leading to flexible micropatterned sheets as seen in (e) with 100 mm letters spelling out the word ‘‘Resolution’’.*

3.4 CONCLUSION

The work presented in this chapter demonstrates the synthesis and application of a novel photocrosslinkable derivative of chitin which can be photopatterned into 2D and 3D structures. Optically transparent and mechanically robust films can be easily formed using a benign solvent. Further, high-resolution microstructures can be patterned on rigid substrates such as glass or

silicon, as well as form flexible micropatterned sheets. This biomaterial can form functional components of tissue scaffolds or bioelectronics that can be fully degraded. As an abundantly available renewable resource and byproduct of the food-processing industry, large quantities of this chitin are produced annually. Thus, through the work described in this chapter, new avenues for its use in biomedical applications and bioelectronics can be envisioned from this material.

Chitin is biodegradable owing to the action of chitinase enzymes that are widely found in nature.[98] Numerous species of microbe such as bacterial, fungi and actinomycetes present in soil contain chitinase enzyme for the degradation of chitin.[238] Human gastric juices contain chitinase that can degrade chitin.[239] However, studies have shown that the rate of degradation of chitin inside physiological environments is very slow which possess the problem of long term reservation of chitin in the body.[240] Taking this into consideration along with the difficulties associated with processing chitin, photoactive silk proteins were selected over photoactive chitin for the fabrication of devices in the subsequent chapters.

[This chapter contains results that have been previously published: Sayantan Pradhan, Kathryn M. Moore, Kristy M. Ainslie, Vamsi K. Yadavalli, "Flexible, microstructured surfaces using chitin-derived biopolymers", J. Mater. Chem. B, 2019,7, 5328-5335.]

CHAPTER 4

IMPARTING CONDUCTIVITY TO INHERENTLY NON-CONDUCTIVE BIOPOLYMERS

4.1 INTRODUCTIOIN

Chapter 2 and 3 explores the development of a platform that allows the photolithographic micropatterning of natural biopolymers such as silk proteins and chitin. This is a crucial towards the realization of functional biodevices using such versatile natural materials. Various components such as electrodes, transducer and other circuit elements of biosensors and bioelectronics (in a broader term) can be easily fabricated using these materials on wide range of rigid and flexible substrates, conferring biocompatibility and degradability. However, to extend their application beyond "passive" substrate materials to active functional components in bioelectronic devices, it is important to imbue them with electrochemical properties. This chapter focuses on the development of biomaterial based conductive inks that allow their application as electroactive components in fully organic, flexible biodevices.

To date, a wide variety of organic and inorganic conductive fillers such as carbon-based materials, metal-based materials, and conducting polymers, have been extensively investigated for flexible conductive composites.[5, 241] Ability to impart intrinsic conductivity has been investigated in

both synthetic and nature derived polymers. Although metals provide excellent conductive properties, there are numerous disadvantages associated with the use of metals. For example, the oxidation of metals is linked to low long-term stability.[242] Metals have also been often known to cause reactions *in vivo* and cannot be contacted with wounds.[243-245] Moreover, deposition and patterning of metals is achieved via high temperature processes involving harsh chemical which can damage natural biopolymers. Carbon based materials such as carbon nanotubes (CNTs) and graphene offer good electrical conductivity along with superior chemical stability, and facile functionalization.[246-249] However, their hydrophobic nature makes it difficult to disperse them efficiently within hydrophilic natural biopolymers.[242]

In comparison, conducting polymers are an excellent alternative due to their intrinsic conductivity and flexibility. Their polymeric nature allows them to be easily coupled with biopolymers and reduces the chance of materials mismatch which is often encountered with metals.[250] They are highly compatible with biopolymers in terms of processability. A number of conducting polymers such as poly(3,4-ethylenedioxythiophene): polystyrene sulfonate (PEDOT:PSS), polypyrrole (PPy), and polyaniline (PANI) have been have been integrated with biopolymers.[5, 45] Biopolymers can help overcome the brittle nature of conducting polymers.[12, 251] These biocompatible conductive composites have been used in a host of biomedical application especially in biodevices for continuous monitoring of human bioinformation.[252] Although numerous commercially developed strategies have been adopted for patterning conductive polymers on biomaterials (screen printing, inkjet printing and stamping), they often demonstrate poor adhesion and stability, causing the patterns to come off during mechanical deformation.[103, 253] In this chapter, the confluence of conducting polymers with biopolymers (viz silk fibroin and sericin proteins) is explored. Moreover, the photocrosslinkable nature of the biopolymers

discussed in previous chapters provide a stable matrix in which the conducting polymers are dispersed while providing patternability using photolithography. In return, the conducting polymers impart electrochemical properties to these biopolymers thus making them suitable for functional device applications.

Alternatively, nature also provide numerous conducting materials that can be coupled with biopolymers to impart electronic activity.[5, 45] Ever since the discovery of eumelanin as a naturally occurring amorphous semiconductor, there has been an interest in eumelanin based organic electronics. Numerous studies have attempted at understanding the conduction mechanism of eumelanin along with its unique physical structure, photoprotective, or antioxidant properties. Additionally, studies have shown that the hydration state of eumelanin has significant effect on its electrical properties. Various melanin-based devices, such as sensors [54]–[56], energy storage devices [18], [57], [58] and OECTs [59], have been reported. A part of the work done in this chapter is extended towards achieving fully nature derived conductive biocomposites by incorporating natural semiconductor melanin in the photofibroin matrix to form a photopatternable conductive ink.

4.2 EXPERIMENTAL

4.2.1 Synthesis of photofibroin and photosericin

Photofibroin and photosericin were prepared following the method described in Chapter 1.

4.2.2 Synthesis and patterning PEDOT:PSS- photosericin conductive ink

PEDOT:PSS dry pellets (Orgacon, Sigma-Aldrich, St. Louis, MO) were dispersed in DI water by sonicating the mixture for 20 minutes followed by ultrasonication for another 20 minutes. The

concentration of the PEDOT: PSS dispersion was 1% (w/v). The dispersion was then doped with 5% (v/v) DMSO in order to increase the conductivity of PEDOT: PSS. Finally, the PEDOT: PSS was mixed with photosericin in varying amounts to form a conductive ink composite with different percentages of PEDOT: PSS. Photoinitiator (Darocur 1173, BASF) was added to the conductive composite (0.2 µl/1 mg of photosericin) and mixed. In order to make patterns, the PEDOT: PSS-photosericin ink was spin coated either on TPM functionalized silicon or glass surfaces or on photofibroin films and air dried under a chemical fume hood. The samples were then exposed under 365 nm UV light (Lumen Dynamics OmniCure 1000 system) for 1 s at 20 mW cm^{-2}. The PEDOT: PSS-photosericin conductive patterns were developed in water to remove the uncrosslinked area.

4.2.3 Synthesis of PANI- photofibroin conductive sheets

A dispersion of polyaniline (PANI) emeraldine salt from p-toluenesulfonic acid (Alfa Aesar, Tewksbury, MA) in formic acid (Acros Organics, 98%) was by sonicating the mixture for 20 minutes followed by ultrasonication for another 20 minutes. The final concentration of the dispersion was maintained at 1% (w/v). The PANI in formic acid dispersion was mixed with photofibroin to make a PANI-photofibroin conductive ink with varying PANI concentration. In order to make PANI- photofibroin films, the composite was mixed with photoinitiator (Irgacure 2959, BASF) 0.6% (w/v) and casted on clean glass slides. Following air drying under a chemical fume hood, the films were crosslinked under 365 nm UV light for 3 s at 20 mW cm^{-2}. The samples were immersed in DI water in order to detach them from the glass slide to form freestanding PANI-photofibroin films.

4.2.4 Preparation of a eumelanin-photofibroin conductive composite

A conductive ink composite composed of photofibroin and eumelanin obtained from cuttlefish ink was prepared. Dry eumelanin powder (obtained from cuttlefish) was dispersed in formic acid (Acros Organics, 98%) by ultrasonicating the mixture for 40 min, resulting in a 1% (w/v) dispersion of eumelanin in formic acid (FA). Photofibroin was mixed with the eumelanin dispersion to form a composite solution. Varying compositions with 12%, 20% and 28% (w/w) of eumelanin blending with photofibroin were studied. A photoinitiator (2-Hydroxy-4'-(2-hydroxyethoxy)-2-methylpropiophenone) (2.5% (w/v) in the solution) was added to the composite. Films were fabricated by casting the solution of eumelanin and photofibroin with appropriate amounts of photo initiator, on clean glass slides (up to 1-inch x 1 inch). The composite was left to dry under ambient conditions (21^{o}C) for 30 mins and crosslinked under 365 nm UV lamp (Lumen Dynamics OmniCure 1000 system) for 3 seconds at 20 mW cm^{-1}. The films were immersed in DI water for ~24 hr to delaminate the films, and to wash off the excess photoinitiator.

4.2.5 Electrochemical characterization

The resistance of the composites was measured using a conventional four-point probe technique using an HP 4156B precision semiconductor parameter analyzer (Agilent Technologies). Cyclic voltammetry (CV), linear scanning voltammetry (LSV) and EIS measurements were performed using a Gamry Interface 1010E Potentiostat (Gamry Instruments, Warminster, PA). 0.1 M PBS Buffer (7.4 pH) was used as the electrolyte. A three- cell configuration consisting of Ag/AgCl as the reference electrode, platinum as the counter electrode, and as-prepared samples as the working electrode was used. Electrical connection to the working electrode was made using silver conducting epoxy or a water pasted carbon paste, and was subsequently scanned from −1.0 to 1.6

V at 100 mV/s. The charge storage capacity (CSC) of the samples were obtained from the area under the CV using OriginPro (Origin Lab). The impedance spectra of the working electrodes in the 0.1 M PBS buffer (7.4 pH) at a frequency range of 10^{-2}Hz to 10^{5}Hz with a 5 mV AC amplitude were obtained using the same three-cell setup.

4.2.6 Electrochemical characterization

Scanning electron microscopy (SEM) images of the conductive silk films and patterns were obtained using a Hitachi SU-FE-SEM to show the fidelity of the patterned structures. The patterns were sputter coated in a 20Å platinum Denton vacuum cold sputtering system (Moorestown NJ) before imaging. The optical images were recorded using a Nikon Eclipse microscope.

4.3 RESULTS AND DISCUSSION

4.3.1 Development of PEDOT: PSS- photosericin conductive ink composite

As discussed in Chapter 1, silk fiber comprises of two protein- the core hydrophobic fibroin, and a glue-like water soluble outer sericin. PEDOT: PSS cannot be dispersed in formic acid or HFIP, the solvents used to dissolve fibroin, they could not be combined together to form a conductive ink composite suitable for biodevice fabrications. Instead, the water-soluble counterpart, photosericin, was selected as the carrier protein which could serve as a stable matrix in which PEDOT: PSS is dispersed. Although PEDOT: PSS dispersion is commercially available (Baytron by Bayer AG, Clevios by Heraeus, and Orgacon by Agfa), a 1% (w/v) dispersion of PEDOT:PSS was prepared in house using ultrasonication. The PEDOT:PSS aqueous dispersion obtained homogenous and could be easily blended with photosericin to form a conductive ink composite. The photosericin helps to overcome the brittle nature of PEDOT:PSS films and improves stability.

Unlike most naturally occurring polymers, photoreactive sericin is soluble in water, which offers great processability when used with most of the biorecognition reagents such as enzymes and antibodies. 5% (v/v) DMSO was added into the composite since it improves conductivity of PEDOT:PSS by inducing better packing and reducing PSS content from the surface of the film.

4.3.1.1 Micropatterning of PEDOT: PSS- photosericin ink

The fabrication of microscale conductive architectures can be achieved via techniques such as inkjet printing, lithography or direct etching. As discussed in Chapter 1, photolithography is a well-developed, high throughput, and high-resolution microfabrication technique. The ink has extremely favorable performance metrics and can be patterned on both rigid and flexible substrates using sustainable process. To form conductive microarchitectures, the ink could be easily spin coated on TPM functionalized silicon or glass surfaces and exposed under the UV light though a photomask to form patterns of in a single step. Due silk sericin being water soluble in nature, the patterns could be immersed in water for development, wherein the area that was not cross-linked could be easily washed off, giving very clean, high resolution and high fidelity micropatterns (**Figure 4.1 a-c**). The design and complexity of the structures formed are restricted only by the nature of the photomasks, and thus user defined microcircuits can be fabricated over microscale to centimeter scale in a precise manner. The ink could also be spin coated on polymeric substrates such as photofibroin and methacrylate functionalized PDMS to flexible sheets with conductive microarchitectures, which is critical for the development of flexible and wearable biodevices. Due to the presence of chemical linkage, the micropatterns can withstand all kinds of mechanical deformations without any delamination or degradation in physio-chemical and electrical properties (**Figure 4.1d**). The entire fabrication process is carried out on a benchtop setup, making it

relatively low cost since no cleanroom facility is required. Hence, a green and sustainable microfabrication of organic bioelectronics could be envisioned in a rapid high throughput process using the approach developed here.

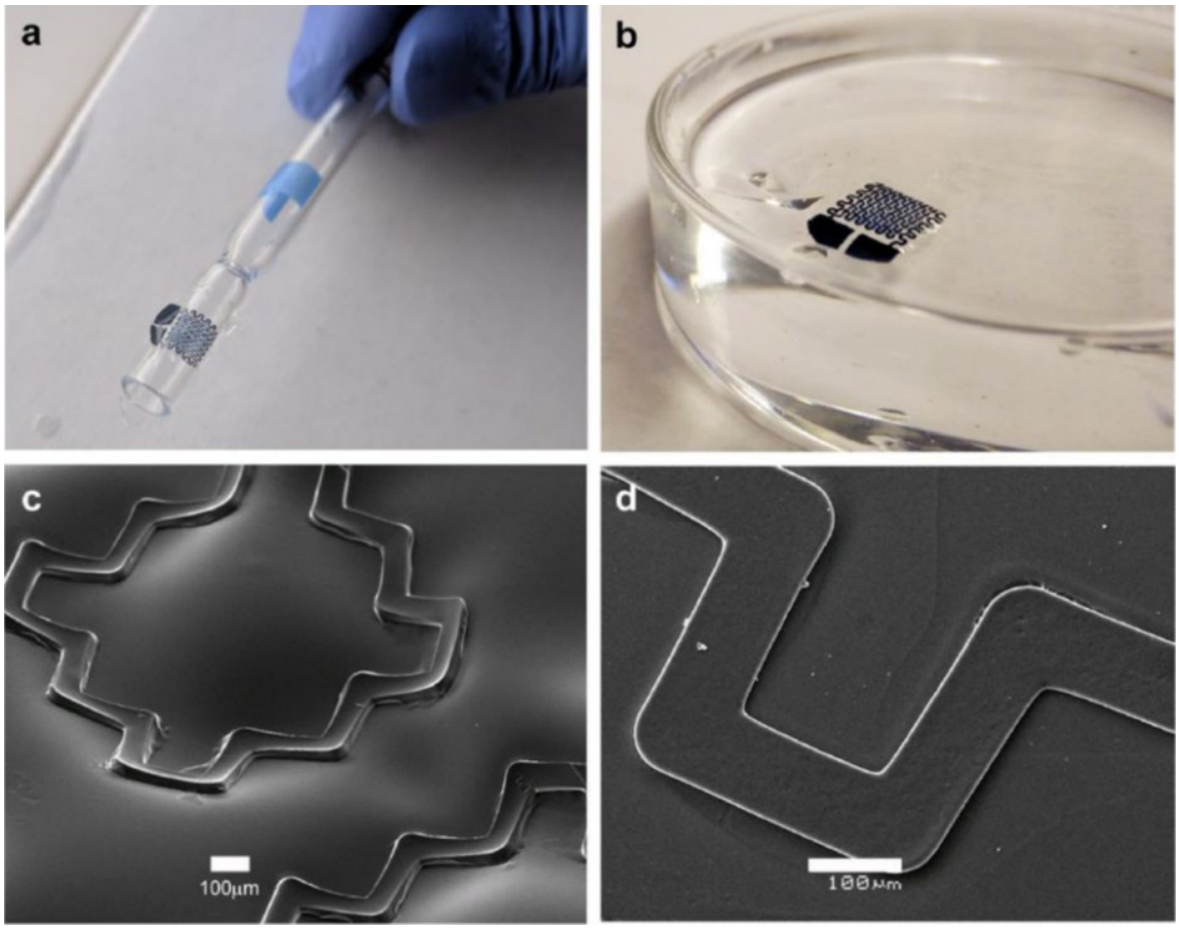

Figure 4.1 *PEDOT: PSS- photosericin patterns on flexible substrates. (a) Pattern flexibility, (b) water stability, (c) SEM image showing pattern fidelity, and (d) pattern adhesion to substrate. Scalebars = 100 µm.*

4.3.1.2 Electrochemical characterization of the conductive ink

Upon electrochemical characterization, the conductive ink composite was found to possess favorable performance metrics. The sheet resistance of the PEDOT:PSS-photosericin was

measured using a 4-point probe. The conductivity of the ink was found to increase (resistivity drops) with the increasing concentration of PEDOT: PSS in the composite. The resistivity trend of the ink (Ω/sq.) is shown in **Figure 4.2a.** However, the ability to photopattern or form high fidelity architectures was lost at higher PEDOT: PSS concentration owing to lack of penetration of the UV light into the ink, causing an incomplete covalent crosslinking at the interface. Consequently, 28% PEDOT:PSS was chosen as an optimal concentration suitable for forming the circuits in biodevices and bioelectronics. This composition of conductive ink was investigated with cyclic voltammetry (CV) to understand electrochemical stability at an electrode-electrolyte interface at physiological pH. The CV showed a wide stable potential window of −1.0 to 1.6 V in PBS buffer (0.1 M, 7.4 pH) without any significant water splitting peaks (**Figure 4.2b**). This indicates its stability and potential usefulness for detecting biomolecules at different oxidation or reduction potentials.

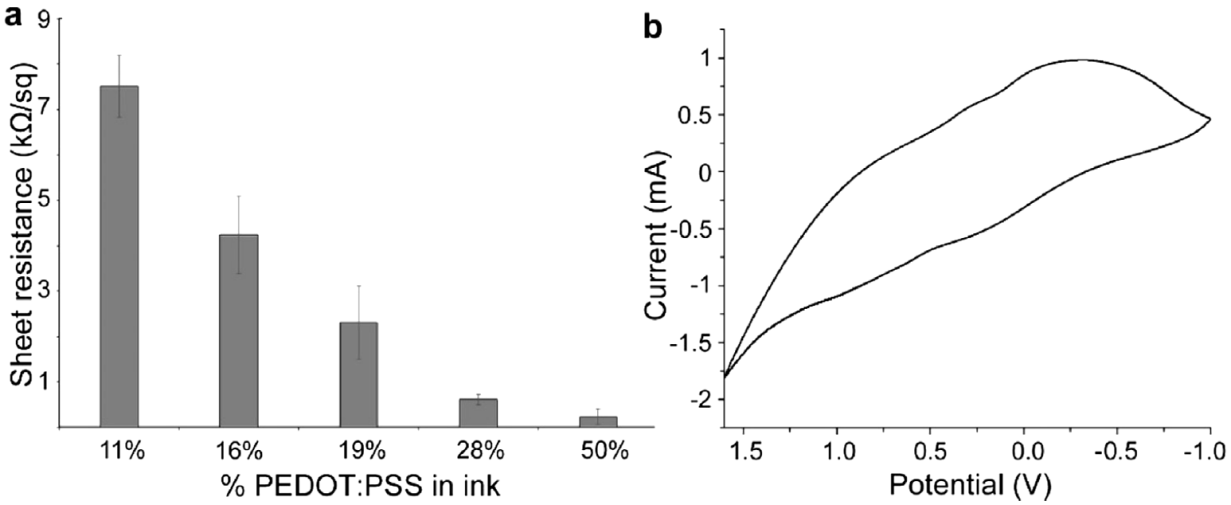

Figure 4.2 *Electrochemical characterization in PBS (7.4 pH). (a) measurement of the sheet resistance/conductivity of the conducting ink at varying concentrations of the conducting polymer (b) CV at 0.1 V/s scan rate for the 28% ink used in the electrodes.*

4.3.2 Development of PANI- photofibroin conductive ink composite

PANI is a widely used polymer among conductive families, with unique properties such as high thermal, electrical, and environmental/chemical stability, as well as reasonable cost. However, one of the major drawbacks of PANI is that it is relatively harder to process in comparison to other well-known conducting polymers. This can be attributed to its rigid backbone, which is related to its high level of conjugation. Initial attempts were made for the synthesis of an aqueous dispersion of PANI using ultrasonication technique which was not successful. However, on subsequent investigation, it was found that PANI could be easily dispersed in formic acid via ultrasonication. This was found to be highly advantageous since formic acid is also used to solubilize photofibroin. Therefore, by mixing photofibroin in the PANI-formic acid dispersion, a PANI- photofibroin conductive ink composite was formed. The dispersion of PANI in formic acid was favorable since doping PANI with acids increases its conductivity.

Conductive PANI-photofibroin sheets were fabricated by casting the conducting ink on clean glass slides and air drying under the chemical hood. This was followed by UV crosslinking. Similar to that of PEDOT: PSS-photosericin composite, it was found the higher concentration of PANI in the composite affected the UV crosslinkability of the films. Hence, 28% PANI in the composite was selected as the optimum concentration. The crosslinked PANI-photofibroin films could be easily detached from the underlying substrate by immersing them in water to form mechanically robust and flexible freestanding films (**Figure 4.3a**). CVs of 28% PANI-photofibroin composite were taken in the range of -1V to 1V at a scan rate of 100 mV/seconds in 7.4 pH PBS buffer. Similar to PEDOT: PSS-sericin composite, a stable CV was obtained with any water splitting peaks. This demonstrates its usefulness in the realization of electrochemical devices for the biological milieu.

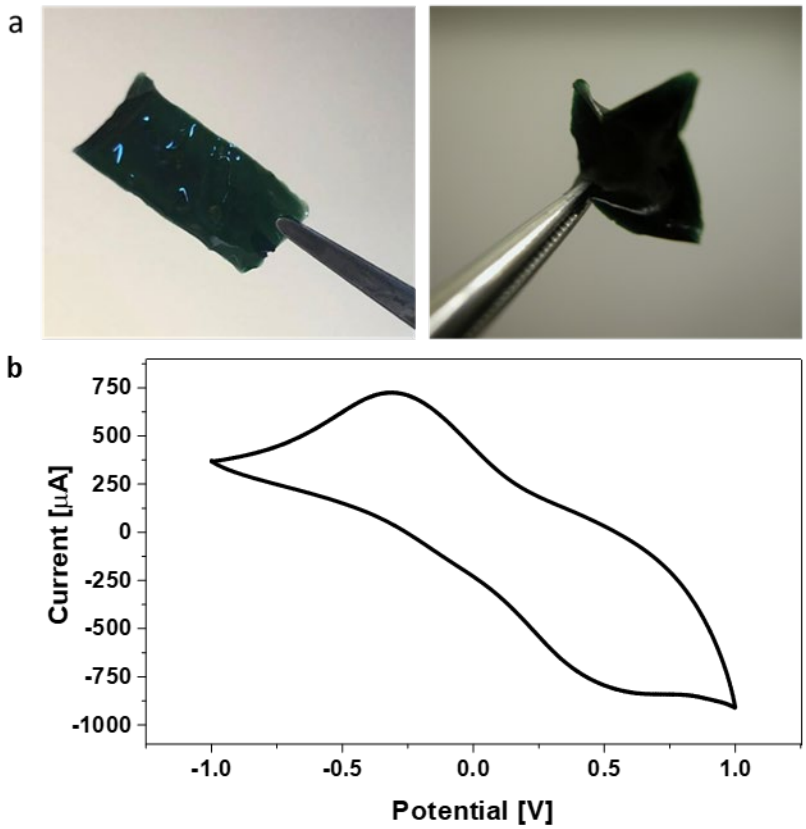

Figure 4.3 *Electrically conducting films of PANI-photofibroin a) mechanically robust and flexible freestanding films and b) CV at 0.1 V/s scan rate for the 28% ink.*

4.3.3 Development of eumelanin- photofibroin conductive ink composite

The ability to form mechanically strong, flexible films and coatings, which are stable in physiological environments using eumelanin, is crucial for the realization of new electroactive applications on tissue engineering and regenerative medicine. Combining eumelanin with fibroin renders electrochemical properties to silk fibroin, while imparting photopatternability to eumelanin. In this work, the combination of eumelanin with the photofibroin is aimed at enhancing the versatility of patterns while rendering it compatible with photolithographic techniques. While eumelanins are insoluble in most organic solvents which hinders their easy processing [45], 1% (w/v) dispersion of eumelanin could be obtained in formic acid by ultrasonication. Thus, a

composite of the two materials could be formed, while varying their relative concentrations.

Films of varying thickness (typical thickness ~ 50 μm) were formed by casting or spin coating the photofibroin/eumelanin composite on clean glass slides followed by exposure to 365 nm UV light. The resulting freestanding films are easily detached from the support on water immersion and are mechanically robust (**Figure 4.4a**). Tensile testing on the films showed that the addition of eumelanin improves the strength of the fibroin films (12 % eumelanin – 28.4 ± 10.2 MPa in comparison to 21.4 ± 5.9 MPa for fibroin films without any eumelanin) (**Figure 4.4b**). Moreover, that the values of tensile strength of regenerated silk fibroin (rSF) are in the same order of the values reported in the literature – from 4 MPa to 30 MPa, depending on the preparation and measurement conditions [46],[47]. This comparison is to show that the photofibroin (PF) films formed by crosslinking do not different substantially from rSF. However, the addition of more eumelanin causes the films to become weaker (28 % eumelanin – 12.1 ± 1 MPa). Importantly, even at this concentration, the films are very robust and can easily be handled without breakage.

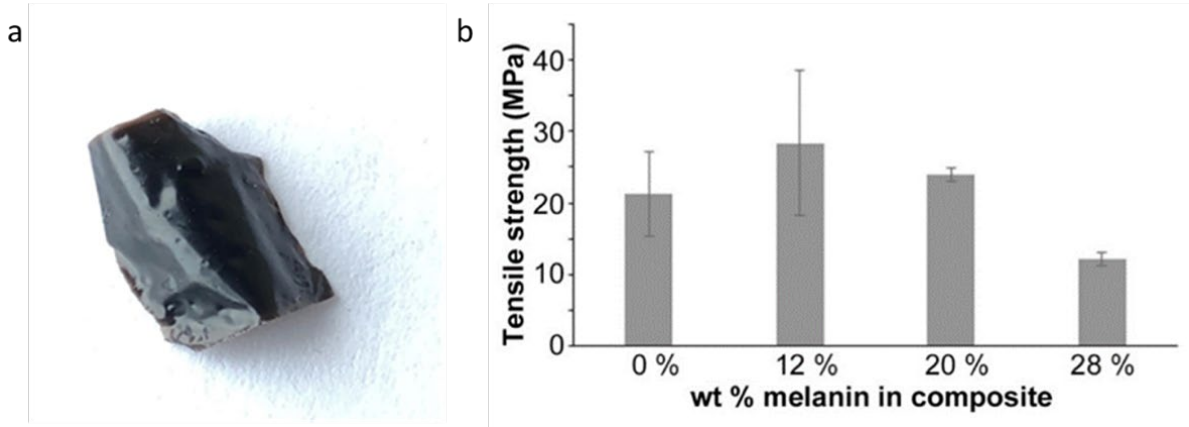

Figure 4.4 *a) Free standing films of crosslinked eumelanin-photofibroin. Films are mechanically robust and flexible. b) Tensile testing of the films of fibroin/eumelanin biocomposite as a function of the % of eumelanin in the film*

4.3.3.1 Micropatterning of eumelanin-photofibroin ink via photolithography

Patterns of eumelanin-photofibroin on glass, ITO glass or silicon substrates were fabricated via photolithography (**Figure 4.5**). The photoreactive fibroin in the composite behaves as a "negative photoresist", providing a stable and biocompatible matrix for entrapping the eumelanin. The fibroin/eumelanin composite solution was spin coated on the functionalized surface and photo-crosslinked through a photomask to form microstructures. Patterns were developed in 1M LiCl/DMSO, wherein the uncrosslinked fibroin/eumelanin dissolved in the developing solution. Upon exposure to UV light, the methacrylate moieties from photofibroin in the composite form covalent bonds with the pendant acrylate groups on the functionalized surface. This chemical conjugation anchors the patterns onto the substrate, thus forming high fidelity structures that are stable in various solvents. Similarly, fibroin films with covalently attached fibroin/eumelanin patterns can be formed as seen in **Figure 4.6**. This implies that fibroin/eumelanin "circuits" can be formed on a variety of substrates including fibroin.

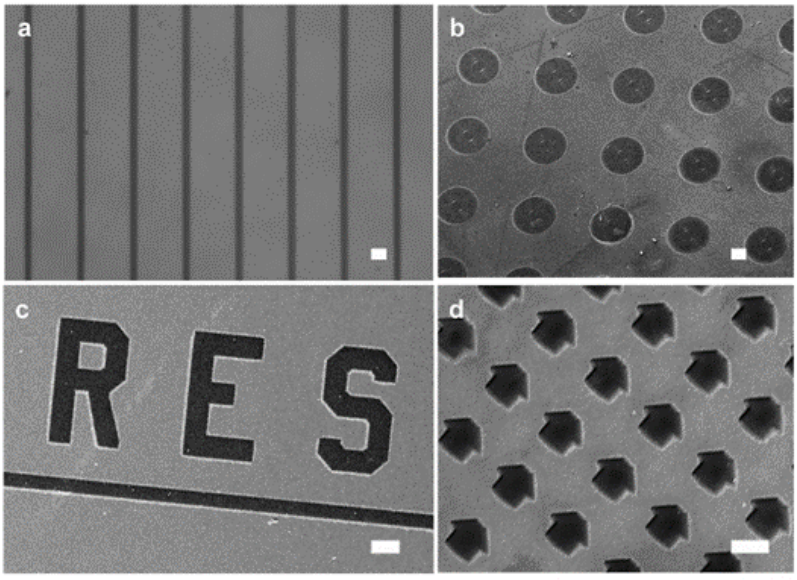

Figure 4.5 *High resolution micropatterning of the eumelanin-photofibroin composite. The composite solution was spin coated on a glass substrate to form various microscale patterns. Scale bar on all the panels = 100 μm.*

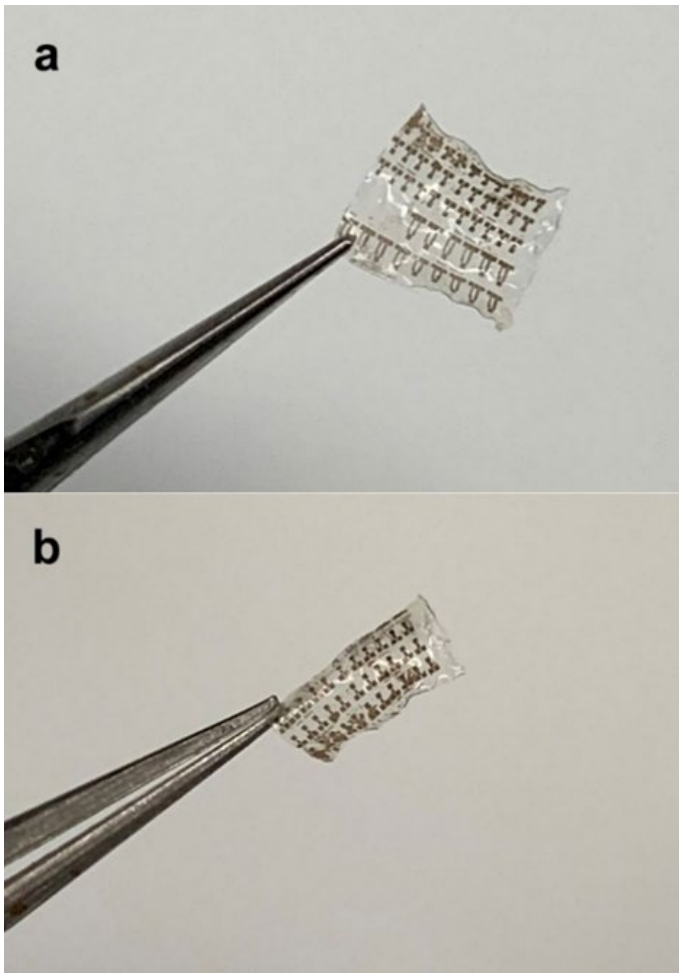

Figure 4.6 *High-resolution patterns of the eumelanin-photofibroin composite can be printed on flexible fibroin sheets resulting in (a) micropatterned films that (b) can be rolled.*

4.3.3.2 Electrochemical characterization of eumelanin-photofibroin composite

Most electrochemical studies have been performed using melanin in ITO/glass, carbon paper or silicon as the substrate. Here, eumelanin-photofibroin electrodes were fabricated on functionalized ITO/glass. Electrochemical characterization of the composite at different compositions was performed using cyclic voltammetry (CV) and electrochemical impedance spectroscopy (EIS). A scan was performed over a wide potential window of -1.0 to 1.6V at a scan rate of 100 mV/sec with varying eumelanin concentrations (**Figure 4.7a)**. A stable CV was obtained with each

composition without any water splitting. The electroactivity and electrochemical stabilities of the eumelanin composites were characterized in terms of charge storage capacity (CSC). The electroactivity of the composite increases with an increase in the concentration of eumelanin (**Figure 4.7b)**. The electrodes with 28% eumelanin (w/w) composite showed a CSC of ~0.3 mC/cm^2. This is comparable to the values reported in literature, where the CSC values of pure eumelanin was found to be 1.8 to 2.8 mC/cm^2 in acidic medium [58]. The electroactivity of eumelanin is affected when blended with fibroin to form a composite. A comparison of the various CSC values of eumelanin reported in literature is presented in **Table 4.1.** Although the CSC values of eumelanin-photofibroin composite is comparable with those reported in literature, it is significantly lower than other silk protein based conducting composites such as PEDOT: PSS-photosericin (~74 mC/cm^2).[103] The stability of eumelanin on ITO substrate is a major concern while performing electrochemical experiments [57]. The presence of fibroin in the composite chemically adhered the film onto the ITO surface, which prevented the film from delaminating. This increased the stability of the entire system. The 28% eumelanin incorporated in fibroin composite was able to retain ~90% of its electroactivity even after 7 days of soaking in PBS. The material was able to retain ~83% of its electroactivity after 100 redox cycles (**Figure 4.7c**).

Table 4.1 *Comparison of the electrochemical properties of the eumelanin composites.*

System	CV range	Scan Rate	CSC	Ref
Eumelanin on carbon paper	-0.4 – 0.4 V	5 mV/s	2.8 mC/ cm^2	[254]
Eumelanin on carbon paper	-0.35 – 0.3 V	5 mV/s	24 mAh/g	[255]
Eumelanin+ AgNW	-0.7 – 0.3 V	1 mV/s	49.3 mAh/g	[256]
Eumelanin-Na	-0.7 – 0.3 V	-	30.4 mAh/g	[257]

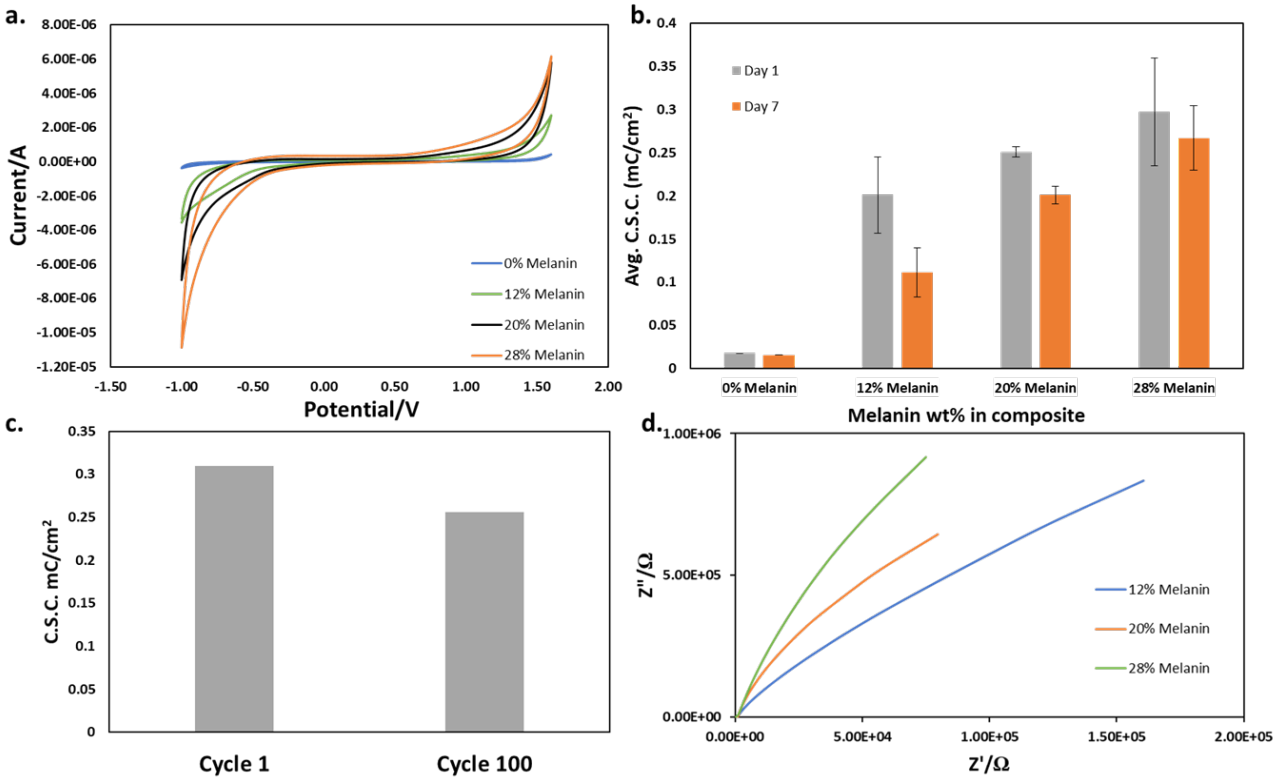

Figure 4.7 *Electrochemical characterization of the eumelanin-photofibroin biocomposite on ITO substrates. (a) Cyclic voltammetry with varying % eumelanin (w/w) in composite, (b) Charge storage capacity of composite over 1 week, (c) Effect of redox cycles on the electroactivity of fibroin/eumelanin composite using 28% of eumelanin, and (d) Nyquist plots for the composite. 0.1M PBS (7.4 pH) was used as the electrolyte.*

EIS spectra of varying eumelanin concentrations in silk fibroin/eumelanin composites was conducted. **Figure 4.7d** shows the Nyquist plots of 3 different electrode compositions. A simple Randles equivalent circuit with a parallel resistance and constant phase element connected in series with a resistance was constructed. The values from the fitting are presented in **Table 4.2.** The resistance of the solution is almost the same in each case, which implies the electrolyte imposes comparable resistance. There is no significant change in the double layer non-ideal capacitance of

the electrodes. This is a clear decrease in the charge transfer resistance from 108 MΩ to 23.05 MΩ upon increasing the concentration of the eumelanin in the composite (**Table 4.1)**.

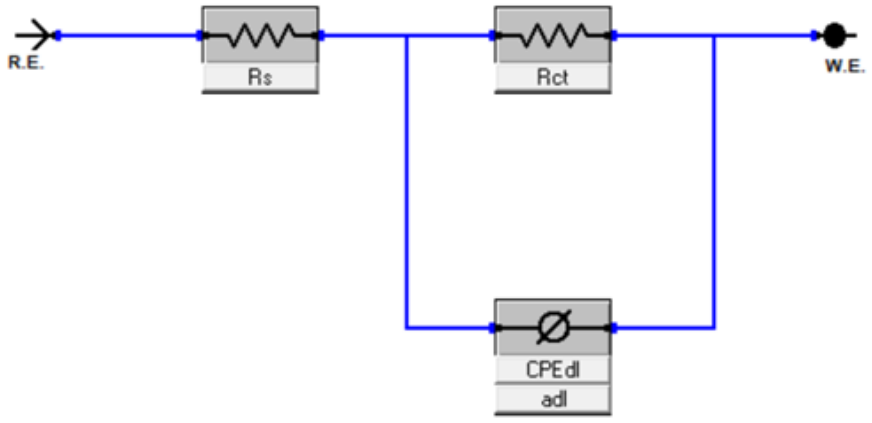

Figure 4.8 *A simple Randles equivalent circuit used for the EIS modelling eumelanin-photofibroin ink.*

Table 4.2 *Equivalent circuit model fit of the electrochemical impedance spectroscopy (EIS) data for varying compositions of the fibroin/eumelanin composite.*

% Eumelanin (w/w)	R_s (Ω)	R_{ct} (MΩ)	CPE_{dl} µF $s^{(a-1)}$	a_{dl}
12	234.3	108	3.27E-06	0.912
20	153.9	46.98	3.34E-06	0.963
28	254.6	23.05	1.41E-06	0.954

4.4 CONCLUSION

This chapter focuses on methods and materials that can be used to imbibe silk proteins- fibroin and sericin with electrochemical properties. A water based PEDOT: PSS dispersion was combined with photosericin whereas water insoluble photofibroin was combined with a dispersion of PANI in formic acid to form conductive ink composites. The silk proteins provide a stable matrix for the entrapment of conducting polymers PEDOT: PSS and PANI. Importantly, these biocomposite inks could be easily combined with simple photolithographic processes to form conducting

microstructures of various complexities which can allow their use as active functional components in organic electronics. Nature also provides a host of active materials. The other part of this work presents a natural electroactive biocomposite formed from silk fibroin (structural component) and eumelanin (electroactive component). This fibroin/eumelanin composites can be formed into films using the simple technique of spin-coating followed by UV crosslinking, and also patterned into microstructures via photolithography. The natural eumelanin-photofibroin composite films with improved mechanical properties and electroactivity could be used for active biomedical applications such as biosensing, theranostics, and regenerative medicine.

[This chapter contains results that have been previously published: Ramendra K. Pal, Sayantan Pradhan, Lokesh Narayanan, Vamsi K. Yadavalli, "Micropatterned conductive polymer biosensors on flexible PDMS films", Sens. Actuators B Chem., 2018, 259, 498-504.]

[This chapter contains results that have been previously published: Yun Hee Youn, Sayantan Pradhan, Lucília P. da Silva, Il Keun Kwon, Subhas C. Kundu, Rui L. Reis, Vamsi K. Yadavalli, Vitor M. Correlo, "Micropatterned Silk-Fibroin/Eumelanin Composite Films for Bioelectronic Applications", ACS Biomater. Sci. Eng. 2021, doi: 10.1021/acsbiomaterials.1c00216.]

CHAPTER 5

FULLY ORGANIC, FLEXIBLE BIOSENSORS FOR PHYSIOLOGICALLY RELEVANT CHEMICAL BIOMARKERS

5.1 INTRODUCTION

In previous chapters, various platforms were shown that facilitate the fabrication of silk protein microstructures photolithographically on a variety of rigid and flexible substrates. Subsequently, these proteins were combined with conducting polymers (PEDOT: PSS and PANI) and natural semi-conductors (eumelanin) to form conductive pathways and circuits that allows us to envision smart and adaptable systems such as wearable or implantable devices, electronic skin and tissue-integrated sensors. In order to demonstrate the utility of such platforms for the development of functional biodevices, this chapter focuses their use as active sensing elements in fully organic biosensors. Moreover, lower charge transfer resistance of these conductive composites can facilitate Faradaic processes suitable for biosensing applications.

A biosensor is a device capable of transforming signals generated at the biological interface into quantifiable analytical forms.[258] A typical biosensor consists of three primary components- a biorecognition element, a signal transducer element, and a signal processing element that processes the transduced signal into quantifiable forms.[259] Based on the types of signal relayed by the

transducer, some of the commonly used biosensors include electrochemical biosensors, optical biosensors, electronic biosensor, piezoelectric biosensor and magnetic biosensors.[260, 261] Among these, electrochemical biosensors are widely used due to their ability to directly convert biological events into electrical signals. However, the process of converting biological information into electrical signals is rather challenging due to the complexity of deploying an electronic device at the biological interface. Hence, there is a need to develop electrochemical sensing platforms that can be easily introduced at dynamic and soft biological environments for the detection of physiologically relevant chemical biomarkers.[262]

The design of successful biosensors requires them to be highly specific to target analytes with a response that is accurate, precise, reproducible and linear over the concentration range of interest.[259] Biosensors targeted for operating at the biological milieu should be small in dimension and biocompatible, without producing toxic or antigenic effects.[15] Finally, to be widely and effectively adopted, biosensors need to be conformable to the sensing surface and to accommodate changes in the surface shape (such as the human body), as well as be compatible with low cost, scalable microfabrication techniques.[263] They should also be free from electrical or other transducer induced noise.[264] State-of-the-art microfabrication techniques can reduce the size of electrochemical sensors which can increase the signal-to-noise ratio for processes designed to occur at the biological interface. While metals present high conductivity and low cost, they tend to be oxidized under ambient and especially, physiological conditions, and can possess a mechanical mismatch in terms of weight and modulus at soft tissue interfaces.[242, 265] They often have low biocompatibility, cytotoxicity, and could induce foreign body reaction.

The PEDOT: PSS- photosericin conductive ink described in Chapter 4 can provide viable and competitive alternative to metal, metal oxides and carbon-based materials as the active sensing

element in organic biosensors. Conducting polymers such as PEDOT: PSS have gained popularity at effective and sensitive transducer material for rapid real-time analysis of Faradaic events taking place at the biological environment due to their ability to transport electrons as well as ions.[266] The PEDOT: PSS – photosericin ink can be photolithographically patterns on a variety of rigid (glass, ITO, silicon) and flexible (silk fibroin, methacrylated PDMS) substrates which can effectively miniaturize biosensor devices. Additionally, the water processability of the PEDOT: PSS- photosericin conductive provides a stable and benign matrix in which specific biorecognition elements such as enzymes, antibodies, DNA, whole cells etc. can be easily immobilized.

The work demonstrated in this chapter shows how silk proteins in conjunction with conducting polymers can be used for the fabrication of functional fully organic, flexible, degradable biosensors. The PEDOT: PSS- photosericin composite was evaluated for its ability to detect electronically active and inactive chemical moieties in a flexible format. In the second part of the study, focuses on the development of an integrated biosensing platform that can be used in wearable or implantable biosensors.

5.2 EXPERIMENTAL

5.2.1 Synthesis of photofibroin and photosericin

Photofibroin and photosericin were prepared following the method described in Chapter 1.

5.2.2 Fabrication of fibroin substrates

The fibroin substrate was fabricated by dissolving 7.5% (w/v) of photoreactive fibroin in formic acid (Acros Organics 98%), and 2.5% (w/v) photo initiator (Irgacure 2959, BASF) was added to the fibroin solution. The solution was drop casted on clean glass slides and air dried for 15 to 20

minutes in order to evaporate the excess formic acid. The samples were exposed under a 365 nm UV lamp (Lumen Dynamics OmniCure 1000 system) for 1.5 seconds at 2000 mW cm^{-2} for cross-linking. To obtain free standing fibroin films, the samples were dipped in DI water which facilitated the delamination of the fibroin films from the glass.

5.2.3 Fabrication of conductive patterns on flexible substrates

1% (wt./vol.) dispersion of PEDOT: PSS (Orgacon™, Sigma-Aldrich, St. Louis, MO) in water was obtained through ultrasonication for 20 minutes. The PEDOT: PSS dispersion was filtered and 5% DMSO (v/v) was added to get the final stock solution. The basic conductive ink containing 2.5% (w/v) of photoreactive sericin, 1% (w/v) PEDOT: PSS, and 0.5% (v/v) of photoinitiator (Darocur 1173, Ciba Specialty Chemicals Inc., Basel, Switzerland) was then casted on the photofibroin substrates and air dried in the dark. Micropatterns were formed by exposure to UV light through a chrome photomask for 1.5 seconds. The patterns were developed in deionized water to obtain flexible bioelectronic components (**Figure 5.1**).

5.2.4. Sensing experiments

Chronoamperometry was used for the electrochemical sensing of the three analytes of interest - dopamine hydrochloride (DA), ascorbic acid (AA), and glucose. 10 mL of a stirred 0.1 M PBS buffer solution (7.4 pH) was used with a polarization potential of 0.3 V for DA and 0.6 V for AA and glucose. 0.01 M AA and DA solutions were prepared for the experiments. For glucose sensing, the PEDOT: PSS-photosericin ink was loaded with 200 U of glucose oxidase (*A. Niger*, Sigma-Aldrich). 0.5 mM of ferrocenyl methyl trimethyl ammonium iodide (Strem Chemicals, Newburyport, MA) was added to the buffer to shuttle electrons from the enzyme active site to the

conductive ink. Following stabilization of the background current, increasing amounts of the analyte was added to the stirred PBS solution to obtain I vs. t curves. Sensitivity was then calculated per ICH guidelines [33]. Sensitivity = $\frac{m}{A}$ µA/ µM.cm^2, where m = slope of the calibration curve (A/µM). The values were obtained from the regression analysis of calibration curves. A = area of sensor exposed to electrolyte (cm^2).

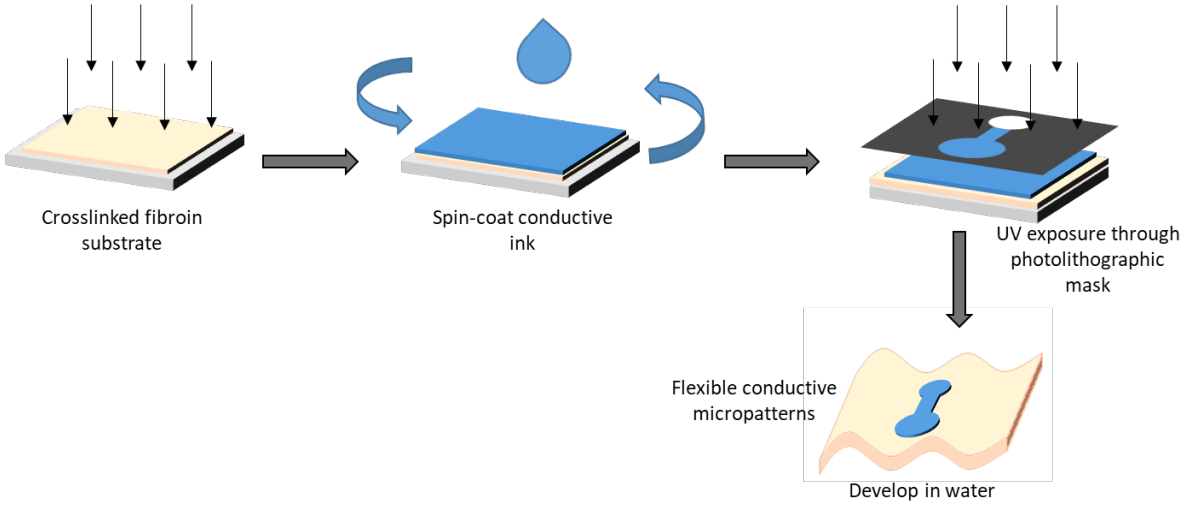

Figure 5.1 *Schematic showing the fabrication of flexible devices based on silk proteins.*

5.3 RESULTS AND DISCUSSION

5.3.1 Fabrication of a flexible biosensor based on silk proteins

Although bio-derived materials possess a variety of properties that enables their use as functional materials in bioelectronics, their electrically insulating natures have limited their use as active components.[5] The biocomposite conductive ink developed in Chapter 4 based on the photoreactive silk sericin and the conducting polymer PEDOT: PSS permits use as active sensing elements in flexible biosensors (**Figure 5.1).** Devices can be easily fabricated on flexible substrates such as methacrylate functionalized PDMS thin films and freestanding fibroin films. However, in

this work biosensors were fabricated on flexible fibroin films to form silk based fully organic devices that are inherently biocompatible and biodegradable in nature. This is crucial to the goal of this dissertation work, where entire device fabrication is envisioned through nature derived materials. The photoreactive sericin is functionalized with the same photo-active moieties as the fibroin so that it can be self-crosslinked as well as covalently bound to fibroin substrates under UV light, thereby producing properly patterned bioelectronics. The rigidity of the devices can be easily altered by modifying the thickness of the substrate by simply modulating the spin coating parameters during film formation. Unlike most naturally occurring polymers, photoreactive sericin is soluble in water, which offers great processability when used with most of the biorecognition reagents such as enzymes and antibodies. It also allows the easy development of patterns once immersed in water. The sericin area that was not cross-linked could be easily washed off, giving very clean, high resolution and high fidelity micropatterns, whose complexity is only limited by the engineering design of the photomasks. The entire fabrication process is carried out on bench-top and low cost using only benign solvents, eliminating the need for clean room procedures. Due to the presence of chemical linkage, the micropatterns can withstand all kinds of mechanical deformations without any delamination or degradation in physio-chemical and electrical properties. This approach therefore has a significant advantage over other techniques where the active patterns tend to dissociate from the substrate under mechanical stress. Moreover, this approach gives rise to a rapid high throughput, green microfabrication of sensors.

5.3.2 Sensing of electrochemically active targets

Electrochemical biosensors can facilitate the detection of chemical analytes using two different sensing mechanisms: i. Direct biosensing and ii. Indirect biosensing. Direct biosensing of chemical

analytes requires them to be electrochemically active so that they can be directly oxidized on electrodes. The sensing of these types of chemical targets is also known as non-specific sensing since they do not require any specific biorecognition molecule such as enzyme or antibody for their recognition. Ascorbic acid and dopamine are some of the common electrochemically active chemical biomarkers that are of great physiological importance. AA, commonly known as vitamin C, plays an important role in the formation of collagen, wound healing, and the maintenance of healthy gums. It also plays an important role in various metabolic activities such as activation of vitamin B, conversion of cholesterol to bile acids, and conversion of amino acids to the neurotransmitter, serotonin. DA is a vital neurotransmitter from catecholamine family, responsible for controlling the reward and pleasure centers of the brain. Neuronal diseases such as Parkinson's, schizophrenia and attention deficit hyperactivity have been linked to dysfunction in the dopamine system, making it an important detection target.

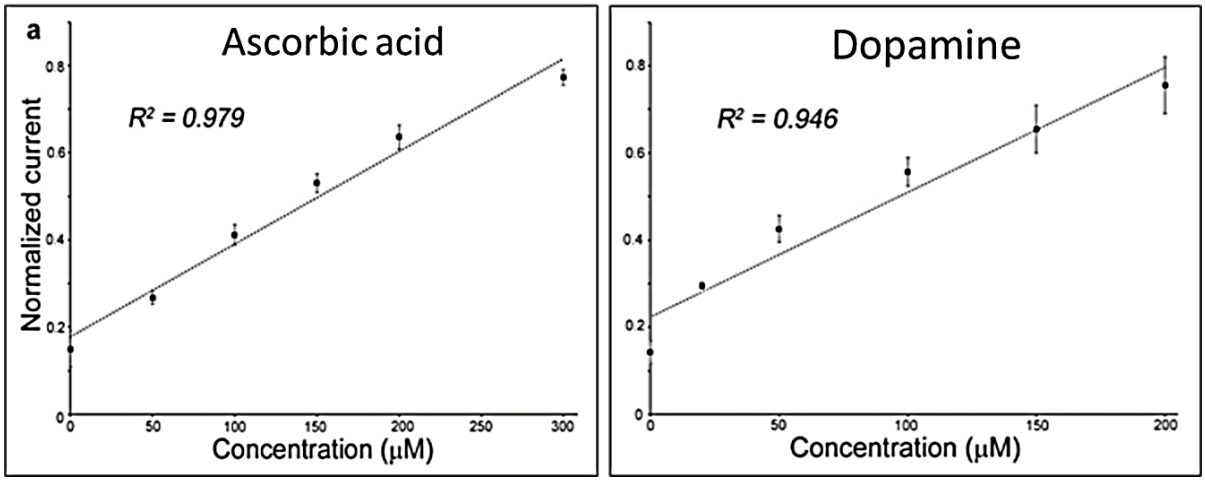

Figure 5.2 *Sensor response curves for (a) ascorbic acid and (b) dopamine.*

Ascorbic acid and dopamine were detected in separate experiments using amperometry. Amperometric biosensors are widely used since continuously measure current resulting from the oxidation or reduction of an electroactive species in a biochemical reaction.[267, 268] Flexible

PEDOT: PSS-photosericin architectures were used as working electrodes, while Ag/AgCl and platinum wire were used as reference and counter electrodes respectively. The sensing experiment was carried out in a 10mL PBS system with continuous stirring. The detection of ascorbic acid and dopamine were carried out at 0.3 V and 0.6 V constant potentials respectively. Following the stabilization of background current, ascorbic acid and dopamine were added in increments from a 0.01M stock solution of each. Each experiment was replicated using at least 3 different sensors. The amperometric response curves of ascorbic acid reveal a linear range from 10 μM to 200 μM. Similarly, the response of dopamine was found to be linear in the range from 10 μM to 300 μM. Current values were normalized to surface area (mA/cm^2) to account for any differences in sensor area of the 3 different fabricated sensors measured (sensor area is ~0.08 cm^2). The sensitivity of the ascorbic acid sensor was found to be 25 nA/ (μM cm^2), whereas the dopamine sensor showed a sensitivity of 113 nA/(μM cm^2) (**Figure 5.2**). The response time (time taken to reach 95% of steady state current) for DA and AA sensors is ~35 s. The linear and dynamic ranges was found to be comparable with earlier reported sensors such as flexible graphite-paper sensor and graphene on plastic freestanding electrodes.[103, 269, 270] Due to the versatility of the PEDOT: PSS-photosericin ink, suitable electroactive species such as graphene can also be added to increase the sensitivity and detection limits.

5.3.3 Sensing of non-electroactive targets

Ever since the development of first glucose sensor by Clark, glucose sensing has become the gold standard of electrochemical sensors. As mentioned previously, the water based ambient temperature processing of the conductive biocomposite makes it possible to encapsulate and stabilize active biomolecules directly in the ink. These include enzymes, DNA, and antibodies for use in specific and "indirect" sensing modalities (e.g., enzymatic reaction, binding etc.). Through

the inclusion of glucose oxidase (GOx) enzyme in the conductive matrix a flexible glucose sensor is realized. Glucose sensing takes place via the breakdown of glucose by the enzyme and the free electrons are shuttled to the conductive polymer by a mediator. Importantly, the glucose sensor developed in this work is free from any metallic and metal oxide-based charge carrying substrates, since the ink is able to function as both the transducer and active electrode. The amperometric response and calibration curve (n = 3 sensors) of the glucose sensor is shown in **Figure 5.3**. 0.1 M glucose solution was added to sensors in PBS at different intervals. The sensor shows a rapid linear response throughout the dynamic range of 0–8 mM, which covers physiologically relevant blood glucose concentrations. The average response time of the sensor (time taken to reach 95% of steady-state current) is 25 s with a sensitivity of 5.06 μA/mM cm^2. The signal change also confirms that the glucose oxidase retains its bioactivity after the fabrication process, implying that the process is indeed benign to biomolecules. The results obtained in this experiment also indicates that other specific targets can be easily detected by incorporating their complementary enzyme or antibody in the ink composition.

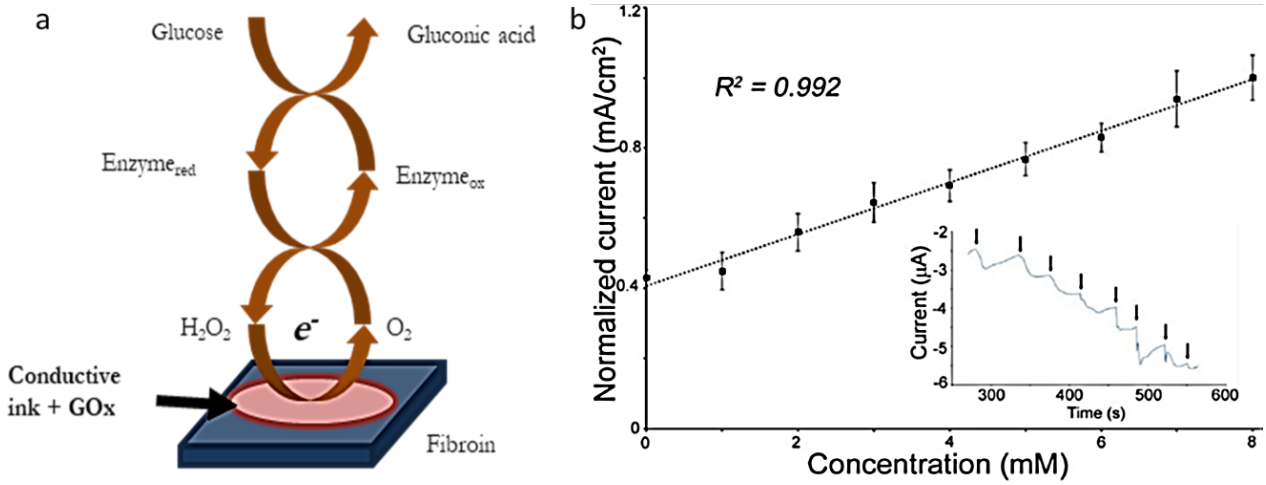

Figure 5.3 *Glucose sensing (a) mechanism and (b) sensor response to glucose concentrations. The inset shows the I-t response of one sensor with the arrows corresponding to addition of glucose.*

5.3.4 Development of a fully organic flexible integrated biosensor

Conventional 3 electrode systems often include metals such as Ag/AgCl and platinum as reference and counter electrodes. Although such systems are simple to design and are cost effective, it is rather difficult to engineer such systems into flexible formats.[265] They are generally not biodegradable. Further, the electrode material often has to be encapsulated with a biocompatible material to minimize inflammatory responses when implanted inside the biological environment.[271] Hence, there is a need to develop better sensor configurations. In this work, the fabrication of functional fully organic, flexible, degradable biosensors has been proposed wherein the working (WE), reference (RE), and counter electrodes (CE) are formed using the PEDOT: PSS-photosericin conductive ink. The electrodes are photolithographically patterned on a flexible fibroin substrate thus making the system compliant to curvy biological surfaces. The proposed sensor has a dimension of ~ 1cm^2 with electrode patterns 1,000μm wide. A cyclic voltammetry scan performed on the sensor shows a wide stable potential window in the range of -1V to 1V without any water splitting window, thus demonstrating the usefulness of the system in detection of various biomolecules. Finally, to demonstrate that such sensor configuration could indeed be used for sensing chemical analytes, electroactive neurotransmitter dopamine was detected. The sensor response was found to be linear in the dopamine concentration range of 0- 400 μM. The sensitivity of the sensor was found to be 160 nA/mM cm^2 which is in the same range as the conventional 3 electrode system with Ag/AgCl and Pt wire as the reference and the counter electrodes respectively.

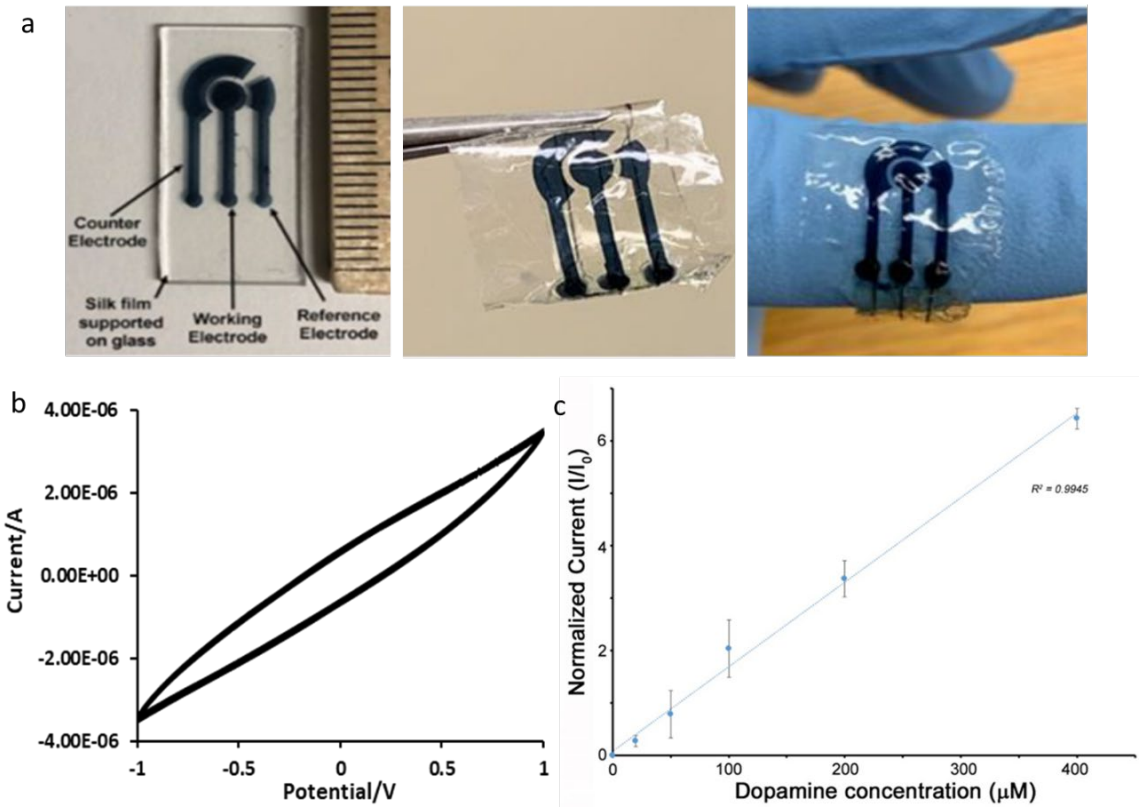

Figure 5.4 *a) Sensor design showing the position of the working, reference, and counter electrodes. The biosensor is conformable, flexible and can be subjected to mechanical deformation b) a stable CV and c) sensor response to dopamine.*

5.4 CONCLUSION

In summary, this work discussed in this chapter demonstrates the application of PEDOT: PSS-silk sericin composite for the detection of physiologically relevant chemical analytes in a flexible format. The PEDOT: PSS-silk sericin composite possess competitive performance metrics along with low charge transfer resistance that can Faradaic processes suitable for biosensing applications. PEDOT: PSS-silk sericin electrodes fabricated on flexible silk fibroin substrates were used to detect electronically active chemicals dopamine and ascorbic acid in a highly sensitive manner. The benign nature of the PEDOT: PSS-silk sericin composite allows the encapsulation of GOx

enzyme which has been exploited for the detection of glucose. The second part of the study demonstrated the fabrication of a fully organic, flexible, degradable biosensors has been proposed wherein the working (WE), reference (RE), and counter electrodes (CE) are formed using the PEDOT: PSS-photosericin conductive ink. The integrated biosensor was applied for the detection of dopamine as a proof of concept. The work presented in this chapter demonstrates the potential of nature derived materials for the realization of complex, state-of-the-art biosensing platforms.

[This chapter contains results that have been previously published: Ramendra K. Pal, Sayantan Pradhan, Lokesh Narayanan, Vamsi K. Yadavalli, "Micropatterned conductive polymer biosensors on flexible PDMS films", Sens. Actuators B Chem., 2018, 259, 498-504.]

CHAPTER 6

SILK-PEDOT: PSS BASED FLEXIBLE TEMPERATURE SENSOR

6.1 INTRODUCTION

Chapter 5 discussed the development of silk based fully organic, flexible biosensors that can sense various biomolecules of physiological importance. However, precise, real-time monitoring of temperature in flexible and bio conformable formats is important for healthcare and disease diagnostics. In this chapter, the expansion of silk-based devices for the detection of physical biomarkers of physiological significance has been explored.

Among the biointegrated and wearable systems that have been studied, the measurement of local temperature is an essential parameter in the monitoring of physiological function.[30] Of interest have been flexible and conformable temperature sensors that can function as wearables for real-time healthcare monitoring.[272, 273] While rigid thermometers have long been in existence, creating direct contact with the body has the potential to provide localized, real-time or continuous sensing, or improve comfort and accuracy. To accomplish conformal contact with uneven and dynamic interfaces, soft, flexible, conformable, and biocompatible sensors have been proposed. Skin is a primary target,[274-276] whereas localized temperature recordings for monitoring soft tissue interfaces for wound healing, or cardiovascular or pulmonary function, may also be

envisioned for disease diagnosis or observing organ function.[277]

The demand for improved, degradable, and conformable sensors continues to motivate research in this field towards ubiquitous sensing.[278, 279] The properties of a flexible temperature sensor may be affected by complex strains/stresses induced by the body. Thus, the presence of skin-like conformability and stretchability is desirable. In addition to conferring degradability, properties such as light weight, thinness, and mechanical flexibility are desirable for improved conformability and comfort. They can promote accurate sensing at tissue interfaces, or for packaging and smart textile applications. Further, sensors capable of operating in wet and dry environments are needed. A challenge lies in providing stable and reliable operation with properties intact for designed operational periods, followed by their degradation. Finally, integration with fabrication techniques makes the devices accessible and easily reproducible at low cost.

There have been prior reports of such flexible sensors for temperature measurement, which operate via different mechanisms (e.g. resistive, capacitive, or thermocouple) or different materials (e.g. carbon based, metals, or conducting polymers), on a variety of substrates (e.g. polyimide (PI), polydimethylsiloxane (PDMS), polyurethane (PU), polyethylene terephthalate (PET)-based films, paper or textiles).[272, 274, 280, 281] Among various conducting inks that have been reported, conducting polymers such as poly(3,4-ethylenedioxythiophene):polystyrene sulfonate (PEDOT:PSS) or polyaniline (PANI) are attractive for the development of flexible and wearable devices.[164] Many sensors incorporate either nondegradable synthetic substrates and/or use metallic electrodes. For example, temperature sensors based on CNT ink and (PEDOT:PSS) solution were printed on PET.[282] A PEDOT: PSS sensing layer was sandwiched between two PDMS layers with sensors pre-strained to improve sensitivity and linearity by creating microcracks.[283] A skin-conformable inkjet printed temperature sensor using

graphene/PEDOT:PSS as the active material was shown with screen printed silver conductors and inkjet-printed graphene/PEDOT:PSS temperature sensors. The functional layer was printed on an adhesive bandage, which had a polyurethane surface and polyacrylate adhesive layer.[284] The negative effect of humidity on the electrochemical behavior of PEDOT:PSS motivated sensors with high humidity stability.[285] A fluorinated passivating polymer with low water permeability was used to provide stability to a crosslinked PEDOT:PSS sensing layer on Ag electrodes printed on a polyethylene naphthalate (PEN) substrate. [286] To date, fully degradable and mechanically flexible temperature sensors based on organic components have not been shown.

Natural biopolymers may provide an avenue for flexible temperature sensing with degradability. The work in this chapter demonstrates the photolithographic fabrication of functional, flexible and degradable temperature sensor using fully organic components. A photoreactive silk fibroin sheet function as a flexible, biocompatible substrate and a humidity protection layer, whereas functionality derives from conductive bioinks. These bioinks comprise the conducting polymer PEDOT: PSS mixed with photoreactive silk sericin, which allow facile fabrication into microelectrodes via photolithography. A silk sericin/reduced graphene oxide (rGO) ink is crosslinked as the temperature sensitive layer. The sensors are mechanically robust, thin and ultralightweight, while possessing humidity stability. The sensors are stable in both air and liquid environments over several days and can be stored in dry and wet conditions. The use of silk proteins to form novel degradable and biocompatible, yet functional (e.g. conducting) substrates provides a ‘green’ future for tissue interfacing (bio) electronics and electronic skins. [4] [228, 287]

6.2 EXPERIMENTAL

6.2.1 Synthesis of photoactive silk proteins

Photofibroin and photosericin were prepared following the method described in Chapter 1.

6.2.2 Formation of conductive composites

A photopatterning conducting ink for the fabrication of sensing microelectrodes was formed using a composite of the conducting polymer PEDOT: PSS with photosericin. The protein matrix forms a stable and biodegradable carrier which entraps the PEDOT: PSS while making it patternable using an aqueous process. A 1% (w/w) dispersion of dry PEDOT: PSS pellets (Sigma-Aldrich, St. Louis, MO) in water was obtained by ultrasonicating for 30 mins and filtering using a 0.25 μm syringe filter. 5% (v/v) DMSO was added to the dispersion to enhance its conductivity and stability. To form the conducting ink, photosericin was mixed with the PEDOT: PSS dispersion at varying concentrations, with appropriate amounts of Irgacure 2959 photoinitiator to facilitate crosslinking.

A composite of photoactive silk sericin and rGO was used to enhance conduction and sensing. GO was reduced to rGO chemically using an aqueous protocol.[288] Briefly, a 2 mg/ml solution of GO (University Wafer, South Boston, MA) was reduced at room temperature using L-ascorbic acid (5 mg per 1 mg of GO) for 1 hour under continuous stirring. Reduction was verified by UV-Vis. Freshly prepared rGO was mixed with the photosericin at varying concentrations with PI added to the solution.

6.2.3 Fabrication of the temperature sensor

Microfabrication of the temperature sensor was carried out via contact photolithography using a benchtop setup (no cleanroom needed) (**Figure 6.1**). The substrate was prepared by casting a solution of 7.5% (w/v) photofibroin and 1.5% PI in formic acid on clean glass slides. The solution

was dried under ambient conditions and crosslinked using an OmniCure S1000 UV Spot Curing lamp (Lumen Dynamics, Ontario, Canada) (365 nm UV (2 mW cm^{-2}) for 2 s) to form flexible substrates. Interdigitated electrodes (IDEs) were formed by spin-coating a solution of photosericin containing 28% (w/w) PEDOT: PSS and PI (0.2 µL/mg) on the substrates and drying under dark conditions in a fume hood. IDEs were patterned by crosslinking the ink under UV light for 2.5 s through a photomask, followed by developing in DI water. The temperature sensing layer was fabricated by casting a solution of 1% (w/w) of rGO and photosericin + PI on the IDEs and drying, followed by UV crosslinking. The top passivation layer was fabricated by casting a solution of 7.5% (w/v) photofibroin and PI in hexafluoro-2-propanol (HFIP, Sigma-Aldrich, St. Louis, MO), and crosslinking to form an integrated, flexible device.

6.2.4 Device characterization and temperature sensing

To perform electrochemical experiments on the flexible silk temperature sensors, connections were made using copper wires. Measurements were performed using a Gamry Interface 1010E potentiostat (Gamry Instruments, Warminster, PA). Conductivity measurements on the sensors were calculated from *I-V* scans performed in the range of −1 to 1 V at 50 mV s^{-1}. A water bath placed on a hotplate with a commercial thermocouple was used to control the temperature at which sensor measurements were taken. To obtain the conductivity at each temperature point, an *I-V* scan was performed after equilibration for 5 minutes. Responses at different humidity was measured by placing the sensors in a controlled humidity desiccator. The sensor was maintained at each humidity level for 30 mins before performing conductivity measurements. For all calculations, room temperature (20°C) was taken as initial temperature (T_0).

Realtime measurement of temperature was performed using chronoamperometry at 1 V potential.

A calibration plot was obtained using amperometric measurements (I vs. t) by varying temperature from 20-45ºC. The temperature was kept stable at each point for 50 seconds. Current values (I) were normalized to the value at 20ºC (I_0) to obtain a calibration curve. For the determination of temperature of a surface, amperometric measurement was obtained at room temperature for 50 seconds followed by placing the sensor on the surface (with fibroin substrate in contact with the surface) and taking a reading for 50 seconds. The final temperature was calculated from the calibration curve.

6.2.5 Degradation and stability in aqueous media

The stability of the devices was observed by storage in PBS over extended period of time (several weeks) followed by electrochemical testing. Degradation of devices was observed under enzymatic conditions. Unsheathed devices (no top fibroin layer) were immersed in 3 ml of PBS solution containing 1 mg ml^{-1} protease (Protease XIV from *Streptomyces griseus*, ≥3.5 U mg^{-1}, Sigma Aldrich) and stored at 37°C. A higher concentration of enzyme was used in order to speed up the process. A control set was designed with devices immersed in PBS buffer at 37°C. To preserve enzyme activity, the solution was replaced every 2 days. Imaging was performed on the devices following removal from the enzyme solution and drying in a gentle N_2 stream.

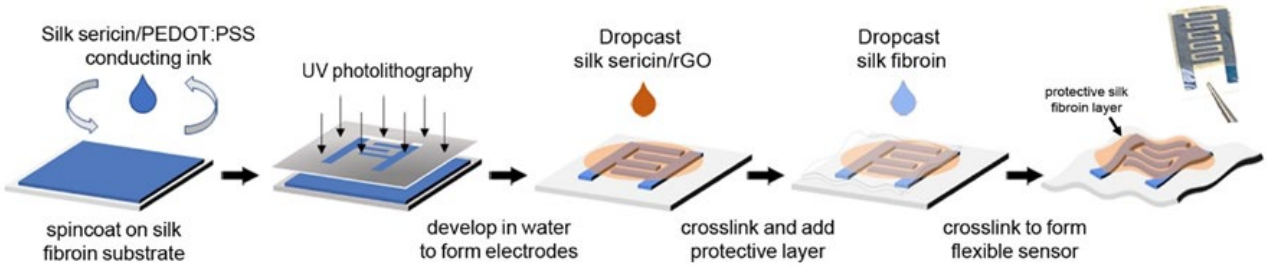

Figure 6.1 *Schematic of formation of flexible silk/PEDOT: PSS temperature sensor.*

6.3 RESULTS AND DISCUSSION

6.3.1 Fabrication of flexible organic temperature sensors

In order to form the flexible, biodegradable temperature sensor, the various components were fabricated using silk protein photolithography discussed in Chapter 2. Fibroin films serve as mechanically robust, biodegradable substrates on which the entire temperature sensor is fabricated. High tensile strength (~100 MPa), optically transparency, and stability in physiological conditions makes them ideal for flexible and bio conformable devices.[289] The photoreactive, conducting ink formed from silk sericin and PEDOT:PSS is a versatile matrix for electrochemical sensing. In this study, temperature sensitivity of PEDOT: PSS was used as the transduction mechanism. Specifically, on applying a thermal stimulus, the charge transport carriers increase along with an increase in the number of charge carriers. This increase in carrier mobility decreases the resistance of the temperature sensor, which is reported as a function of temperature.[290, 291]

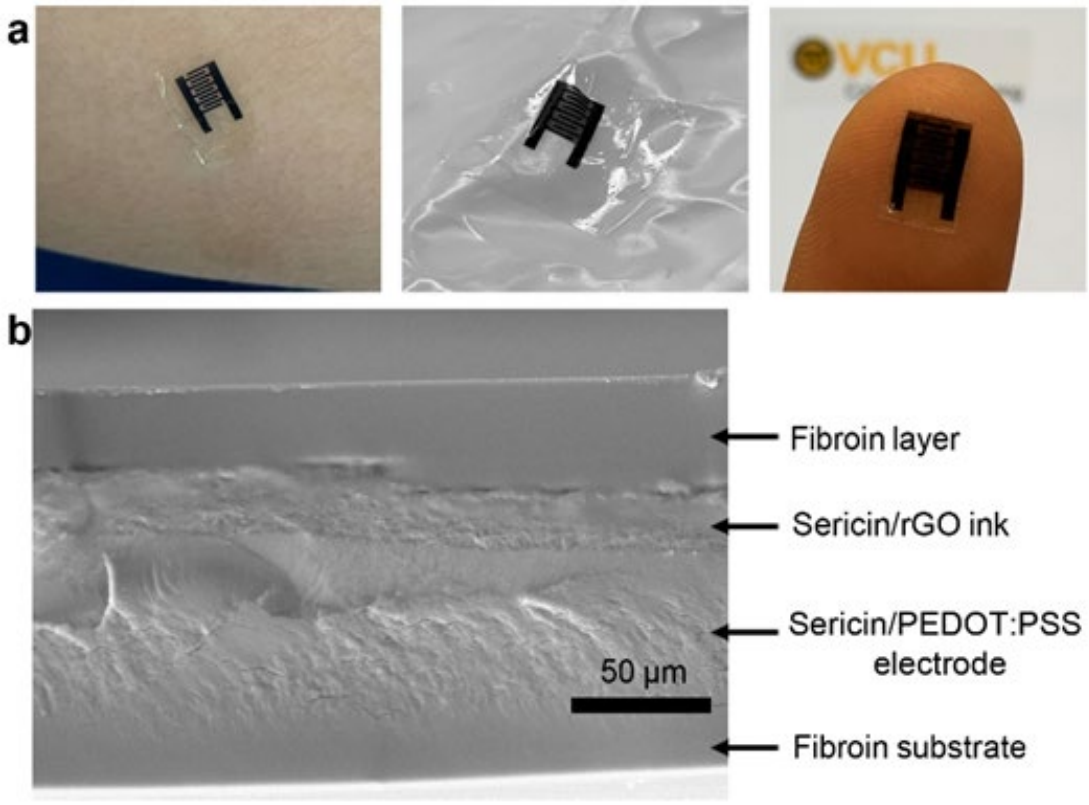

Figure 6.2*: Images showing the flexible temperature sensor formed using silk proteins. a) the sensor may be placed on skin or integrated into a wrinkled surface (e.g., a textile) with a small form factor. b) SEM imaging of the cross-section of the sensor showing the layers that are covalently integrated, preventing delamination and improving stability.*

The flexible substrates are formed as thin, smooth, mechanically robust silk fibroin films crosslinked on glass supports. The PEDOT: PSS ink was patterned on these substrates by spin coating, followed by photolithography. The process schematic is shown in **Figure 6.1**. Interdigitated electrodes (IDEs) with 250 µm finger width were fabricated to have a small form factor for the sensors (IDEs cover ~ 1 mm x 2 mm area on a substrate that is ~10 mm x 10 mm). The films were soaked in water for development and to delaminate them from the support and form free-standing devices (**Figure 6.2a**). A conducting composite of rGO and photosericin was

cast on the electrodes and covalently crosslinked, taking advantage of the same pendant methacrylate moieties present in the substrate and electrodes to form interpenetrating layers. rGO is used as the temperature sensing element due to its well-known phenomenon of temperature dependent charge transport behavior. Upon thermal excitation, the mobility of charge carriers in rGO increases, thus increasing the conductivity of the material. Finally, to provide stability against humidity, a fibroin layer was used to sheath the top of the sensor. The use of water as the developing solvent makes the entire process benign and environmentally friendly. The chemical crosslinking of the different layers using the same chemistry makes the entire device more robust, durable and less prone to failure under multiple mechanical deformations and flexure. By incorporating the PEDOT: PSS in the photosericin matrix, which contains residual methacrylate groups, the IDEs are covalently attached to the underlying fibroin substrate. **Figure 6.2b** shows an SEM image of the cross-section of the device, showing how the layers are integrated.

6.3.2 Device characterization and optimization

The temperature sensor reported here utilizes two different conducting composites- rGO-photosericin and PEDOT: PSS- photosericin. The inclusion of the (photoreactive) sericin offers a stable, patternable matrix for the rGO and PEDOT: PSS, while also providing biodegradation under proteolysis. Both rGO and PEDOT: PSS have been used as the active sensing elements in temperature sensors.[275, 286] Hence, the temperature sensitivity of each layer was separately investigated. The effect of temperature on the resistance of PEDOT: PSS-photosericin and rGO-photosericin was studied, while keeping the configuration (amount of material and area) similar (**Figure 6.3**). In order to characterize each sensor configuration, linear voltammetry scans were performed while varying the temperature from 20-50^{o}C. The temperature sensitivity is expressed

in terms of the Temperature Coefficient of Resistance (TCR):

$$\text{TCR} = \frac{R - R_0}{R_0 * \triangle T} \times 100.$$

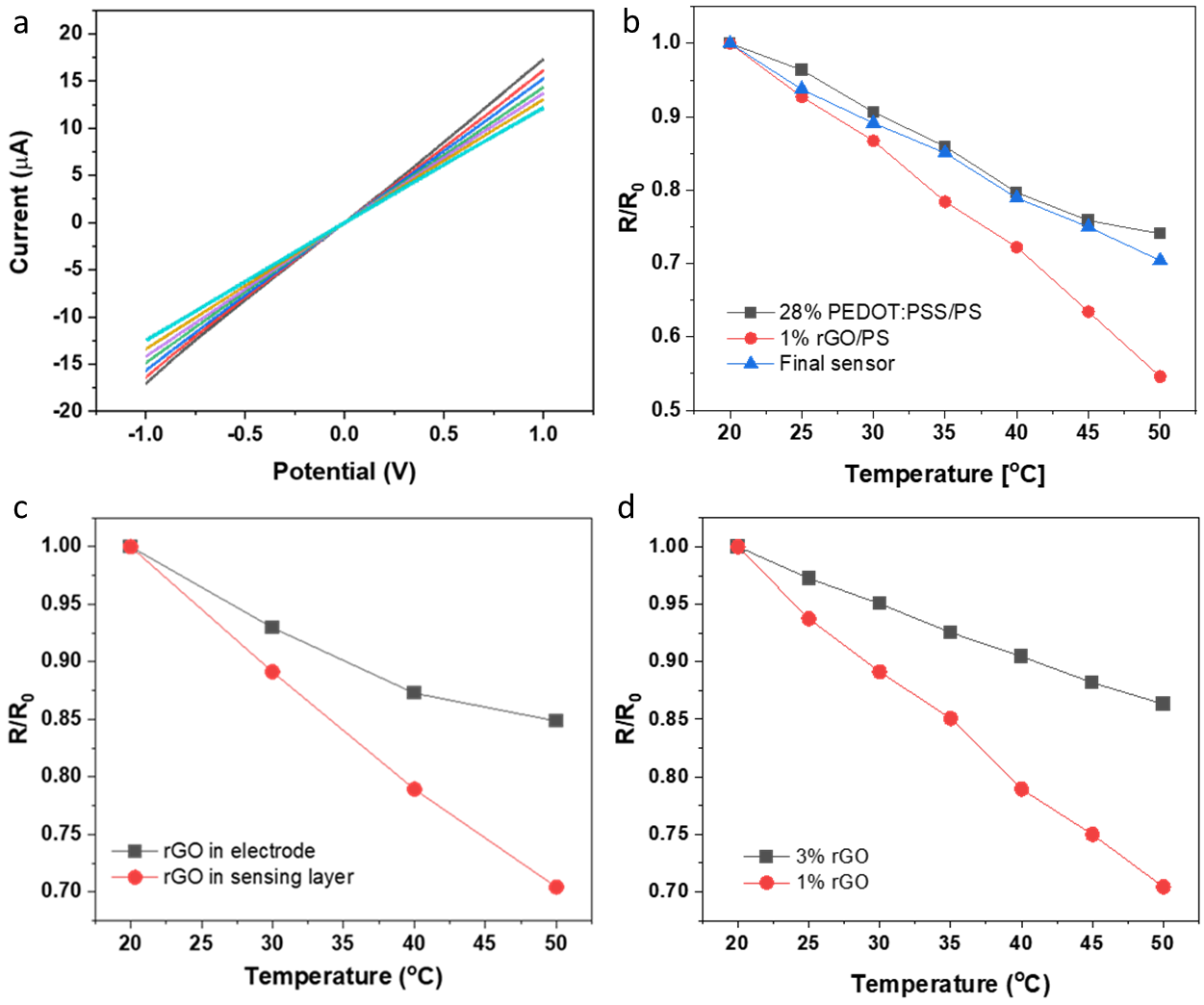

Figure 6.3 *a) I-V curves as a function of temperature for temperature sensors in liquid environment (PBS buffer) b) Comparison of the effect of temperature on resistance from each of the individual composites with the final temperature sensor. c) Difference in sensitivity as a function of rGO in the electrode ink vs. rGO in the top sensing layer and d) effect of increasing the concentration of rGO in the conduction layer.*

The temperature sensitivity of the 1% rGO-photosericin layer (-1.51% $^{o}C^{-1}$) is higher compared to

the 28% PEDOT: PSS-photosericin layer (-0.86% $^{o}C^{-1}$). In comparison to the individual composites, the TCR of the temperature sensor is -0.99% $^{o}C^{-1}$ (**Figure 6.3b**). Although the change in resistance is not linear for either of the composites, the response of the final sensor was found to be linear. Since the sensitivity of the 1% rGO-photosericin is higher than the 28% PEDOT: PSS-photosericin layer. To optimize device characteristics, the use of rGO dispersed within the IDEs instead of using it as a separate layer was investigated. The temperature sensitivity of electrodes with 1 wt.% rGO in the PEDOT: PSS-photosericin ink composite was estimated at -0.5% $^{o}C^{-1}$, which is almost half the sensitivity of devices with 1% rGO in the top layer (-0.99% $^{o}C^{-1}$) (**Figure 6.3c**). The presence of rGO in the PEDOT: PSS-photosericin ink did not lead to any noticeable enhancement of sensing behavior.

Table 6.1 *Some comparative reports of sensors showing the temperature coefficient of resistance (TCR) response.*

Temperature sensing active material	**Temperature range ^{o}C**	**TCR ($^{o}C^{-1}$)**	**Reference**
PEDOT:PSS + GOP sensing layer on Ag electrode	25-50	-0.77%	[286]
PBH-rGO composite	20-65	-0.3% - 0.8%	[275]
rGO	25-45	-1.30%	[276]
Silk fibroin and Ca (II) ions	0-40	-1.9%	[292]
Silk based graphitic nanocarbon	25-80	-0.81%	[293]
Gr/SF/Ca^{2+}	20-50	-2.1%	[294]
PEDOT:PSS	30-55	-0.42%	[295]
Graphene/PEDOT:PSS	30-45	-0.064%	[284]
PDMS/ PEDOT:PSS/ rGO	30-50	-1.69%	[296]
Silk/PEDOT:PSS	**20-50**	**-0.99%**	**This work**

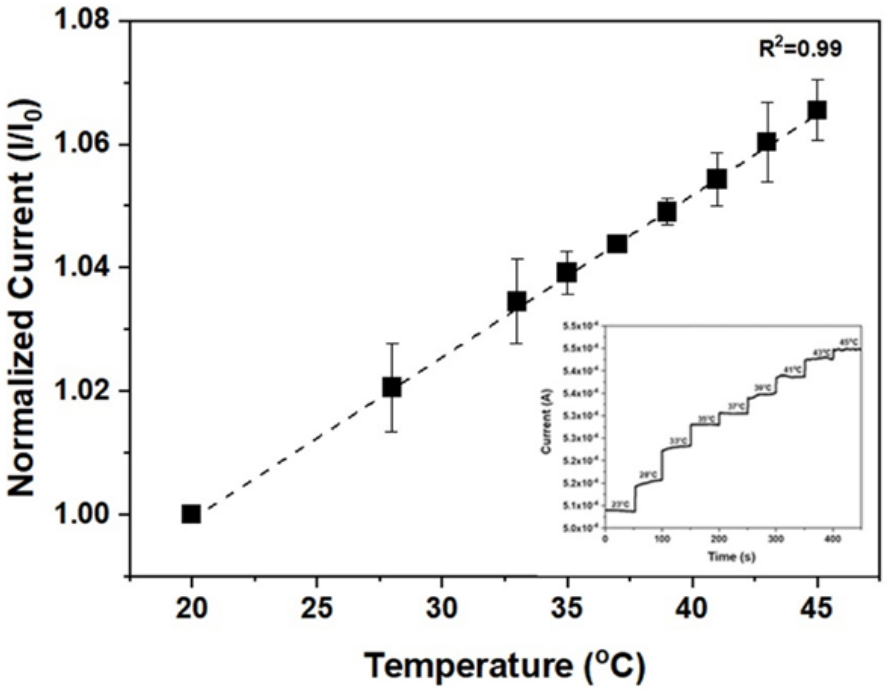

Figure 6.4 *Calibration curve showing the temperature response of the flexible sensors. The inset shows the signal vs. time measured by chronoamperometry in steps of 5°C. (n=3 different sensing experiments).*

Similarly, increasing the concentration of rGO in the top layer was studied. The temperature dependent *I-V* characteristics of devices with varying rGO loading was obtained from 20 to 50°C. Even though the overall resistivity of the devices decreased while increasing the rGO concentration from 1 wt.% to 3 wt.%, the temperature sensitivity of the devices decreased (**Figure 6.3d**). This can be explained by the percolation threshold and dispersion of rGO in the photosericin matrix. 1% rGO-photosericin is more efficiently dispersed, making it more sensitive to temperature changes. The charge carrier mobility of the rGO-photosericin composite might be impeded at higher temperatures with higher rGO loading. Hence, the configuration as shown in **Figure 6.2** was proposed. Finally, a calibration curve was obtained by suspending the sensor in a temperature-controlled water bath and varying the temperature of the water bath from 20-50°C, covering the

physiological temperature. A liner chronoamperometric response in current was observed upon increasing the temperature (**Figure 6.4)**.

6.3.2.1 Temperature response to humidity

The change of conductivity depending on the environmental conditions such as humidity and temperature are important for device operation. The influence of relative humidity (RH) on the electrical and optical properties of PEDOT:PSS is known.[297] A significant cause of degradation of organic PEDOT:PSS devices in air is the adsorption of moisture from the atmosphere.[298] In PEDOT:PSS, the polycationic PEDOT chains are interspersed in the polyanionic poly(4-styrenesulfonate) (PSS) matrix, making it water dispersible. However, the presence of the PSS renders the material to be hygroscopic. This degradation of the PEDOT:PSS layer is spatially inhomogeneous, and related with the formation of insulating patches causing loss of device current, an increase in the resistivity, and consequently decrease in device efficiency.[299]

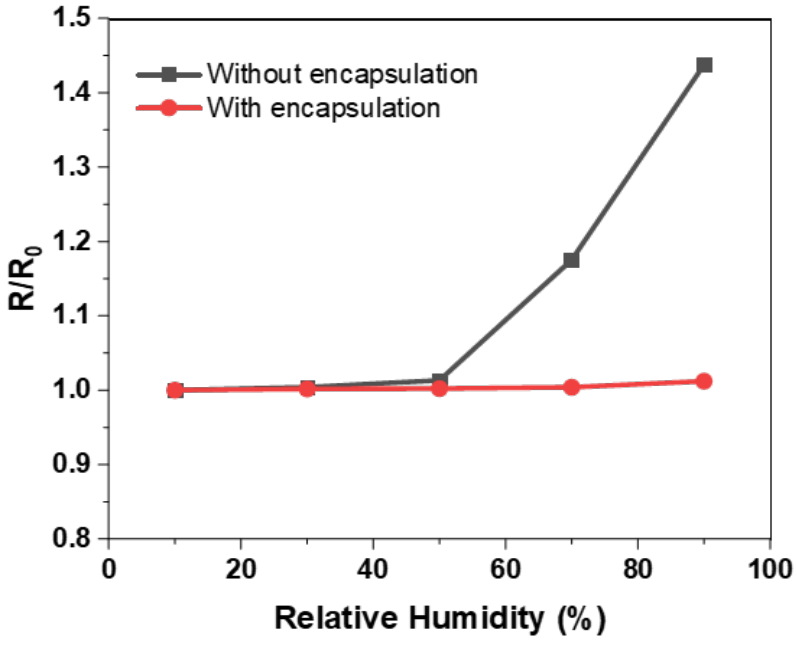

Figure 6.5 *Effect of humidity on the temperature sensor with and without fibroin encapsulation layer.*

While the calibration curve in Figure 3 was obtained under fully hydrated conditions, the effect of humidity on the conductivity of the temperature sensor was estimated by measuring the *I-V* characteristics while varying the relative humidity level from 10% to 90% by placing them in desiccator. Further, the effect of sheathing of the sensing layers using a photofibroin layer (top layer shown in **Figure 6.2b**) in order to enhance stability towards humidity was studied. In the devices without a photofibroin passivation layer (unsheathed), the resistance of the sensor was relatively unchanged till ~60% RH. However, the resistance increased by 6% and 11% upon increasing the humidity level to 70% and 90% respectively (**Figure 6.3**). However, when a photofibroin layer was introduced, the resistance of the sensors increased by only ~1.2 % even under high humidity (90% RH) conditions. This demonstrates that a degradable fibroin encapsulation/sheath provides excellent protection against humidity interference while enhancing stability in wet environments.

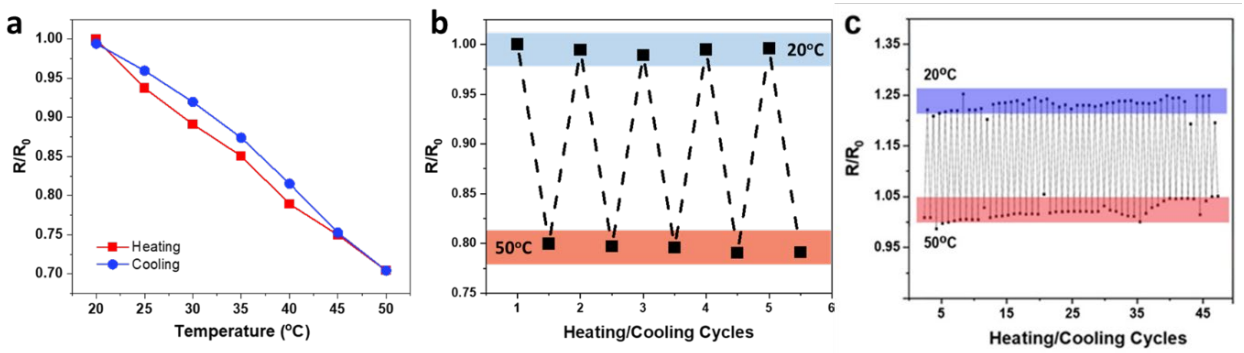

Figure 6.6 *Effect of heating and cooling. a) Measurement of TCR hysteresis of the sensor in a single heating and cooling cycle. Repeated heating and cooling over b) 5 cycles and c) 50 cycles.*

6.3.2.2 Effect of heating and cooling

The characteristics of the temperature sensors for heating and cooling cycles was measured. The response of the devices for heating and cooling is similar with a very small hysteresis between the

heating and cooling curves. The TCR of the device while heating (-0.989% $^{o}C^{-1}$) was very close to the co-efficient on cooling (-0.973% $^{o}C^{-1}$) (**Figure 6.6a**). This suggests that the reported temperature sensor can be used in multiple heating and cooling cycles. The sensors displayed excellent cycling stability over multiple heating cooling cycles (**Figure 6.6b**). Only minuscule changes in response were observed over even 50 cycles of consecutive heating and cooling, demonstrating the exceptional consistency of the sensors (**Figure 6.6c**). This suggests that the reported temperature sensor can be used in multiple heating and cooling cycles without compromising on precision.

6.3.3 Application of the sensor for measuring surface temperatures

The ability to detect surface temperature, especially on the human body, reliably in a flexible and conformable format finds potential applications in healthcare, disease diagnostics and in developing e-skins. As seen in **Figure 6.2a**, the sensors are conformable and can be easily applied to surfaces including skin and wrinkled fabric. The experiments noted in the prior section were performed using a water bath to maintain a steady and measurable temperature. The response of the flexible sensors was tested in contact with surface temperatures, including human skin. In the first series of experiments, a flexible, soft, synthetic skin surface (commercially available silicone matrix product) was used. A temperature calibration in the range of 23^{o}C to 45^{o}C was used. The synthetic skin slab was immersed in a water bath (40^{o}C) till an equilibrium temperature was reached. The skin slab was removed, and the sensor placed on it to obtain the current response. From the calibration plot, the temperature was calculated to be 39.4^{o}C, which was extremely close to the surface temperature of 39^{o}C as measured by two different commercial thermometers.

The developed temperature sensor was subsequently deployed on skin for measuring the surface

temperature. The conformable nature of the sensor allows it to be easily placed on the forearm surface (**Figure 6.2a**). After taking a reading at room temperature (23ºC, 60% RH), the sensor was placed on the arm and the response was monitored. The current signal response is practically instantaneous as the sensor was placed on the skin and stabilized once the skin temperature was reached (**Figure 6.7a**). The current signal at the skin temperature was taken for 50 seconds, with the sensor giving a stable response for the entire duration. Once the sensor was removed from the skin, the current value dropped back to the signal observed at room temperature observed initially. The temperature reading of skin obtained from the calibration curve previously generated was calculated to be 30.4ºC. For the purpose of validation, the skin temperature was measured using a commercial IR skin thermometer which gave a reading of 30.5ºC (**Figure 6.7a inset**). While the skin temperature is below the normal physiological temperature. The agreement in temperature response illustrates the fidelity of the sensor developed in this work. From the current vs time graph, an increase in current signal is observed as soon as the sensor was placed on skin, showing that this flexible sensor is rapid and conformable to the underlying surface. It may be noted that the biocompatible fibroin substrate through which the conduction occurs is in contact with the surface, rendering it useful for soft interfacial measurements. The application of the sensor for touch detection was also considered. A current response was recorded as soon as a finger was placed on the sensor, indicating its utility for flexible touch panels using an array of sensors.

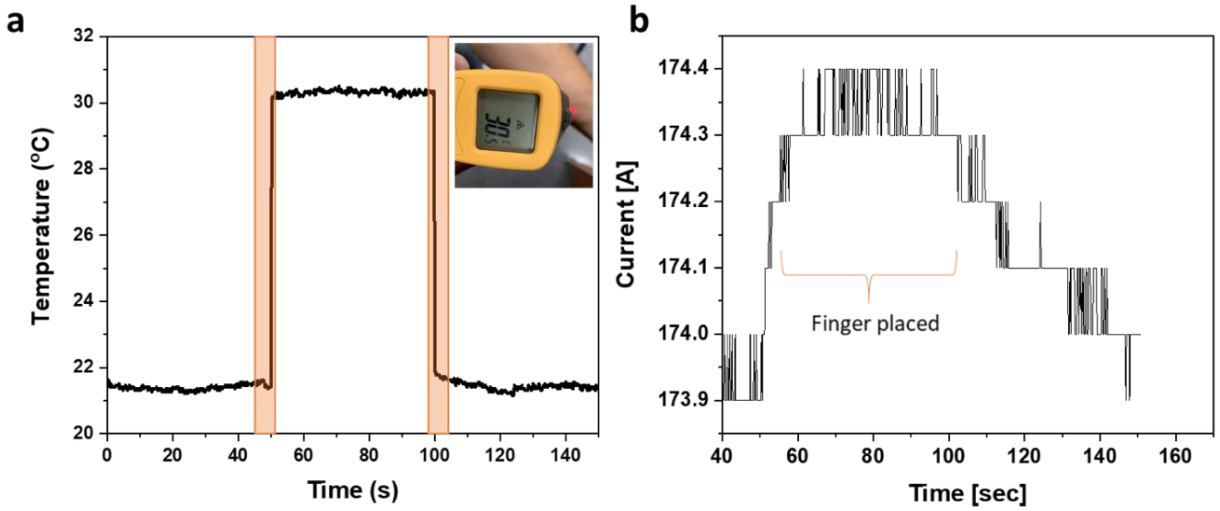

Figure 6.7 *a) Temporal sensor measurement of skin surface temperature (forearm). The inset shows the temperature reading taken using a commercial IR thermometer. b) Current response upon placing a finger on the sensor.*

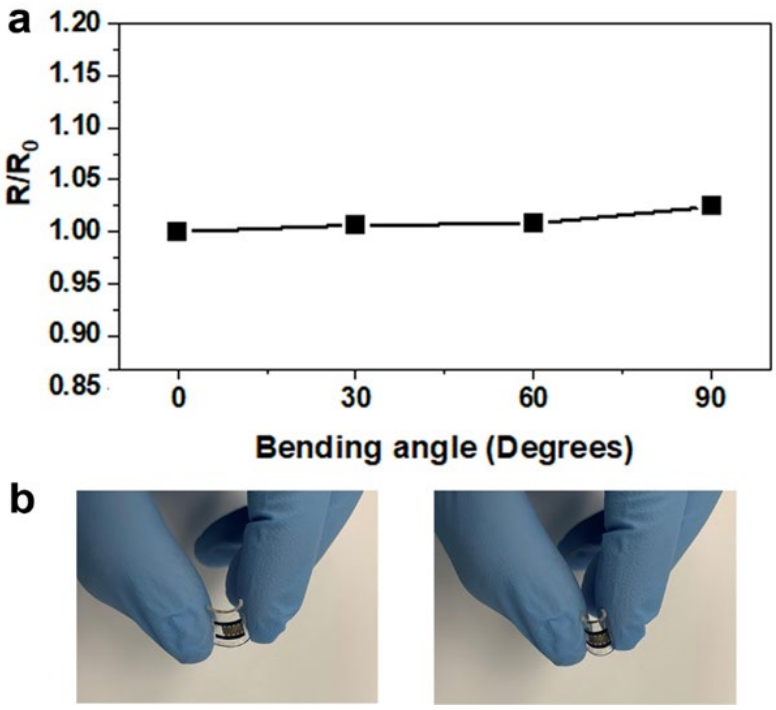

Figure 6.8 *Response of the temperature sensor to bending. The resistance (a) was measured by generating I-V curves at different bends. Representative bending (b) is shown by placing the sensors on a PDMS support that can be flexed.*

6.3.4 Flexibility and bendability of temperature sensor

Flexibility and conformability against soft curvilinear surfaces are two basic requirements for sensors designed for applications on the human body. As shown above, these sensors are easily placed on, and function, on non-rigid and non-planar surfaces. It is important to measure the retention of electrical and mechanical properties under non-planar deformations. We studied the effect of bending on the electrical properties of the sensors by subjecting them to 30º, 60º and 90º bends, which may be encountered in the body. The resistance of the sensor under different bend conditions was compared to the resistance of a "flat" sensor. At small bends, no change in the resistance is noted. Even at a 90º bending angle, the resistance increased by only 2.4% showing the high stability of this device (**Figure 6.8**). Importantly, the sensor retains its structural integrity when subjected to mechanical deformations, without any structural failures such as delamination of the electrodes, fracture, or cracking of the layers. Collectively, these experiments demonstrate the utility of the proposed sensor for real-time and continuous monitoring of temperature of arbitrary, dynamic surfaces including soft tissue interfaces.

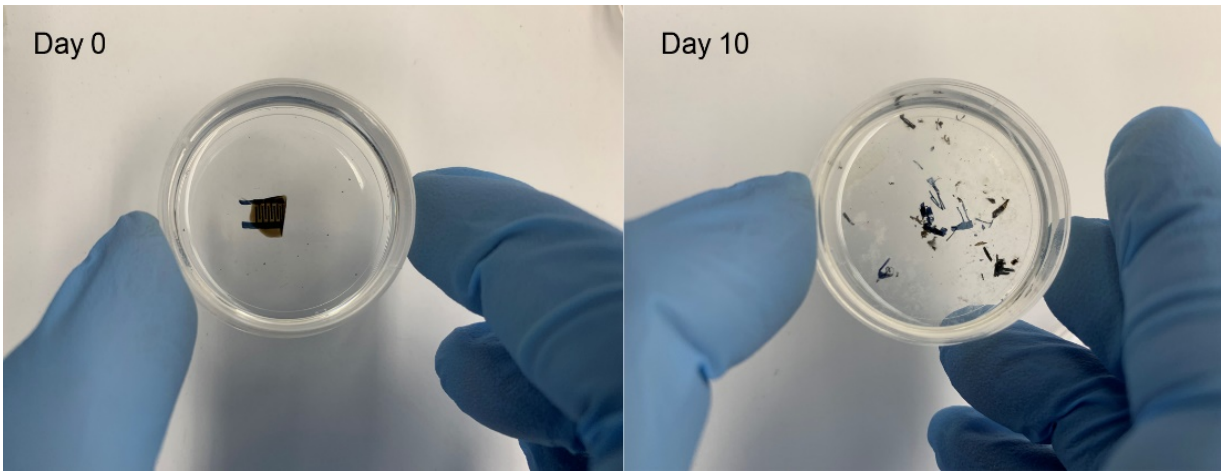

Figure 6.9 *Degradation of the flexible temperature sensor in 10 days in an enzymatic (protease) environment.*

6.3.5 Degradation studies:

One of the primary advantages of using an organic, biomaterial-based fabrication strategy is the ability to form a degradable device. While the applications demonstrated above are primarily *ex vivo* (e.g., on skin), this property can permit the sensor to be bioresorbed or disappear in a physiological microenvironment after a stable operation lifetime. Silk proteins are known to be enzymatically degraded [300, 301]. A simulation of enzymatic degradation of the temperature sensors was carried out *in vitro* to demonstrate their transient nature. The devices were immersed in a 3.5 U/ml solution of protease at 37ºC. The control consisted of devices immersed in 1M PBS buffer. In the presence of the enzyme, the devices lose their structural integrity in a few days and break apart completely in ~ 10 days (**Figure 6.9**). A higher protease concentration was employed to accelerate this process. This implies that a sensor in a standard environment can be designed to last longer. A lower protease concentration of 1 U/ml was studied, resulting in proteolytic degradation over 1 month (**Figure 6.10**). Similarly, by controlling the thickness of the substrates and the degree of crosslinking, this degradation rate may be further modulated to a period of several weeks. It must be noted that the devices in the control group retain their structural integrity and function, even after 1 month of immersion in buffer. We note that in these experiments, it is the supportive matrix (silk fibroin and sericin) that degrades in the presence of protease enzyme. While PEDOT: PSS and rGO are not known to be degradable inside the human body, the loss of the sericin ink matrix results in their dispersal in the form of fine particles that can be eventually expelled. We can therefore envision such flexible and degradable devices to be used for short periods of time, in external operation (on body or in textiles) or *in vivo*.

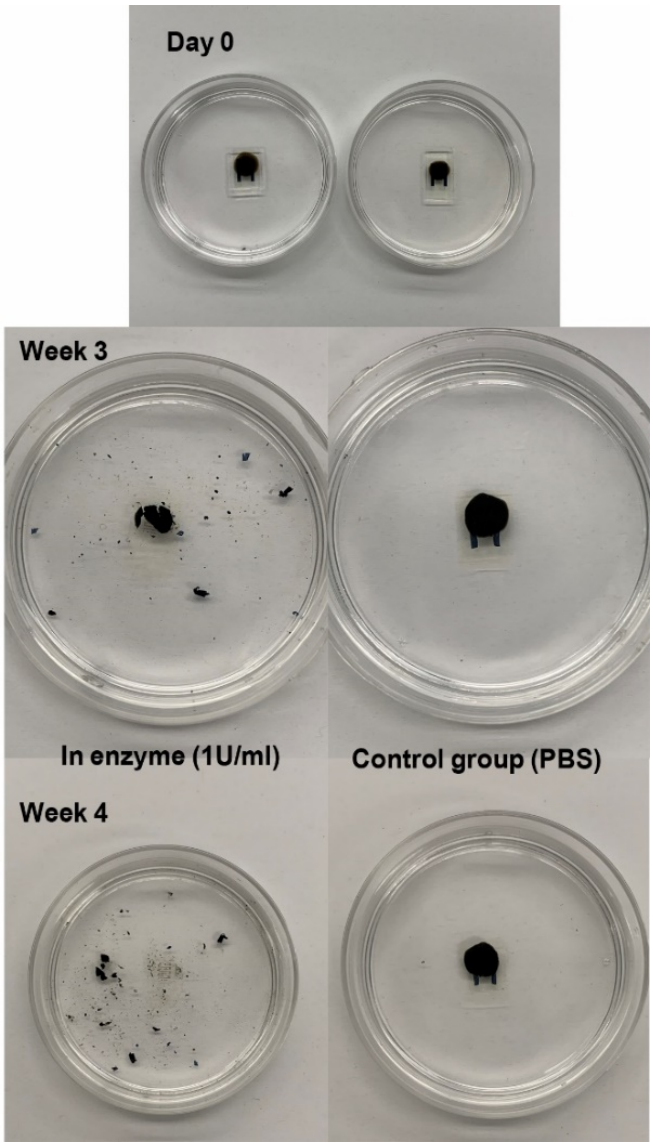

Figure 6.10 *Degradation of the temperature sensors in different proteolytic conditions weaker enzyme solution (1 U/ml protease solution). In this case, the sensor begins to fall apart after about 2.5 weeks, with almost complete degradation in 4 weeks.*

6.4 CONCLUSION

In summary, a flexible silk/PEDOT: PSS device is shown in this chapter for the monitoring of surface temperature. This demonstrates the usefulness of natural polymeric materials combined with conductive materials for the development of temperature sensitive composites which further

allow the realization of fully organic sensors for physical biomarkers. The device is a fully organic, degradable temperature sensor that possesses several useful features including small size with high-resolution, reproducible microstructured electrodes. The entire device is optically transparent, mechanically robust while being flexible and conformable to complex surfaces. Notably, this sensor is formed from protein matrices that comprise an organic framework for the device, while allowing it to be proteolytically degraded over a period of several weeks. The sensing performance was stable against humidity variations while being able to function in fully hydrated environments. Sensor response is rapid, repeatable and cyclable and functions under various mechanical challenges. Such degradable systems may be applied for wearable and degradable applications for on-body, tissue interfacing, implantable physiological monitoring of temperature, or as e-skins that can provide temperature response to touch.

[This chapter contains results that have been previously published: Sayantan Pradhan, Vamsi K. Yadavalli, "Photolithographically Printed Flexible Silk/PEDOT: PSS Temperature Sensors", ACS Appl. Electron. Mater. 2021, 3, 1, 21–29.]

CHAPTER 7

A KIRIGAMI INSPIRED APPROACH TOWARDS FLEXIBILITY AND COMFORMABILITY

7.1 INTRODUCTION

The ability to produce flexible, thin, mechanically robust, and compliant interfaces that perform in dynamic environments is an ongoing challenge. Devices imbued with such multifunctionality can establish adaptive interfaces with the body. The biosensor devices reported in Chapters 5 and 6 have been developed on silk fibroin substrates which are inherently flexible and robust, making them ideal for wearable or conformable electronics. However, there is a scope to enhance their flexibility, stretchability and conformability to soft biological interfaces by introducing new structural design concepts. A variety of structural design concepts have been integrated with functional materials to form biodevices and surfaces for health monitoring. This chapter explores such a possibility by taking inspiration from the concept of Kirigami (Japanese art of paper cutting) to engineer flexibility in materials through the creation of patterned defects.

The successful designing of flexible biodevices for application at the biological milieu requires them to possess a host of important features. However, one of the most important property of such devices is stretchability, i.e., the ability of the device to maintain normal functionality under mechanical strain.[302] This is crucial to the realization of biodevices that are mechanically robust

and are able to conform to soft non-planar surfaces commonly encountered when dealing with the human body. Stretchability can be imbued to such devices via two strategies: i. material design strategies wherein either novel stretchable materials are synthesized, or elastomeric materials are blended with non-stretchable materials and ii. Structural design strategies which involve subjecting existing materials to new structural conformations and geometries.[303, 304] Recently, the second strategy has gained much attention in the field of flexible and wearable electronics because of its ability to include to a wider selection of materials, as traditional non stretchable materials or components can simply adapt the specially designed structure to achieve device-level stretchability.[181] For examples, flexibility can be imparted to rigid materials such as metals metal oxides and semiconductors simply by altering their thickness.[37] Stretchability has been introduced to various active components in devices such as electrodes, sensors, transistors etc., through structural designs such as wrinkles, arches, serpentines interconnections and island-bridge structures.[304, 305] Of interest is the use of kirigami-inspired cuts to transform materials toward multifunctional bio interfaces. While designed to enhance elasticity for traditionally stiff materials, kirigami architectures can transform intrinsically flexible and soft materials in interesting ways.

Kirigami cuts have been mostly achieved using material substation using techniques such as microscale laser cutting,[306] optical lithography,[307] etching (e.g., plasma, masked ion),[308] and macroscopic cutting (e.g., x-acto knife).[309] Kirigami has been successfully shown on flexible materials including traditional paper, elastomers (polydimethylsiloxane, PDMS), metal foils, plastics (polyimide, polyethylene terephthalate, polyester films), and graphene-silk composite are among materials reported.[191, 308] The use of kirigami with active functional components in devices using conductive materials such as metal electrodes (Au, Ag, Pt, and Al), indium tin oxide, carbon nanomaterials (nanotubes, graphene), conducting polymers, and 2D

layered materials such as MoS_2 have also been shown.[188, 305, 310, 311] At present, kirigami design strategies have been effectively demonstrated in stretchable and conformable devices such as light-emitting diode (LED), stretchable supercapacitor, thin-film GaAs solar cells, wearable health monitoring device and strain sensors.[312] However, the use of fully biodegradable and biocompatible materials with kirigami strategies has not been shown.

In this chapter, for the first time, photolithographic fabrication of biofunctional, biodegradable silk kirigami via a facile, single-step subtractive process is demonstrated. The photolithographic process described in Chapter 2 was used as a route to form precise cuts on photoreactive silk fibroin over a large (centimeter scale) area. This results in flexible, freestanding, optically transparent, macroscale sheets with precisely defined microscale cuts. The PANI-photofibroin conductive composite developed in Chapter 4 was combined with kirigami to form intrinsically conducting silk kirigami films that are flexible, stretchable, and can be bent and twisted while retaining electrical properties.

7.2 EXPERIMENTAL

7.2.1 Fabrication of kirigami films using photocrosslinkable fibroin

Photocrosslinkable fibroin (referred to as photofibroin) was prepared following the protocol discussed in Chapter 2. The photofibroin (7.5% (w/v)) was dissolved in hexafluoroisopropanol (HFIP) with the 2.5% (w/v) Photoinitiator (Irgacure 2959, BASF). The solution was drop cast on plain glass slides and air-dried for 15 min to evaporate the excess solvent. Samples were crosslinked using 365 nm UV (Lumen Dynamics OmniCure 1000) at 20 mW/cm2. Uncrosslinked areas (cuts) were developed by soaking in 1 M LiCl/dimethyl sulfoxide (DMSO). Freestanding films were obtained by soaking developed films in deionized water to delaminate them from the

glass support. Films were washed in water and stored in air or water. To form conducting fibroin films, polyaniline (PANI) emeraldine salt from p-toluenesulfonic acid (Alfa Aesar, Tewksbury, MA) (11% w/w) was dispersed in formic acid (1 wt.%) using ultrasonication and mixed with photofibroin along with appropriate amounts of photoinitiator. Similar fabrication steps were followed to make cuts.

7.2.2 Tensile tests

Kirigami samples were fixed on a paper frame with a window of 0.5 cm side. The tensile test was performed on an MTS 300 series tensile testing machine (MTS Systems Corporation, Eden Prairie, MN) equipped with a 50 N load cell. Measurements were taken at a strain rate of 0.1 mm/s, and data was collected at a rate of 10 Hz. All other parameters are sample-specific such as thickness, width, and length. Typically, films were 20−25 μm thick.

7.2.3 Electrochemical characterization

Linear sweep voltammetry (LSV) was used to characterize the electrochemical properties of the silk-PANI kirigami films. The measurement was conducted by a Gamry Interface 1010E Potentiostat (Gamry Instruments, Warminster, PA). The scanning range of applied potential was from −0.5 to 0.5 V (over 1 V) with a rate of 100 mV/s. The electrochemical data was analyzed using the Gamry Echem Analyst software. Electrical connections were tested by connecting to a DC power source.

7.2.4 Proteolytic degradation in vitro

Silk fibroin films can be proteolytically degraded over time in the presence of enzymes. In the

present work, the degradation of silk kirigami films in the presence of protease (Protease XIV from Streptomyces griseus, ≥3.5 U/mg, Sigma- Aldrich) was demonstrated. Films, 20 μm thick with 100 μm cuts (containing ~2.5 mg fibroin), were incubated in 5 mL of protease (1 U/mg of protein) at 37 °C, and the degradation was studied over 2 weeks. Another set of samples was incubated in PBS buffer under the same environment, which served as the negative control. The enzyme solution was replaced every 3 days to maintain protease activity. Samples from each set were taken out on different days, rinsed with deionized (DI) water, and imaged under a microscope to record their degradation over time.

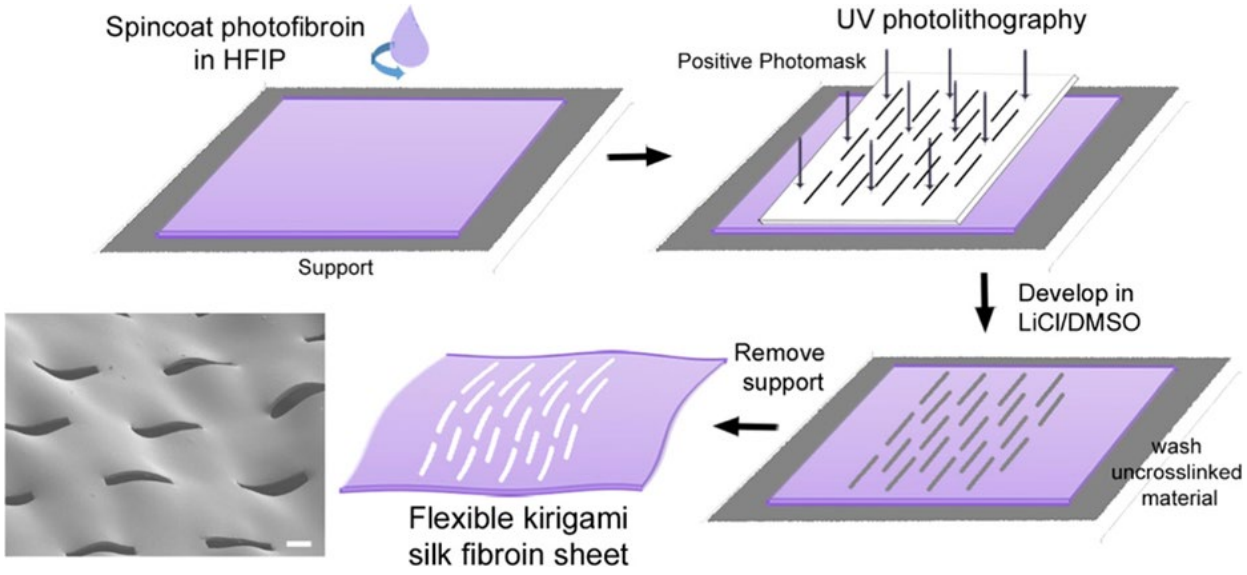

Figure 7.1 *Schematic diagram showing the single-step fabrication of kirigami cuts in silk fibroin films via photolithography.*

7.3 RESULTS AND DISCUSSION

7.3.1 Fabrication of silk kirigami films

In previous chapters, the use of silk fibroin films as a mechanically robust, optically transparent

and flexible substrate on which devices can be easily fabricated using bench top photolithographic techniques was discussed. The incorporation of kirigami inspired cuts can enhance the stretchability of such devices by aiding the substrate material (silk fibroin) to withstand more strain, thus enabling better conformability to curvilinear surfaces. In this Chapter, kirigami-inspired cuts/patterns using degradable and biocompatible polymer silk fibroin were used to add a new dimension to their function. Material subtraction or cutting is photolithographically accomplished in a single-step process.

Initially, a solution of photofibroin in formic acid was spin coated on glass substrates and crosslinked under 365 nm UV light through a photomask. The photofibroin acts as a negative photoresist and the uncrosslinked material is removed by developing the films in 1M LiCl/ DMSO solution. Here, the cuts comprise the uncrosslinked regions from where the material is removed during the development process. Following the development step, inspection under an optical microscope revealed the presence of residual crosslinked material which prevent the cuts from opening up. It was hypothesized that after the spin coating step, even though formic acid is relatively volatile, it took around 20-30 minutes for it to evaporate completely, which is sufficient for the formation of a thin crosslinked layer at the bottom (**Figure 7.2a)**. To overcome this problem, formic acid was replaced with 1,1,1,3,3,3-hexafluoro-2-propanol (HFIP) to dissolve the fibroin for solvent casting. HFIP is a highly volatile fluorinated polar solvent and its use resulted in a smooth dry layer of photofibroin in less than 5 minutes which could significantly reduce the bottom layer crosslinking. Additional care was also taken to avoid any exposure to light, and samples were kept under aluminum foil during the drying process.

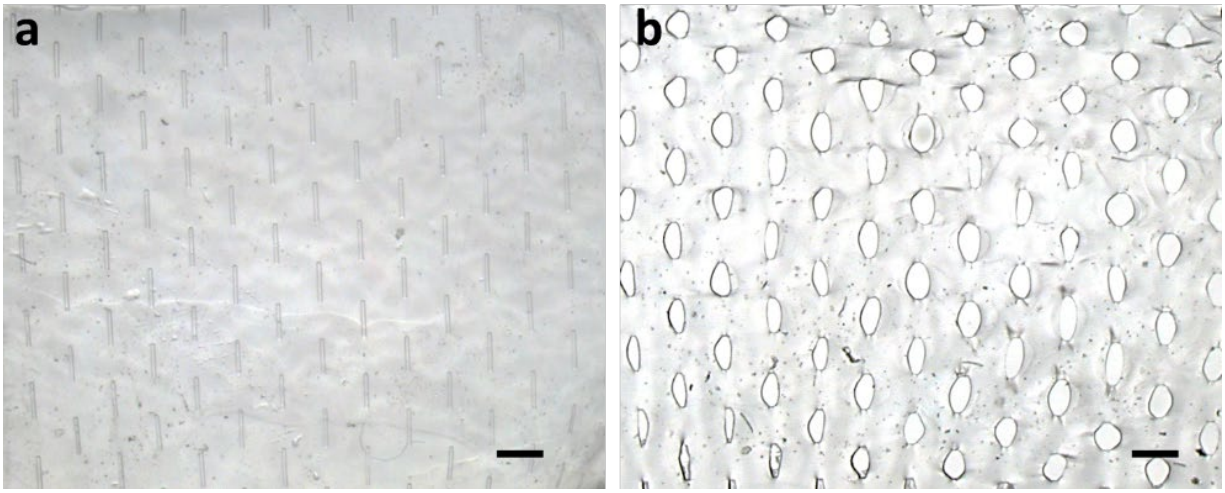

Figure 7.2 *Kirigami cuts fabricated on silk fibroin films using a) glass substrate and formic acid solvent and b) silicon substrate with HFIP solvent after stretching. Scale bar = 500 µm.*

However, this was sufficient enough to completely overcome the problem of residual crosslinking. In subsequent trials, the glass substrate was replaced with silicon one which the photofibroin-HFIP solution was spin coated since the transparent nature of glass led to the combination of refraction and scattering of UV light from the bottom of the glass surface, thus resulting in a thin crosslinked bottom layer. Silicon being opaque in nature along with a highly polished surface did not pose any problems pertaining to refraction. This finally resulted in cuts that have high structural fidelity and spatial resolution demonstrating the scalability and accuracy of this photolithographic process to form micropatterns over large areas (**Figure 7.2b)**.

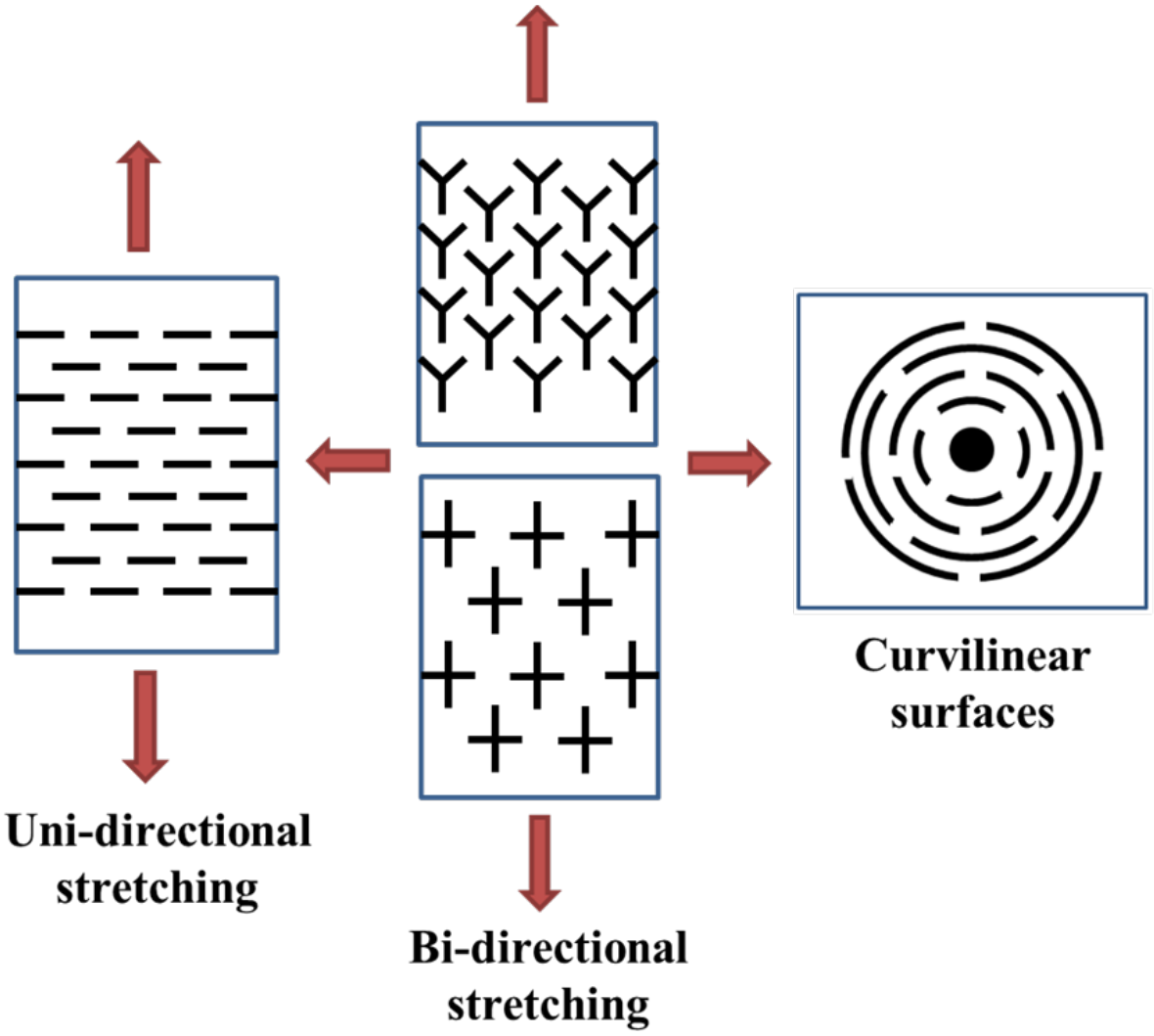

Figure 7.3 *Designing of various cut geometries depending on the direction of strain tolerance.*

A variety of cuts of different complex geometries could be formed easily which is only restricted to the designing of the photomask. A representative photomask is shown in **Figure 7.3a.** The designing of the cut geometries is largely governed by the intended direction of stretching or strain tolerance. For example, the cuts shown in **Figure 7.3b** (left) represents single slit geometries that are suitable for unidirectional stretching. On the other hand, cuts shown in **Figure 7.3b** (center) are more suitable for accommodating strains from multiple directions. Finally, cuts such as the one

shown in **Figure 7.3b** (right) can conform around complex curvilinear surfaces easily. Additionally, the silk kirigami films are optically transparent which could enable their application in stretchable optics and transparent devices. Cuts down to 10 μm resolution could be easily fabricated using simple bench top photolithography without requiring any cleanroom procedures. Moreover, the fabrication of nano-scale cuts can be envisioned via state-of-the-art nanofabrication techniques such as electron beam lithography (EBL). SEM images taken on the kirigami films shows ordered patterns of various complexities over a large area (cm scale) of flexible fibroin sheets. The mechanical robustness of the kirigami films allows for their easy handling wherein they can be bent, stretched and rolled into tubes without generating any faults or loss in mechanical properties. Bending certain patterns such as branches, saddles, or chevrons results in interesting and useful microscale openings and out-of-plane deformations.

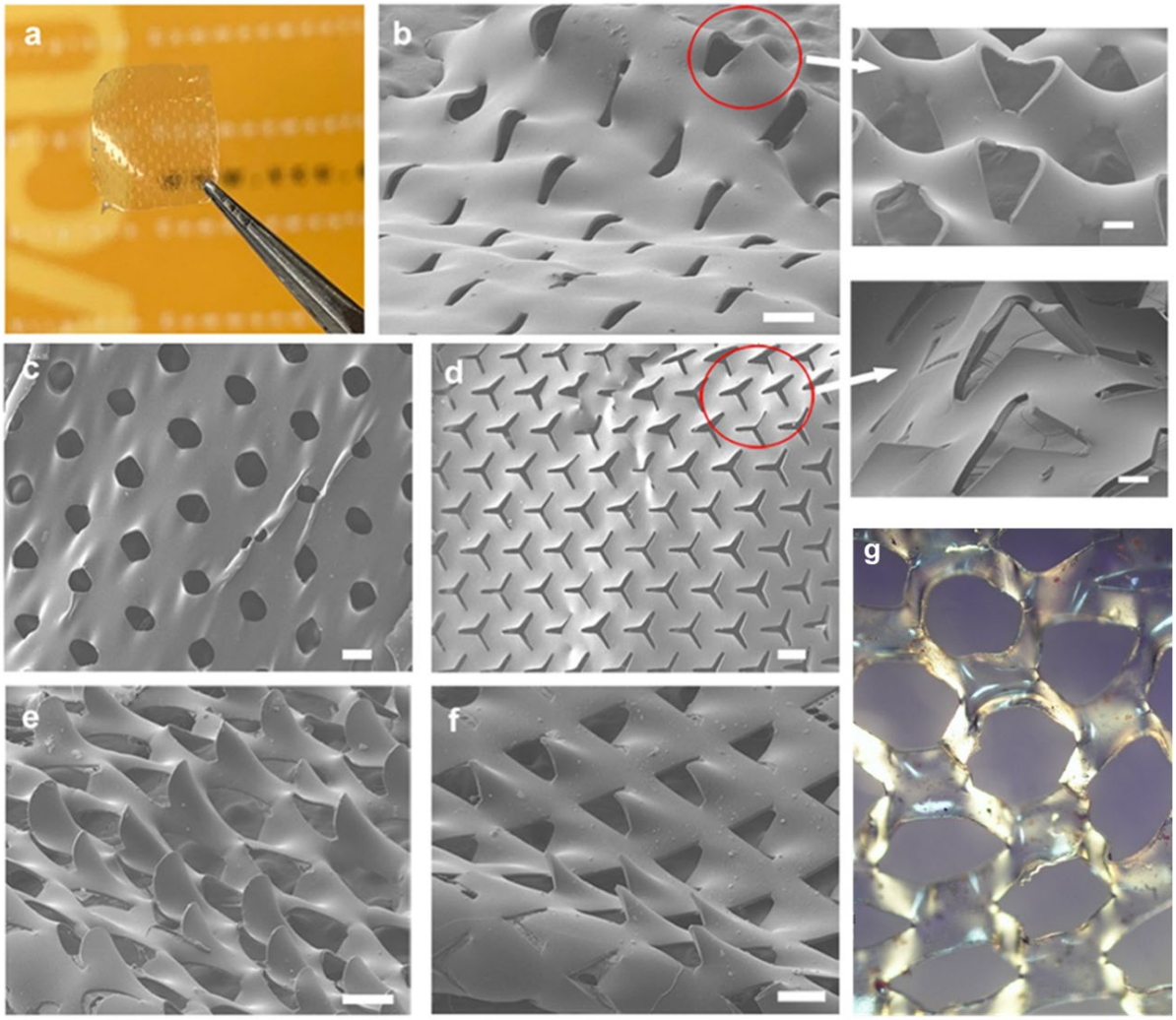

Figure 7.4 *Images of silk kirigami (a) large-scale silk kirigami films can be formed that are optically transparent (shown here are cuts 50 μm wide × 500 μm long). SEM images showing the diversity of geometries of cuts that can be formed using photolithography—(b) linear cut geometry with 25 μm cuts, (c) crosscuts that can be stretched biaxially, (d) branched ("Y"-cuts), (e) saddles, and (f) chevrons. The top right insets show the out-of-plane deformation of the cuts. (g) Optical image of a fully stretched silk kirigami film. The scale bar on all images = 100 μm. Film thickness = 25 μm.*

Finally, in a simple experiment, the conformability of the reported kirigami films to nonplanar

surfaces was tested. As discussed in Chapter 2, by altering the amount of material cast, and the spin coating parameters, thin silk fibroin films could be fabricated. These films can effortlessly conform to soft biological interfaces. However, with the addition of precisely designed cuts, this attribute is further enhanced. The kirigami films reported in this work possess a thickness of ~20 - 25 µm thick which was confirmed using SEM and optical microscopy. Human skin is known to be stretchable to 75% strain, with surface strain ~55% at the knees. The introduction of deformability in silk kirigami sheets, with fracture-resistant openings to accommodate stretch, allows conformable interfaces or attachment at interfaces. While the dry films are flexible but not compliant, moist films can be applied to and readily conform to irregular surfaces such as that of a bent finger. In comparison, a pristine film of a similar size and thickness is quickly delaminated on bending the finger. Expectedly, it was found that certain cut geometries such as 'Y' cuts conform better to irregular surfaces due to their ability to stretch in all directions when compared to simple slit cuts which can only stretch in one direction (**Figure 7.5)**.

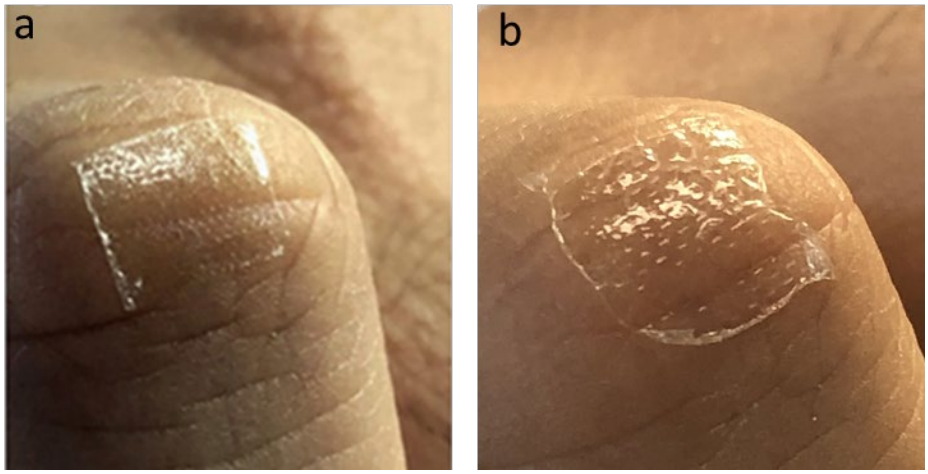

Figure 7.5 *Adherence of a) Y cut and b) simple slit cuts. The Y shaped cuts provide better conformability and remain on during flexure.*

7.3.2 Evaluation of mechanical properties using tensile testing

Following the fabrication of silk fibroin kirigami films, tensile tests were conducted on the films with various cuts to understand their mechanical behavior. Kirigami-based structural designs can achieve dynamic shaping toward stretchability and foldability.[313] Kirigami sheets possess a mechanical regime in which they are stretchable and soft in comparison to pristine (uncut) sheets.[314] Initially, tensile tests were performed on 3 types of silk kirigami films with cut dimensions- 100 μm wide × 500 μm long, 100 μm wide × 1000 μm long and pristine films (without any cuts). MTS 300 series tensile testing machine equipped with a 50 N load cell was used.

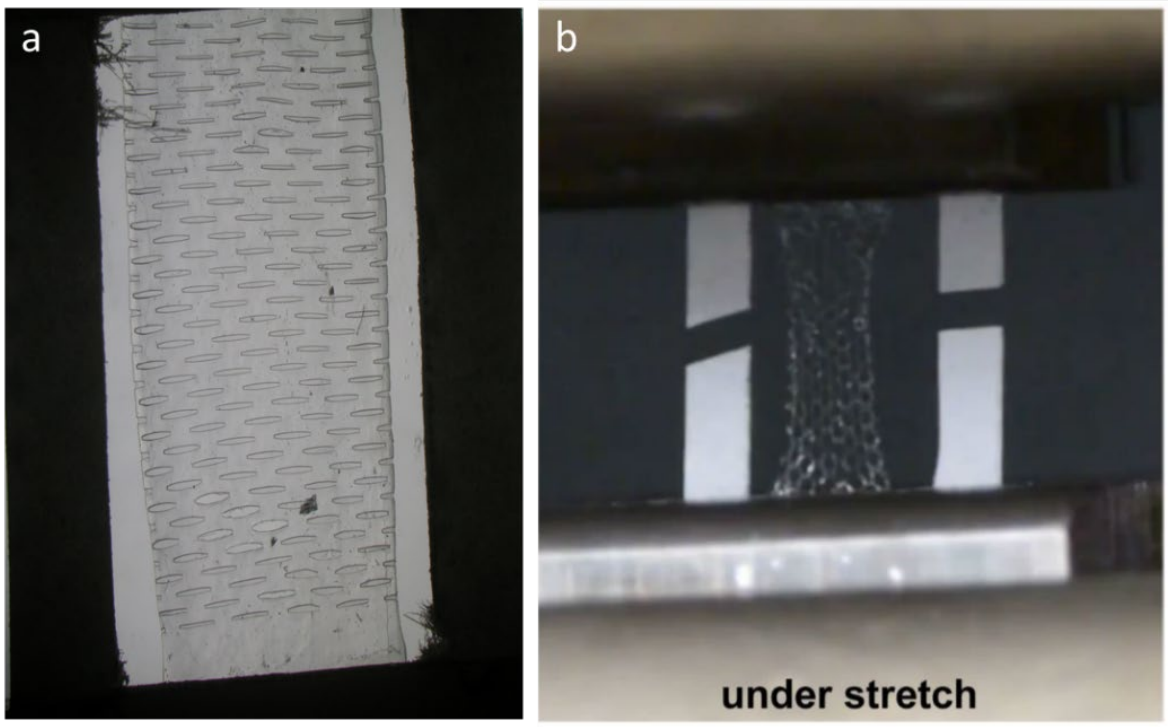

Figure 7.6 *Tensile testing of kirigami films. a) kirigami film placed inside a paper window and b) kirigami film mounted on tensile testing machine.*

Due to the flexible nature of the films, it was extremely difficult to mount the films to the tensile

testing machine without damaging them. Hence, the silk kirigami films were placed between a paper window to allow easy handling during the tensile tests (**figure 7.6a, b)**. This made the process of mounting the films between the clamps of the tensile testing machine relatively easier. Strain rate is an important parameter that critically affects the tensile data obtained. Hence, it is important to set the strain rate of measurement carefully to obtain an accurate representation of the mechanical properties of the samples. In initial experiments, the strain rate of measurement was set around 5 mm/sec. However, it was found that the kirigami samples failed instantly and gave incorrect tensile data, thus indicating that such high strain rates are not suitable for soft biological samples. After a series of careful investigations, the strain rate was optimized to 0.1 mm/sec (**Figure 7.7**).

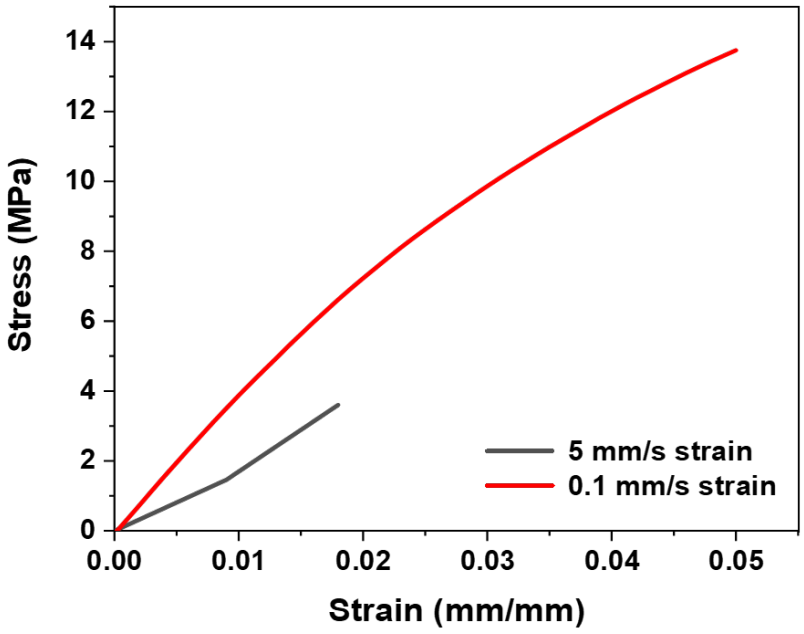

Figure 7.7 *Stress vs. Strain curves of plain fibroin films at 5mm/s and 0.1mm/s strain rates.*

To evaluate the effect of cut dimensions on the stress-strain response of the kirigami films, a simple tensile test was performed wherein the width of the cuts were kept constant at 100 µm while

varying the length of the cuts to 500 µm and 1000 µm. The tensile response of these kirigami films were also compared with pristine films (**Figure 7.8**). It was found that although the pristine fibroin films displayed a higher tensile strength of ~16 - 30 MPa, they could tolerate strain levels only up to ~7%. On the other hand, even though the kirigami films with 500 µm cut length possessed lower tensile strength (~8 -10 MPa), they could easily tolerate up to ~20% strain. Finally, the kirigami films with 1000 µm cuts had an even lower tensile strength of ~ 4 -6 MPa but their maximum strain tolerance increased significantly to ~70%. The decrease in tensile strength could be attributed to the kirigami cuts, which in this case acts at faults (or cracks) in the films, thus decreasing their capability to withstand high mechanical stress. Nevertheless, the primary objective of introducing kirigami cuts is to increase the strain tolerance levels of nature derived materials so that they can be successfully integrated with soft nonplanar biological surfaces.

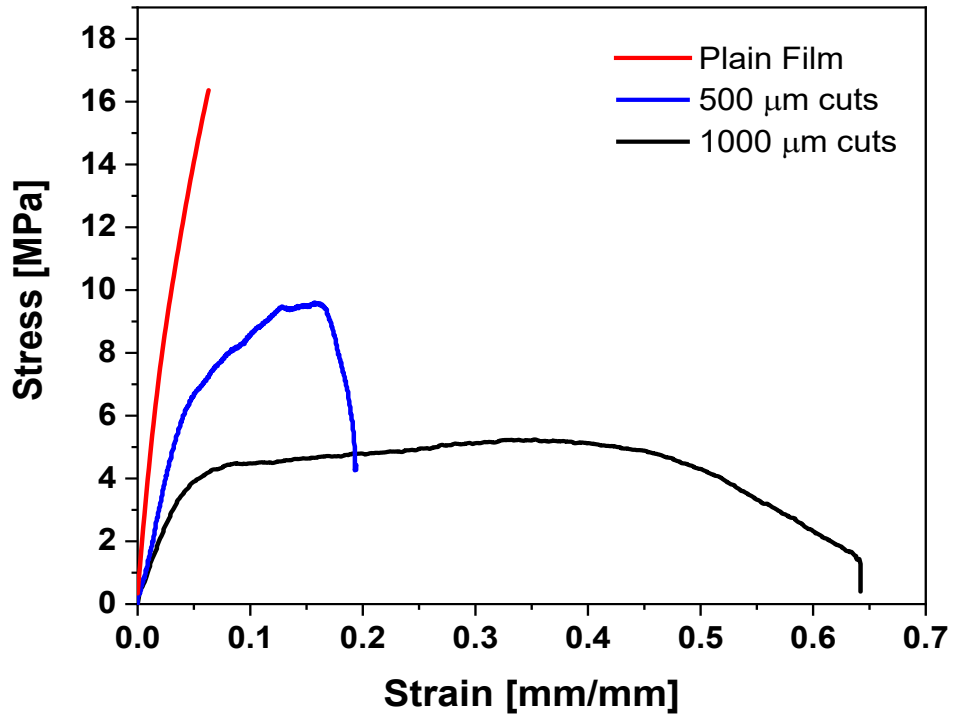

Figure 7.8 *Comparison of Stress vs. Strain curves of plain fibroin films with kirigami films with 500 and 1000 µm cut length.*

For thin films to be successfully applied to soft-biological samples, it is very important to reduce

the Young's modulus.[37] Reducing the modulus results in a decrease of the stress induced in devices due to strain generated during mechanical deformation. Due to the low Young's modulus of elastomeric materials such as PDMS (0.73 MPa), they have been widely adopted as materials of choice for the realization of flexible and stretchable electronics. The modulus of the kirigami films were calculated and compared to that of pristine silk films. Young's modulus (also known as elastic modulus) is defined as the ratio of the stress acting on a substance to the strain produced and was calculated using the formula- $E = \frac{\sigma}{\varepsilon}$, where E= Young's modulus, [MPa], σ = Uniaxial stress, [MPa], ε = Strain/ deformation [Dimensionless]

The Young's modulus at 0.1 strain was calculated for the kirigami and pristine films. It was found that modulus of the kirigami films were much lower that the pristine film. Additionally, the modulus decreased further upon increasing the length of the cuts from 500 μm to 1000 μm. The modulus values of the films are reported in **Table 7.1**. This proves the usefulness of Kirigami as a tool to fine tune the mechanical properties of nature derived polymeric materials.

Table 7.1 *Young's modulus of kirigami films with 500 and 1000 μm cut length and pristine films.*

Film Type	Young's modulus (MPa)
Plain Film	340
500 μm cuts	162
1000 μm cuts	112

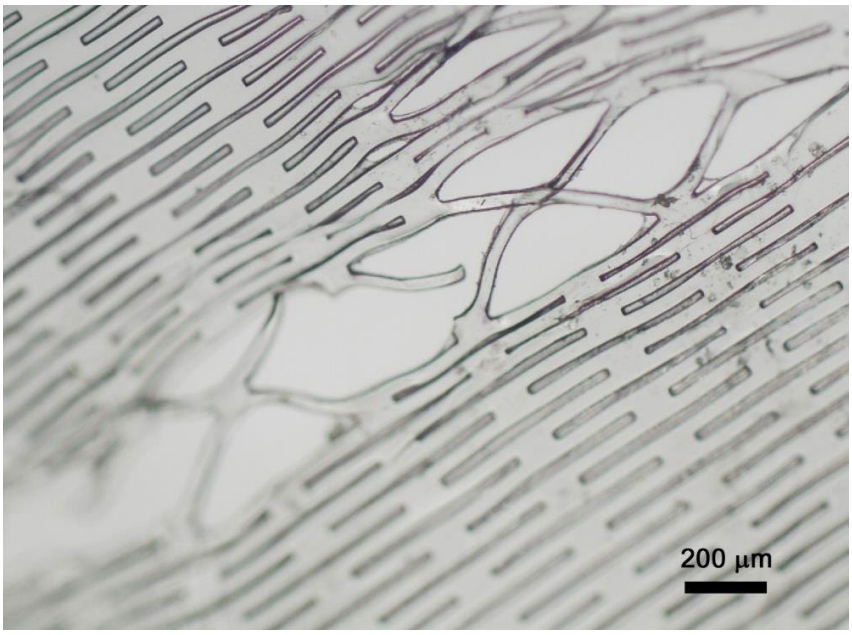

Figure 7.9 *Optical image showing one of the modes of failure on stretching a silk kirigami film with a slit geometry.*

Upon further investigation it was observed that the strain at which the pristine films failed (~7%, 0.07 mm/mm), the kirigami films underwent a mechanical transformation and entered a stretchable regime. It is hypothesized that beyond ~7% strain level, the tensile behavior of the films is governed by the kirigami cuts, whose absence in pristine films causes them to fail. The tolerance of strain beyond 7% is thus attributed to the opening of the kirigami cuts and not the inherent stretchability of the films. Further, it was observed that the kirigami films did not break at once and rather had a slow and gradual mode of failure. This was associated to the tearing of the kirigami films across the line of the cuts (**Figure 7.9**). Even though some of the cuts tear, the entire structure does not come apart at once. The stills from the tensile test with the point of failure (red arrow) under load are shown in **Figure 7.10**.

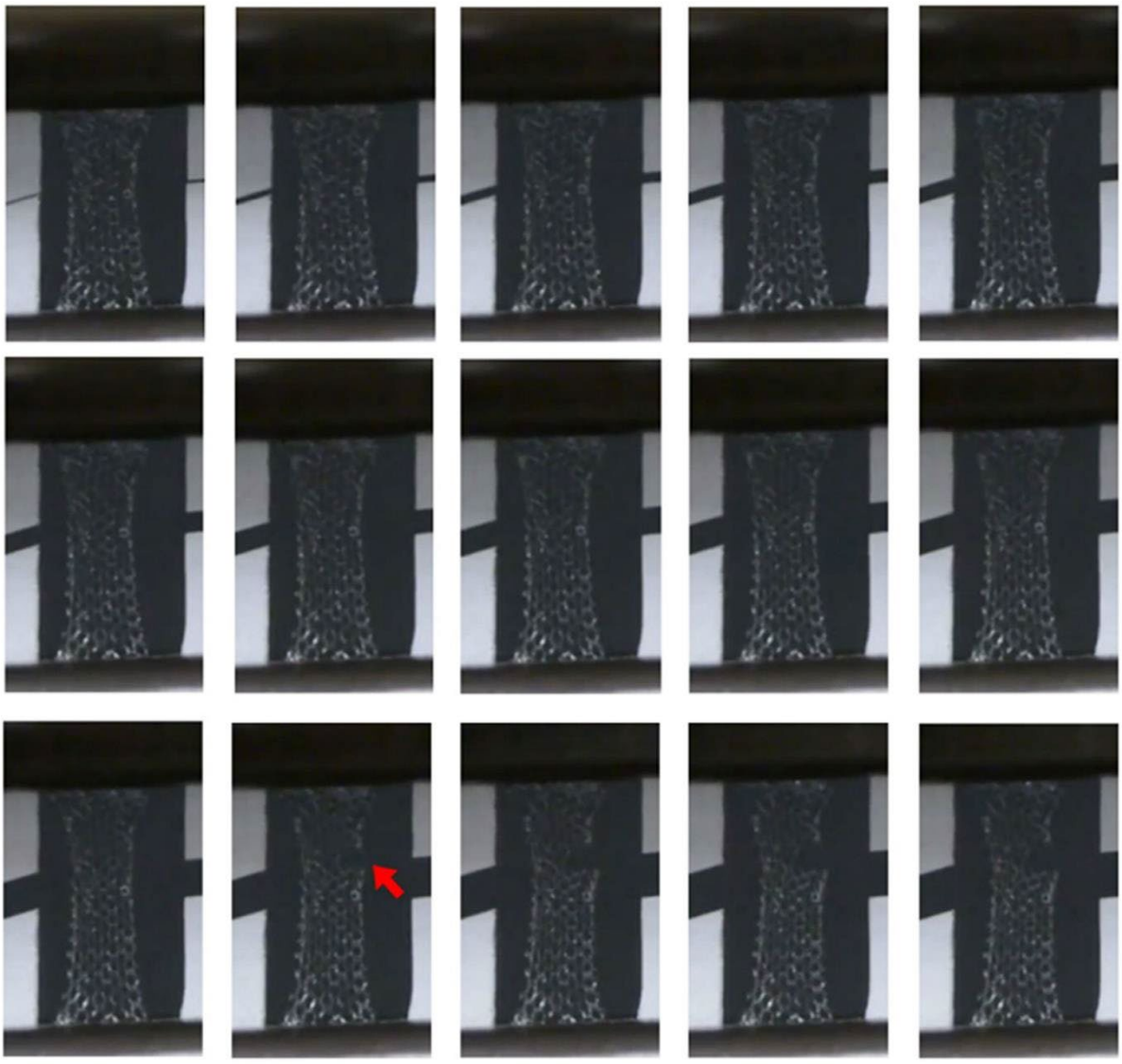

Figure 7.10 *Stills from video taken for kirigami stretch. The red arrow in the bottom row indicates the point of failure of the film. The failure then propagates through the entire film.*

7.3.3 Degradation of silk kirigami sheets

As discussed in previous chapters, the advantage of using nature derived organic materials for the realization of kirigami inspired stretchable systems is their ability to confer controlled biodegradability in physiological environments. The degradation of photocrosslinked silk films

were studies under enzymatic condition as a function of their loss in mass. In this work, the biodegradation of silk kirigami films were studied. An enzymatic biodegradation experiment was conducted on silk kirigami films incubated in the phosphate-buffered saline (PBS) solution with or without protease (control) at 37 °C. It was observed that kirigami films in the control set retained their structural integrity and flexibility whereas the films incubated in the enzyme started broking down after 10 days. This is consisted with the results previously observed in Chapter 2. Moreover, the degradation rate and subsequently the lifetime of the silk kirigami films can be tuned by varying the degree of crosslinking, film thickness and the number of cuts introduced on the films. Stretchable devices and bio interfaces with precisely engineered lifetimes can therefore be fabricated using the kirigami films, which can be useful as flexible biomimetic cellular constructs for tissue regeneration, drug delivery platforms, and biosensors.

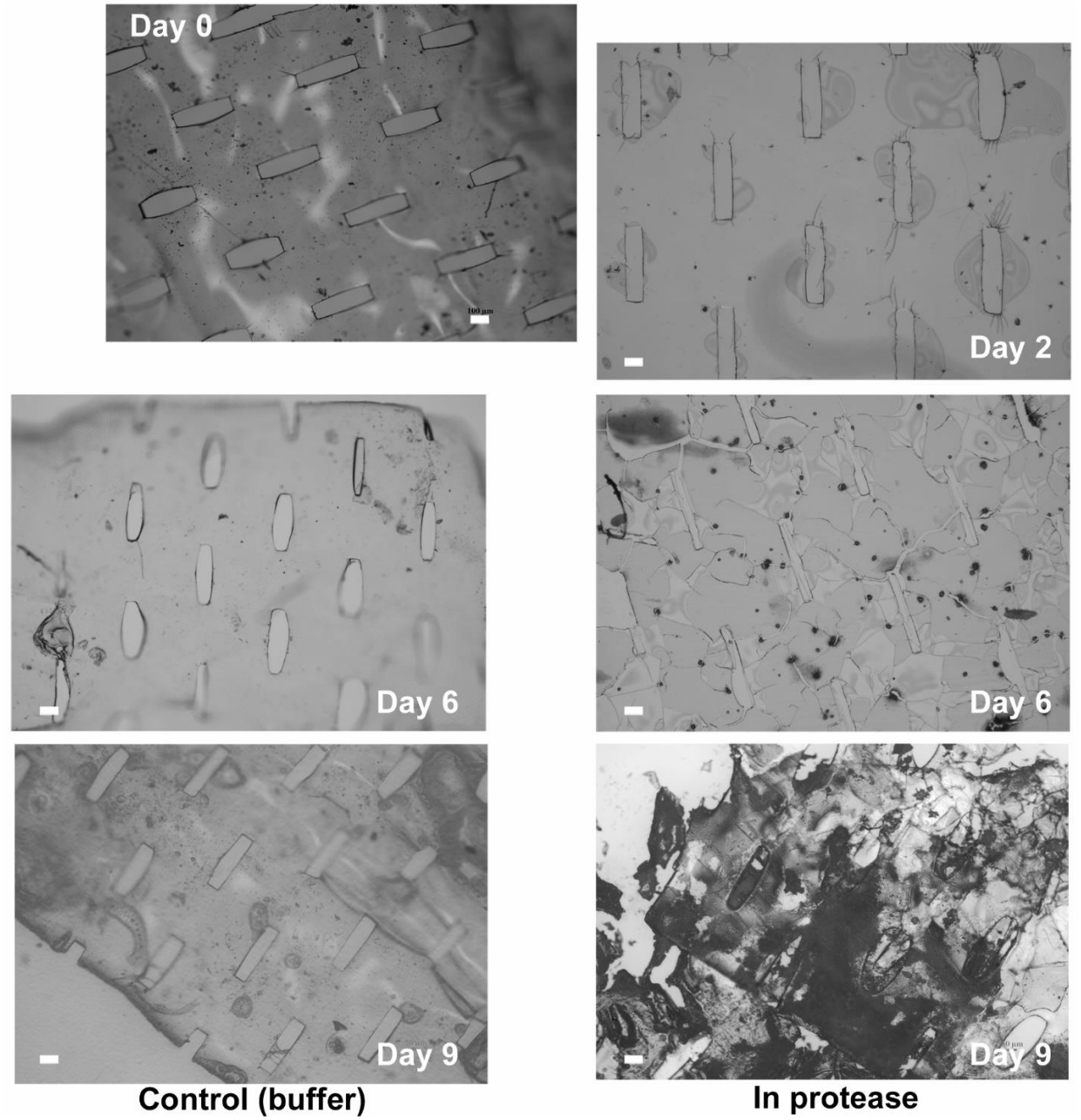

Figure 7.11 *Proteolytic degradation of silk kirigami sheets. On the left, films in (control) PBS buffer remain stable over several days (stored for a month with no loss in properties or morphology). On the right, a thin film (~10 μm) is completely biodegraded in solution of proteolytic enzyme (protease XIV), showing for the first time, a kirigami film that can be degraded. By controlling the thickness of the films, the rate of degradation can be controlled. Scale bar = 100 μm.*

7.3.4 Imparting conductivity to silk kirigami

So far, the development of a facile process was explored that can enhance the strain tolerance of a natural biopolymer (viz silk fibroin) has been discussed. They can be used as stretchable substrates on which devices are fabricated. However, the concept of kirigami can also be used to imbibe active functional components with enhanced strain tolerance and flexibility. Moreover, while many soft materials are not potentially degradable or resorbable, conducting polymer composites with silk and auxetic patches using chitosan have been used toward tissue-interfacing electronics and e-textiles.[315-318] In this work, multifunctional kirigami with intrinsic electrical conductivity is demonstrated on fully organic electroactive sheets fabricated using the PANI-photofibroin biocomposite developed in Chapter 3. A similar photolithographic procedure was followed by spin coating the PANI-photofibroin ink on silicon substrate and dying under a chemical hood. The samples were then exposed under UV light through a photomask and developed in 1M LiCl/ DMSO solution. After washing thoroughly using DI water, flexible, intrinsically electroactive kirigami sheets were formed.

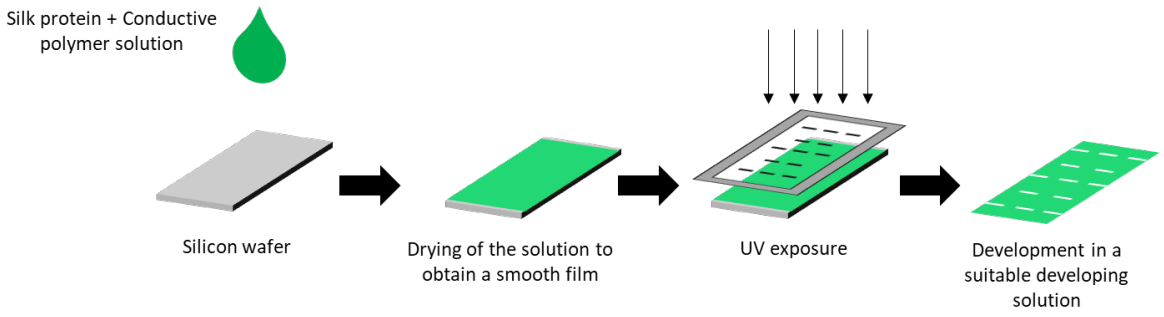

Figure 7.12 *Schematic diagram showing the fabrication of conducting silk kirigami sheets via photolithography.*

The PANI-photofibroin conductive composite is formed using a 1 wt.% dispersion of PANI in formic acid in which the photofibroin is mixed. As discussed previously, following the spin coating step, use of formic acid as the solvent increases the drying time to 20-30 mins which results in the formation of a thin crosslinked bottom layer. However, such effect was not observed in this case since the dark color of PANI prevented light from penetrating though the film during the drying process. Due to the same phenomenon, the higher concentration of PANI in the composite make the photolithography process difficult and affected the formation of cuts. Hence, 11% (w/w) PANI in the composite was found to be optimum for the formation of high-resolution cuts. The higher concentration of PANI in the composite can also cause the films to be brittle due to the presence of H-bonding between the benzene ring structures of the molecular backbone.

Following the fabrication of PANI-photofibroin based conductive kirigami sheets, the electrochemical properties of the sheets were evaluated as a function of mechanical deformation. In order to take electrochemical measurements, the films were connected to copper pads for electrical connections. *I-V* scans were taken on the sheets in the range of -0.5 V to 0.5V. while subjecting them to mechanical deformations. The experiments were performed on simple silt geometries with cut dimensions- width 100 μm, length 500 μm, gap spacing −500 μm, and gap width 500 μm, 25 μm thick, in order to maintain simplicity. In the first set of investigations, the kirigami sheets were compared with pristine PANI-photofibroin conductive sheets. Both films displayed excellent conductive behavior in the range of μS with kirigami films showing slightly better conductivity.

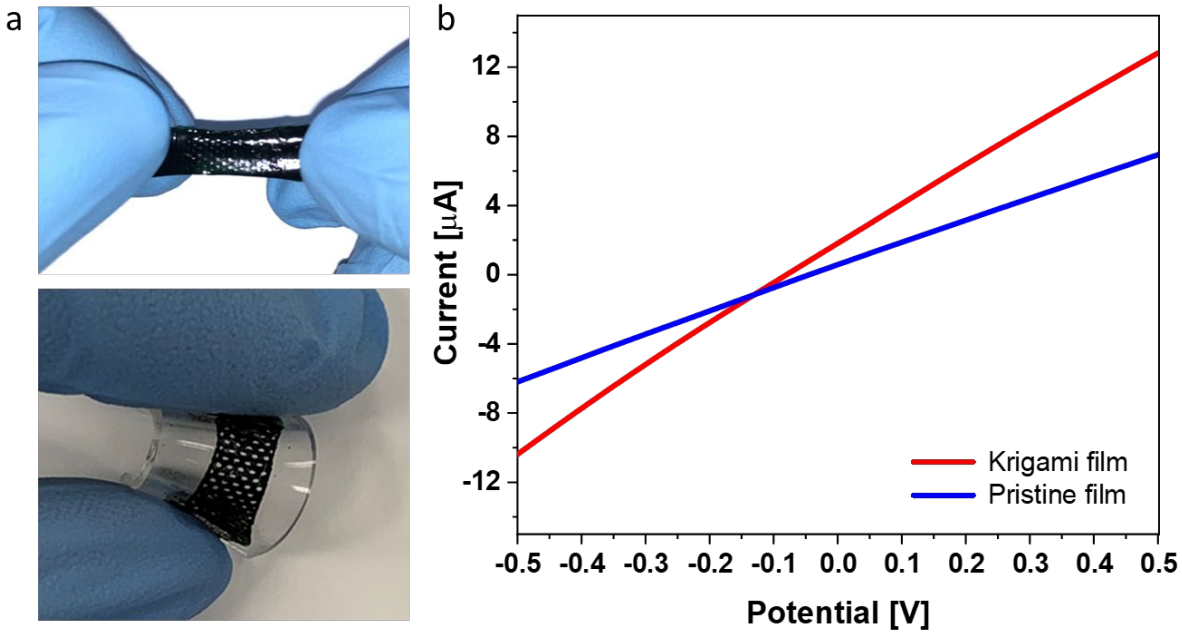

Figure 7.13 *a) PANI-photofibroin based conductive silk kirigami sheets and b) Kirigami films vs. pristine film I-V comparison.*

I-V scans were performed on the kirigami samples under relaxed condition and subjecting them to ~10% strain. It was found that the films retained their conductivity at such strain level although a decrease in conductance by ~40% was observed. This was attributed to the well-known phenomenon of reduced electron coupling due to the increase in π-π stacking distance which is caused due to stretching. In the final investigation, the films were placed on PDMS supports and subjected to ~50 – 55^{O} bends to simulate bends commonly encountered on the human body such as the knee. PDMS was chosen as a support to mimic a soft stretchable surface similar to human skin. Upon bending the conductance of the films decreased by ~22% from 3.03 to 2.35 μS which is again a result of the increase in π-π stacking distance. Further understanding of the effect of mechanical deformation of conductance can be useful in design strain or pressure sensors where the stain or deformations are measured as a function of current change.

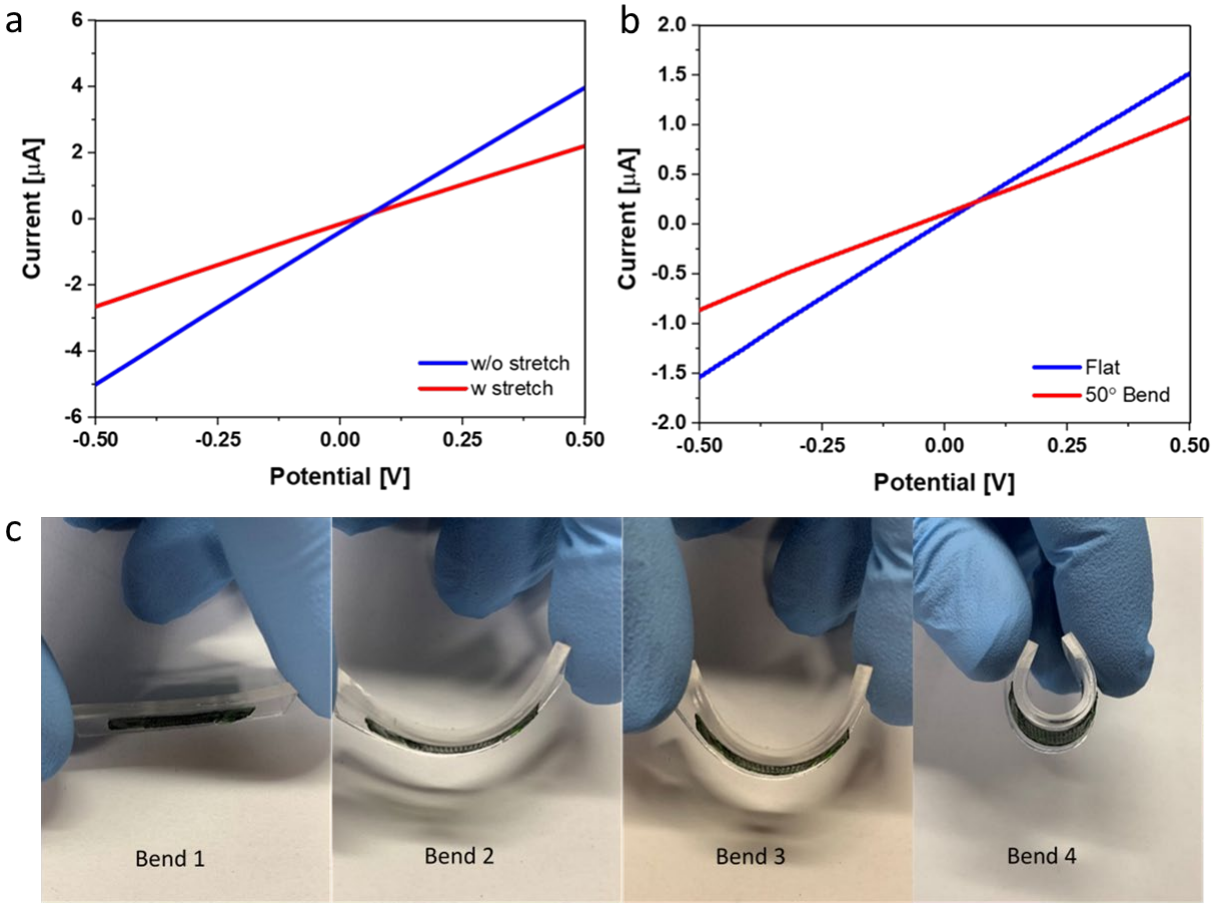

Figure 7.14 *a) Comparison of electrical behavior between stretched and unstretched conductive kirigami sheets. b) Comparison of behavior in relaxed (0°) and bent (50°) conditions. c) Bending experiment bend 2 is 20°, bend 3 is 50° (knee), bend 4 is 180°. Film thickness = 25 μm.*

The conducting kirigami sheets were used to complete an electrical circuit connected to a DC power source and an LED bulb to evaluate their capability to retain satisfactory electrical conductivity under mechanical deformations. It was observed that the kirigami films were able to retain their conductivity even under 180^{O} bends and twists can maintain current flow from the power source to the LED bulb. All these results indicate that such bioinspired and degradable systems can used to design skin-like devices while addressing sustainability in bioelectronics.

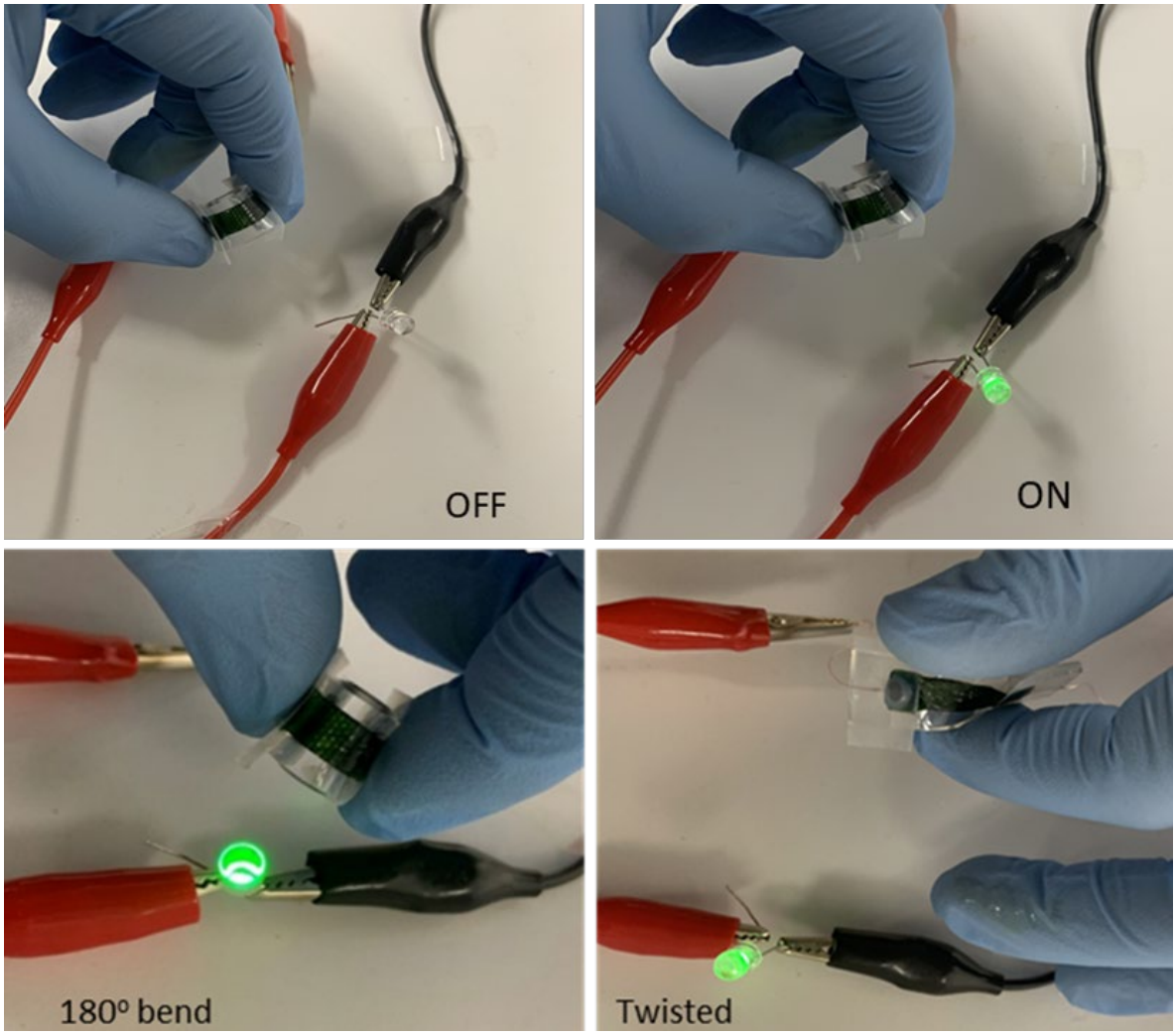

Figure 7.15 *Electrically conducting, mechanically robust kirigami sheets that can be bent and twisted. Films are conductive enough to illuminate a light-emitting diode (LED) under both bending and twisting.*

7.4 CONCLUSION

In summary, this chapter discusses the development of silk kirigami films to address the issue of stretchability and conformability at the bio interface. Through the formation of precisely designed cuts using benchtop photolithography, the silk fibroin films are imbued with enhanced strain

tolerance when compared to pristine films. Limited by the design of photomask, a large variety of cuts can be fabricated easily over a large-scale area in a single step process. Further, the mechanical properties of the silk fibroin films can be fine-tuned by modulating the cut dimensions. Importantly, the silk kirigami film can be degraded under enzymatic condition in a controllable fashion. This chapter also demonstrates the fabrication of conductive silk kirigami sheets by incorporating conducting polymer PANI in the fibroin matrix. The conductive kirigami sheets displayed excellent electrochemical properties. Additionally, the conductive kirigami sheets are also able to retain their electronic properties even under extreme mechanical deformations. These results suggest that silk kirigami can provide exceptional bioinspired and biodegradable structures toward flexible and stretchable biodevices.

[This chapter contains results that have been previously published: Sayantan Pradhan, Leonardo Ventura, Francesca Agostinacchio, Meng Xu, Ettore Barbieri, Antonella Motta, Nicola M. Pugno, Vamsi K. Yadavalli, "Biofunctional Silk Kirigami With Engineered Properties", ACS Appl. Mater. Interfaces 2020, 12, 11, 12436–12444.]

CHAPTER 8

CONCLUSIONS AND FUTURE WORK

8.1 CONCLUSIONS

The research discussed in this dissertation is focused on the exploration of the application of nature derived materials for the realization of functional biodevices. Among the host of biomaterials available in nature, silk and chitin were chosen as materials of choice, due to their well-established characteristics and prevalence in modern biomedical research. However, lack of proper fabrication techniques that can be combined with these materials have hindered their use beyond substrate materials for tissue engineering and biodegradable electronics. The combination of high throughput fabrication techniques along with doping with suitable conducting materials can enable their applications in functional biodevices.

The studies performed in this dissertation can be summarized as follows:

1. **Development of processing and microfabrication strategies that allow the formation of precise microstructures of silk and chitin on a variety of substrates.** Photolithography was chosen over other fabrication techniques as a tool to micropattern high resolution structures over large areas due to its simplicity, low cost, and prevalence in modern systems. A key step to this process is the chemical modification of silk proteins and chitin to impart photoactivity. Chemical modification of silk proteins and subsequent

silk protein photolithography were developed in prior work. In this work, fabrication of fibroin micropatterns on flexible fibroin sheets was demonstrated. This is possible due to the dissolution of photofibroin in different solvents. The micropatterned silk fibroin sheets can be degraded in a controlled fashion under proteolytic conditions. Similar to silk proteins, we showed synthesis and application of photocrosslinkable derivatives of chitin which can be photopatterned into 2D and 3D structures.

2. **Development of conductive composites with silk proteins that can be used for the realization of active functional components in flexible biodevices.**

   Inherently non-conductive photocrosslinkable silk proteins were combined with electroactive materials wherein the silk proteins provide a stable matrix in which the conducting polymer was crosslinked. The application of well-known conducting polymers PEDOT: PSS and PANI was explored due to their popularity in flexible bioelectronics research. PEDOT: PSS was combined with photosericin to develop a water processable conducting composite in which other biomolecules can be entrapped due to its benign nature. On the other hand, fibroin, due to its limited solubility, was combined with a dispersion of PANI in formic acid to form a conductive biocomposite with competitive performance metrics. Finally, the study was extended to the utilization of the natural semiconductor melanin to induce electrochemical activity in photofibroin.

3. **Development of silk based fully organic, flexible and degradable biosensors.**

   Electrochemically active silk based biocomposites using photolithography was utilized for the formation of fully organic and flexible biosensors. The photopatternability of the composites was harnessed to form conducting microarchitectures which act as the active sensing element in these biosensors. The devices can be formed on various synthetic

(PDMS) and natural (silk fibroin) flexible polymeric substrates. The devices formed are optically transparent, mechanically robust, degradable in a controlled fashion, and are formed using water based green processing techniques. Their usefulness in the detection of various electroactive and non-electroactive chemical analytes was studied. Further, they were used for the development of flexible and degradable temperature sensors.

4. **Application of structural design strategies to address conformability at the bio interface.**

   Conformability to soft nonplanar surfaces is a key challenge in the development of systems intended for use on the human body. Stretchability is a key requirement in such devices that allows higher strain levels without the loss of mechanical or electrochemical properties. The work presented in this dissertation aimed at applying the concept of kirigami for the formation of structural defects or cuts that enabled silk fibroin films to tolerate high strain. The cuts were formed in a simple single step process using photolithography. The mechanical properties of the films were modulated by altering the geometry and dimension of the cuts. By doping silk fibroin films with conducting polymer PANI, intrinsically conducting silk kirigami films were demonstrated, that were flexible, stretchable, and could be bent and twisted while retaining electrical properties.

In conclusion, the research emphasizes the usefulness of nature derived biopolymers in the development of fully organic functional devices for biomedical applications. Although biopolymers silk and chitin are widely studied for applications such as tissue engineering, regenerative medicine and drug delivery, their application in active functional devices is limited. Of specific interest is the use of such materials for the realization of sensors for the detection of

chemical and physical biomarkers which finds importance in disease diagnostics and therapeutics. However, the work done in this dissertation represents only a small part of the immense potential of these materials. There is further scope of these materials in unique applications which can pave the path forward.

8.2 FUTURE WORK

8.2.1 Deposition of ZnO on biopolymers

Among all the bioresorbable metal oxides, ZnO has gained much attention in opto /electronic/bio/chemical applications as a wide-band gap semi-conductor.[319] Combining ZnO with flexible biopolymers silk and chitin can lead to interesting applications. Initials attempts were aimed at forming ZnO thin films on silk fibroin. In the first step, ZnO was deposited on ITO glass using electrochemical methods from Zn $(NO_3)_2$ (Zinc nitrate) solution. A smooth ZnO film was obtained on the ITO within 15 minutes (**Figure 8.1a**). In the second step, the ZnO film was transferred to a flexible silk fibroin film (**Figure 8.1b**). Since highly conductive Aluminum-doped ZnO (AZO) has been successfully deposited on cellulose films using atomic layer deposition technique, such procedures can be easily translated to other polysaccharides such as chitin.[320]

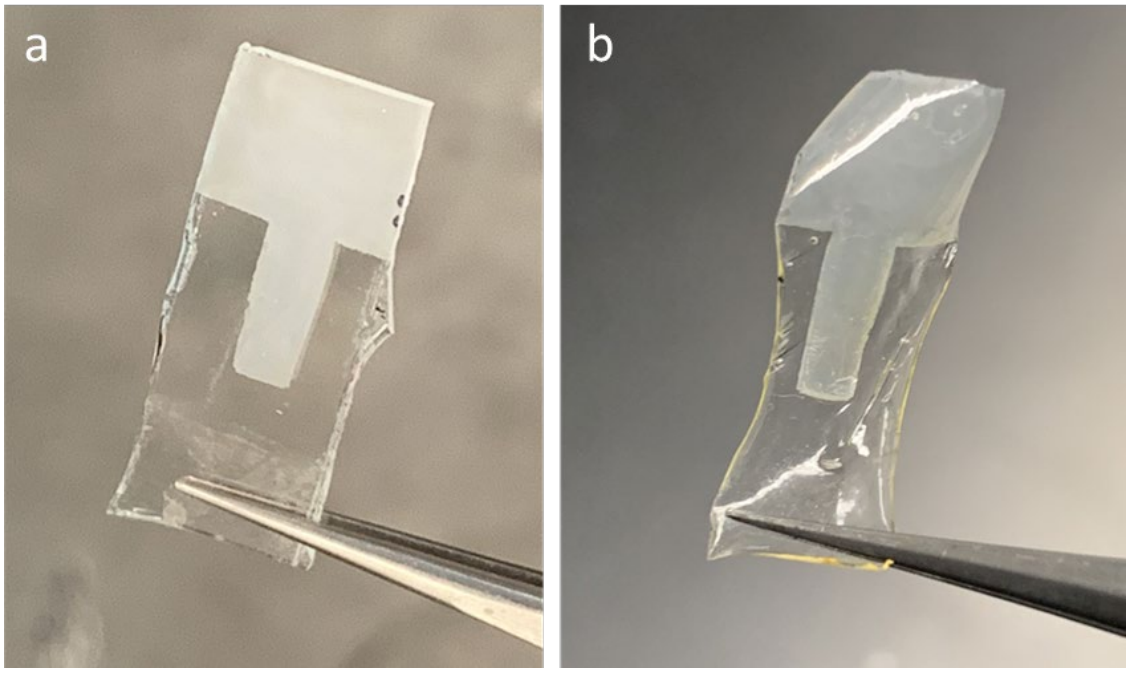

Figure 8.1 *a) electrochemically deposited ZnO film on ITO glass and b) ZnO layer transferred onto a flexible silk fibroin film.*

8.2.2 Silk based adhesives

One of the key challenges in interfacing flexible biodevices with the biological surfaces such as the human skin is crucial for obtaining accurate, reliable, and stable signals. Tissue adhesives are also of great importance in wound care where there are used as sealants for ruptured tissues.[321] Currently there are a wide variety of tissue adhesives to meet different clinical requirements and can be broadly classified as (1) natural tissue adhesives, (2) synthetic and semisynthetic tissue adhesive, and (3) biomimetic tissue adhesives.[322] Recently, calcium-modified silk fibroin was reported as adhesive for epidermal electronics.[323, 324] The Ca-modified silk exhibits physical adhesive characteristics because Ca ions act as both cross-links for random coil chains of silk via metal–chelate complexes and water-capturing points. Such biomimetic adhesives can be useful for the attachment of the biofunctional devices described in this work, where the adhesives themselves

degrade over time along with the devices.

8.2.3 Flexible and biodegradable sensors for sensing of analytes on a surface

The ability to detect targets of physiological importance from surfaces such as the human skin finds applications in healthcare and disease diagnostics. For example, such sensors can be mounted on the skin for detecting physical cues (temperature, strain, pressure) as well as valuable analytes found in sweat (Na^+, K^+, glucose, pH).[325] Flexible and biocompatible sensors find critical importance in wound monitoring, since they can conformally cover the wound and do not apply excessive force/stress to the healing area.[326] Therefore, the fully organic, flexible and biocompatible silk based sensors developed can be rationally extended towards the detection of chemical targets from a wound surface. Preliminary studies show that a 2-electrode system with GOx enzyme immobilized in the working electrode can be used for the detection of glucose on a surface. Following baseline measurement of 0 mM glucose, the sensor was placed on a surface containing glucose wherein an instant increase in current signal can be observed (**Figure 8.2**). However, significant work needs to be done on understanding and optimizing such systems. Critical performance metrics such as behavior under dynamic conditions (mechanical deformations, effect of temperature and humidity), accuracy, stability and operational lifetime have to be investigated meticulously before they can be successfully adopted in a clinical setting.

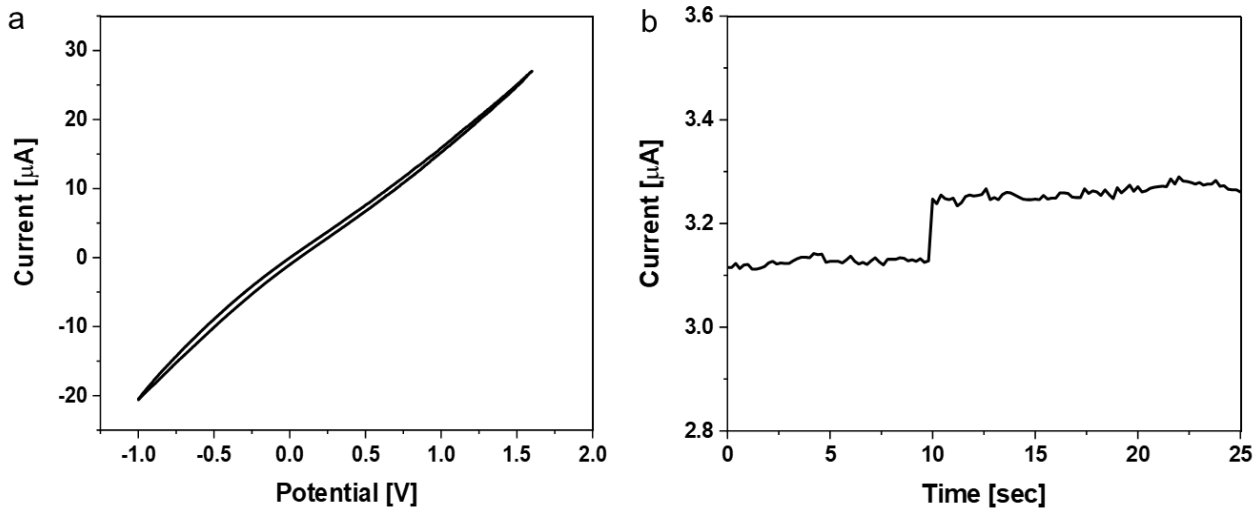

Figure 8.2 *Electrochemical measurements performed on a random surface using flexible silk-based biosensor. a) A stable CV obtained from PBS electrolyte on a surface and b) increase in current signal (after 10s) after the sensor was deployed on a surface with glucose.*

8.2.4 Silk based multianalyte sensors

The ability to detect multiple analytes using the same device can further enhance the continuous monitoring of human health, thus improving patient care. Such devices are expected to detect multiple analytes which high accuracy and sensitivity. Additionally, the specificity of each individual electrode to a particular analyte without any interference from other analytes should also be considered while engineering such systems. For this purpose, the ability to encapsulate large number of biorecognition molecules such as enzymes and antibodies can prove to be advantageous for the realization of such a platform. With the sensing techniques and platforms developed in this dissertation work, it is possible to envision a multianalyte sensor for the continuous monitoring of various chemical and physical targets using nature derived materials.

REFERENCES

[1] A. W. Lloyd, "Interfacial bioengineering to enhance surface biocompatibility," *Medical device technology,* vol. 13, pp. 18-21, 2002.

[2] U. G. Wegst, H. Bai, E. Saiz, A. P. Tomsia, and R. O. Ritchie, "Bioinspired structural materials," *Nature materials,* vol. 14, pp. 23-36, 2015.

[3] J. Aizenberg and P. Fratzl, "Biological and biomimetic materials," ed: Wiley Online Library, 2009.

[4] R. Feiner and T. Dvir, "Tissue–electronics interfaces: From implantable devices to engineered tissues," *Nature Reviews Materials,* vol. 3, p. 17076, 2018.

[5] S. Pradhan, A. K. Brooks, and V. K. Yadavalli, "Nature-derived materials for the fabrication of functional biodevices," *Materials Today Bio,* vol. 7, p. 100065, 2020/06/01/ 2020.

[6] C. Wang, K. Xia, Y. Zhang, and D. L. Kaplan, "Silk-based advanced materials for soft electronics," *Accounts of chemical research,* vol. 52, pp. 2916-2927, 2019.

[7] Q. Sun, B. Qian, K. Uto, J. Chen, X. Liu, and T. Minari, "Functional biomaterials towards flexible electronics and sensors," *Biosensors and Bioelectronics,* vol. 119, pp. 237-251, 2018.

[8] T. Someya, M. Kaltenbrunner, and T. Yokota, "Ultraflexible organic electronics," *MRS Bulletin,* vol. 40, pp. 1130-1137, 2015.

[9] T. Sekitani, U. Zschieschang, H. Klauk, and T. Someya, "Flexible organic transistors and circuits with extreme bending stability," *Nature materials,* vol. 9, pp. 1015-1022, 2010.

[10] C. Wang, C. Pan, and Z. Wang, "Electronic skin for closed-loop systems," *ACS nano,* vol. 13, pp. 12287-12293, 2019.

[11] D. Rus and M. T. Tolley, "Design, fabrication and control of soft robots," *Nature,* vol. 521, pp. 467-475, 2015.

[12] R. Balint, N. J. Cassidy, and S. H. Cartmell, "Conductive polymers: Towards a smart biomaterial for tissue engineering," *Acta biomaterialia,* vol. 10, pp. 2341-2353, 2014.

[13] Y. Chen, S. Lu, S. Zhang, Y. Li, Z. Qu, Y. Chen*, et al.*, "Skin-like biosensor system via electrochemical channels for noninvasive blood glucose monitoring," *Science advances,* vol. 3, p. e1701629, 2017.

[14] Y. Yang, X. Yang, Y. Tan, and Q. Yuan, "Recent progress in flexible and wearable bio-electronics based on nanomaterials," *Nano Research,* vol. 10, pp. 1560-1583, 2017.

[15] M. Xu, D. Obodo, and V. K. Yadavalli, "The design, fabrication, and applications of flexible biosensing devices," *Biosensors and Bioelectronics,* vol. 124, pp. 96-114, 2019.

[16] S. Bhatia, "Natural polymers vs synthetic polymer," in *Natural Polymer Drug Delivery Systems*, ed: Springer, 2016, pp. 95-118.

[17] M. Irimia-Vladu, "“Green” electronics: biodegradable and biocompatible materials and devices for sustainable future," *Chemical Society Reviews,* vol. 43, pp. 588-610, 2014.

[18] H.-S. Sun, Y.-C. Chiu, and W.-C. Chen, "Renewable polymeric materials for electronic applications," *Polymer Journal,* vol. 49, pp. 61-73, 2017.

[19] Y. Fang, L. Meng, A. Prominski, E. N. Schaumann, M. Seebald, and B. Tian, "Recent advances in bioelectronics chemistry," *Chemical Society Reviews,* vol. 49, pp. 7978-8035, 2020.

[20] Y. Zhou, C. Fuentes-Hernandez, T. M. Khan, J. C. Liu, J. Hsu, J. W. Shim*, et al.*, "Recyclable organic solar cells on cellulose nanocrystal substrates," *Sci Rep,* vol. 3, p. 1536, 2013.
[21] A. R. Murphy and D. L. Kaplan, "Biomedical applications of chemically-modified silk fibroin," *Journal of materials chemistry,* vol. 19, pp. 6443-6450, 2009.
[22] E. M. Pritchard and D. L. Kaplan, "Silk fibroin biomaterials for controlled release drug delivery," *Expert opinion on drug delivery,* vol. 8, pp. 797-811, 2011.
[23] J. G. Hardy and T. R. Scheibel, "Composite materials based on silk proteins," *Progress in Polymer Science,* vol. 35, pp. 1093-1115, 2010.
[24] G. Yao, C. Yin, Q. Wang, T. Zhang, S. Chen, C. Lu*, et al.*, "Flexible bioelectronics for physiological signals sensing and disease treatment," *Journal of Materiomics,* vol. 6, pp. 397-413, 2020/06/01/ 2020.
[25] S. Wang, J. Xu, W. Wang, G.-J. N. Wang, R. Rastak, F. Molina-Lopez*, et al.*, "Skin electronics from scalable fabrication of an intrinsically stretchable transistor array," *Nature,* vol. 555, pp. 83-88, 2018.
[26] A. Chortos, J. Liu, and Z. Bao, "Pursuing prosthetic electronic skin," *Nature materials,* vol. 15, pp. 937-950, 2016.
[27] C. Wang, X. Li, H. Hu, L. Zhang, Z. Huang, M. Lin*, et al.*, "Monitoring of the central blood pressure waveform via a conformal ultrasonic device," *Nature biomedical engineering,* vol. 2, pp. 687-695, 2018.
[28] Y. Yang and W. Gao, "Wearable and flexible electronics for continuous molecular monitoring," *Chemical Society Reviews,* vol. 48, pp. 1465-1491, 2019.
[29] C. Choi, Y. Lee, K. W. Cho, J. H. Koo, and D.-H. Kim, "Wearable and Implantable Soft Bioelectronics Using Two-Dimensional Materials," *Accounts of Chemical Research,* vol. 52, pp. 73-81, 2019/01/15 2019.
[30] T. R. Ray, J. Choi, A. J. Bandodkar, S. Krishnan, P. Gutruf, L. Tian*, et al.*, "Bio-integrated wearable systems: A comprehensive review," *Chemical reviews,* vol. 119, pp. 5461-5533, 2019.
[31] T. Someya, Z. Bao, and G. G. Malliaras, "The rise of plastic bioelectronics," *Nature,* vol. 540, pp. 379-385, 2016/12/01 2016.
[32] J. Koo, M. R. MacEwan, S.-K. Kang, S. M. Won, M. Stephen, P. Gamble*, et al.*, "Wireless bioresorbable electronic system enables sustained nonpharmacological neuroregenerative therapy," *Nature medicine,* vol. 24, pp. 1830-1836, 2018.
[33] S. H. Jin, S.-K. Kang, I.-T. Cho, S. Y. Han, H. U. Chung, D. J. Lee*, et al.*, "Water-Soluble Thin Film Transistors and Circuits Based on Amorphous Indium–Gallium–Zinc Oxide," *ACS Applied Materials & Interfaces,* vol. 7, pp. 8268-8274, 2015/04/22 2015.
[34] S. W. Hwang, J. K. Song, X. Huang, H. Cheng, S. K. Kang, B. H. Kim*, et al.*, "High-performance biodegradable/transient electronics on biodegradable polymers," *Advanced Materials,* vol. 26, pp. 3905-3911, 2014.
[35] R. Li, L. Wang, and L. Yin, "Materials and Devices for Biodegradable and Soft Biomedical Electronics," *Materials (Basel, Switzerland),* vol. 11, p. 2108, 2018.
[36] M. D. Dickey, "Stretchable and soft electronics using liquid metals," *Advanced Materials,* vol. 29, p. 1606425, 2017.
[37] J. A. Rogers, T. Someya, and Y. Huang, "Materials and mechanics for stretchable electronics," *science,* vol. 327, pp. 1603-1607, 2010.

[38] X. Li, W. Huang, G. Yao, M. Gao, X. Wei, Z. Liu*, et al.*, "Highly sensitive flexible tactile sensors based on microstructured multiwall carbon nanotube arrays," *Scripta Materialia,* vol. 129, pp. 61-64, 2017.
[39] A. Maziz, E. Özgür, C. Bergaud, and L. Uzun, "Progress in conducting polymers for biointerfacing and biorecognition applications," *Sensors and Actuators Reports,* vol. 3, p. 100035, 2021/11/01/ 2021.
[40] Y. Liu, K. He, G. Chen, W. R. Leow, and X. Chen, "Nature-inspired structural materials for flexible electronic devices," *Chemical reviews,* vol. 117, pp. 12893-12941, 2017.
[41] C. Hassler, T. Boretius, and T. Stieglitz, "Polymers for neural implants," *Journal of Polymer Science Part B: Polymer Physics,* vol. 49, pp. 18-33, 2011.
[42] M.-S. Hong, G.-M. Choi, J. Kim, J. Jang, B. Choi, J.-K. Kim*, et al.*, "Biomimetic Chitin–Silk Hybrids: An Optically Transparent Structural Platform for Wearable Devices and Advanced Electronics," *Advanced Functional Materials,* vol. 28, p. 1705480, 2018.
[43] K. Kim, M. Ha, B. Choi, S. H. Joo, H. S. Kang, J. H. Park*, et al.*, "Biodegradable, electro-active chitin nanofiber films for flexible piezoelectric transducers," *Nano Energy,* vol. 48, pp. 275-283, 2018/06/01/ 2018.
[44] R. K. Pal, S. C. Kundu, and V. K. Yadavalli, "Fabrication of Flexible, Fully Organic, Degradable Energy Storage Devices Using Silk Proteins," *ACS Applied Materials & Interfaces,* vol. 10, pp. 9620-9628, 2018/03/21 2018.
[45] V. R. Feig, H. Tran, and Z. Bao, "Biodegradable Polymeric Materials in Degradable Electronic Devices," *ACS Central Science,* vol. 4, pp. 337-348, 2018/03/28 2018.
[46] S. Pradhan, K. M. Moore, K. M. Ainslie, and V. K. Yadavalli, "Flexible, microstructured surfaces using chitin-derived biopolymers," *Journal of Materials Chemistry B,* vol. 7, pp. 5328-5335, 2019.
[47] H. Hamouche, S. Makhlouf, A. Chaouchi, and M. Laghrouche, "Humidity sensor based on keratin bio polymer film," *Sensors and Actuators A: Physical,* vol. 282, pp. 132-141, 2018.
[48] S. Moreno, M. Baniasadi, S. Mohammed, I. Mejia, Y. Chen, M. A. Quevedo-Lopez*, et al.*, "Biocompatible Collagen Films as Substrates for Flexible Implantable Electronics," *Advanced Electronic Materials,* vol. 1, p. 1500154, 2015.
[49] M. Xu, Y. Jiang, S. Pradhan, and V. K. Yadavalli, "Use of silk proteins to form organic, flexible, degradable biosensors for metabolite monitoring," *Front. Mater. 6: 331. doi: 10.3389/fmats,* 2019.
[50] A. Kumar, H. Gullapalli, K. Balakrishnan, A. Botello-Mendez, R. Vajtai, M. Terrones*, et al.*, "Flexible ZnO-Cellulose Nanocomposite for Multisource Energy Conversion," *Small,* vol. 7, pp. 2173-2178, 2011.
[51] E. Fortunato, N. Correia, P. Barquinha, L. Pereira, G. Goncalves, and R. Martins, "High-Performance Flexible Hybrid Field-Effect Transistors Based on Cellulose Fiber Paper," *IEEE Electron Device Letters,* vol. 29, pp. 988-990, 2008/09// 2008.
[52] S. Liu, Y. Qiu, W. Yu, and H. Zhang, "Highly Stretchable and Self-Healing Strain Sensor Based on Gellan Gum Hybrid Hydrogel for Human Motion Monitoring," *ACS Applied Polymer Materials,* vol. 2, pp. 1325-1334, 2020/03/13 2020.
[53] M. Rinaudo, "Main properties and current applications of some polysaccharides as biomaterials," *Polymer International,* vol. 57, pp. 397-430, 2008.
[54] P. Scott, *The book of silk*, 1993.
[55] T. M. Muffly, A. P. Tizzano, and M. D. Walters, "The history and evolution of sutures in pelvic surgery," *J R Soc Med,* vol. 104, pp. 107-12, Mar 2011.

[56] T. D. Sutherland, J. H. Young, S. Weisman, C. Y. Hayashi, and D. J. Merritt, "Insect silk: one name, many materials," *Annual review of entomology,* vol. 55, pp. 171-188, 2010.
[57] G. Bhat, *Structure and properties of high-performance fibers*: Woodhead Publishing, 2016.
[58] G. H. Altman, F. Diaz, C. Jakuba, T. Calabro, R. L. Horan, J. Chen*, et al.*, "Silk-based biomaterials," *Biomaterials,* vol. 24, pp. 401-16, Feb 2003.
[59] D. Kaplan and K. McGrath, *Protein-based materials*: Springer Science & Business Media, 1997.
[60] D. N. Rockwood, R. C. Preda, T. Yücel, X. Wang, M. L. Lovett, and D. L. Kaplan, "Materials fabrication from Bombyx mori silk fibroin," *Nature protocols,* vol. 6, p. 1612, 2011.
[61] Y. Qi, H. Wang, K. Wei, Y. Yang, R. Y. Zheng, I. S. Kim*, et al.*, "A Review of Structure Construction of Silk Fibroin Biomaterials from Single Structures to Multi-Level Structures," *Int J Mol Sci,* vol. 18, Mar 3 2017.
[62] C. Z. Zhou, F. Confalonieri, N. Medina, Y. Zivanovic, C. Esnault, T. Yang*, et al.*, "Fine organization of Bombyx mori fibroin heavy chain gene," *Nucleic Acids Res,* vol. 28, pp. 2413-9, Jun 15 2000.
[63] W. Huang, S. Ling, C. Li, F. G. Omenetto, and D. L. Kaplan, "Silkworm silk-based materials and devices generated using bio-nanotechnology," *Chem Soc Rev,* vol. 47, pp. 6486-6504, Aug 28 2018.
[64] A. T. Nguyen, Q. L. Huang, Z. Yang, N. Lin, G. Xu, and X. Y. Liu, "Crystal networks in silk fibrous materials: from hierarchical structure to ultra performance," *Small,* vol. 11, pp. 1039-54, Mar 2015.
[65] R. Liu, Q. Deng, Z. Yang, D. Yang, M. Y. Han, and X. Y. Liu, "“Nano-Fishnet” Structure Making Silk Fibers Tougher," *Advanced Functional Materials,* vol. 26, pp. 5534-5541, 2016.
[66] Z. Shao and F. Vollrath, "Surprising strength of silkworm silk," *Nature,* vol. 418, p. 741, Aug 15 2002.
[67] J. Pérez-Rigueiro, C. Viney, J. Llorca, and M. Elices, "Silkworm silk as an engineering material," *Journal of Applied Polymer Science,* vol. 70, pp. 2439-2447, 1998.
[68] J. Melke, S. Midha, S. Ghosh, K. Ito, and S. Hofmann, "Silk fibroin as biomaterial for bone tissue engineering," *Acta Biomater,* vol. 31, pp. 1-16, Feb 2016.
[69] B. Kundu, N. E. Kurland, S. Bano, C. Patra, F. B. Engel, V. K. Yadavalli*, et al.*, "Silk proteins for biomedical applications: Bioengineering perspectives," *Progress in polymer science,* vol. 39, pp. 251-267, 2014.
[70] M. Santin, A. Motta, G. Freddi, and M. Cannas, "In vitro evaluation of the inflammatory potential of the silk fibroin," *Journal of Biomedical Materials Research,* vol. 46, pp. 382-389, 1999.
[71] K. Numata, P. Cebe, and D. L. Kaplan, "Mechanism of enzymatic degradation of beta-sheet crystals," *Biomaterials,* vol. 31, pp. 2926-2933, 2010.
[72] L. Fernández-García, N. Marí-Buyé, J. A. Barios, R. Madurga, M. Elices, J. Pérez-Rigueiro*, et al.*, "Safety and tolerability of silk fibroin hydrogels implanted into the mouse brain," *Acta biomaterialia,* vol. 45, pp. 262-275, 2016.
[73] Y. Hu, Q. Zhang, R. You, L. Wang, and M. Li, "The relationship between secondary structure and biodegradation behavior of silk fibroin scaffolds," *Advances in Materials Science and Engineering,* vol. 2012, 2012.

[74] R. F. Pereira, M. M. Silva, and V. de Zea Bermudez, "Bombyx mori silk fibers: an outstanding family of materials," *Macromolecular Materials and Engineering,* vol. 300, pp. 1171-1198, 2015.
[75] L.-D. Koh, Y. Cheng, C.-P. Teng, Y.-W. Khin, X.-J. Loh, S.-Y. Tee*, et al.*, "Structures, mechanical properties and applications of silk fibroin materials," *Progress in Polymer Science,* vol. 46, pp. 86-110, 2015/07/01/ 2015.
[76] M. Gulrajani, "Sericin: A Bio-moecule of Value," in *Souveni 20^< th> congress of the international sericultural commission Bangalore, India 15-18^< th> December 2005*, 2005, pp. 21-29.
[77] M. Padamwar and A. Pawar, "Silk sericin and its applications: A review," 2004.
[78] T. Gamo, T. Inokuchi, and H. Laufer, "Polypeptides of fibroin and sericin secreted from the different sections of the silk gland in Bombyx mori," *Insect Biochemistry,* vol. 7, pp. 285-295, 1977/01/01/ 1977.
[79] K. KATAOKA, "On the solubility of sericin in water," *The Journal of Sericultural Science of Japan,* vol. 46, pp. 227-230, 1977.
[80] S. Nayak, S. Talukdar, and S. C. Kundu, "Potential of 2D crosslinked sericin membranes with improved biostability for skin tissue engineering," *Cell and Tissue Research,* vol. 347, pp. 783-794, 2012/03/01 2012.
[81] H. Oh, J. Y. Lee, M. K. Kim, I. C. Um, and K. H. Lee, "Refining hot-water extracted silk sericin by ethanol-induced precipitation," *International Journal of Biological Macromolecules,* vol. 48, pp. 32-37, 2011.
[82] B. Panilaitis, G. H. Altman, J. Chen, H. J. Jin, V. Karageorgiou, and D. L. Kaplan, "Macrophage responses to silk," *Biomaterials,* vol. 24, pp. 3079-85, Aug 2003.
[83] P. Aramwit, S. Kanokpanont, W. De-Eknamkul, and T. Srichana, "Monitoring of inflammatory mediators induced by silk sericin," *J Biosci Bioeng,* vol. 107, pp. 556-61, May 2009.
[84] L. Lamboni, M. Gauthier, G. Yang, and Q. Wang, "Silk sericin: A versatile material for tissue engineering and drug delivery," *Biotechnol Adv,* vol. 33, pp. 1855-67, Dec 2015.
[85] M. Rinaudo, "Chitin and chitosan: Properties and applications," *Progress in polymer science,* vol. 31, pp. 603-632, 2006.
[86] I. Younes and M. Rinaudo, "Chitin and chitosan preparation from marine sources. Structure, properties and applications," *Mar Drugs,* vol. 13, pp. 1133-74, Mar 2 2015.
[87] K. Kurita, "Controlled functionalization of the polysaccharide chitin," *Progress in polymer science,* vol. 26, pp. 1921-1971, 2001.
[88] D. Elieh-Ali-Komi and M. R. Hamblin, "Chitin and Chitosan: Production and Application of Versatile Biomedical Nanomaterials," *Int J Adv Res (Indore),* vol. 4, pp. 411-427, Mar 2016.
[89] L. R. R. Berger, T. C. M. Stamford, T. M. Stamford-Arnaud, S. R. C. De Alcântara, A. C. Da Silva, A. M. Da Silva*, et al.*, "Green conversion of agroindustrial wastes into chitin and chitosan by Rhizopus arrhizus and Cunninghamella elegans strains," *International journal of molecular sciences,* vol. 15, pp. 9082-9102, 2014.
[90] M. Benhabiles, N. Abdi, N. Drouiche, H. Lounici, A. Pauss, M. F. Goosen*, et al.*, "Protein recovery by ultrafiltration during isolation of chitin from shrimp shells Parapenaeus longirostris," *Food Hydrocolloids,* vol. 32, pp. 28-34, 2013.
[91] P. R. Austin, "Chitin solvents and solubility parameters," in *Chitin, Chitosan, and Related Enzymes*, ed: Elsevier, 1984, pp. 227-237.

[92] V. Zargar, M. Asghari, and A. Dashti, "A Review on Chitin and Chitosan Polymers: Structure, Chemistry, Solubility, Derivatives, and Applications," *ChemBioEng Reviews,* vol. 2, pp. 204-226, 2015.
[93] U. Shahbaz, "Chitin, Characteristic, Sources, and Biomedical Application," *Curr Pharm Biotechnol,* vol. 21, pp. 1433-1443, 2020.
[94] F. Ding, H. Deng, Y. Du, X. Shi, and Q. Wang, "Emerging chitin and chitosan nanofibrous materials for biomedical applications," *Nanoscale,* vol. 6, pp. 9477-9493, 2014.
[95] F. Croisier and C. Jérôme, "Chitosan-based biomaterials for tissue engineering," *European polymer journal,* vol. 49, pp. 780-792, 2013.
[96] X. Liu, L. Ma, Z. Mao, and C. Gao, "Chitosan-based biomaterials for tissue repair and regeneration," *Chitosan for Biomaterials II,* pp. 81-127, 2011.
[97] K. Madhumathi, P. S. Kumar, S. Abhilash, V. Sreeja, H. Tamura, K. Manzoor*, et al.*, "Development of novel chitin/nanosilver composite scaffolds for wound dressing applications," *Journal of Materials Science: Materials in Medicine,* vol. 21, pp. 807-813, 2010.
[98] S. Beier and S. Bertilsson, "Bacterial chitin degradation—mechanisms and ecophysiological strategies," *Frontiers in microbiology,* vol. 4, p. 149, 2013.
[99] S. Nikolov, H. Fabritius, M. Petrov, M. Friák, L. Lymperakis, C. Sachs*, et al.*, "Robustness and optimal use of design principles of arthropod exoskeletons studied by ab initio-based multiscale simulations," *J Mech Behav Biomed Mater,* vol. 4, pp. 129-45, Feb 2011.
[100] C. Sun, X. Li, J. Zhao, Z. Cai, and F. Ge, "A freestanding polypyrrole hybrid electrode supported by conducting silk fabric coated with PEDOT: PSS and MWCNTs for high-performance supercapacitor," *Electrochimica Acta,* vol. 317, pp. 42-51, 2019.
[101] S. Wang, H. Ning, N. Hu, Y. Liu, F. Liu, R. Zou*, et al.*, "Environmentally-Friendly and Multifunctional Graphene-Silk Fabric Strain Sensor for Human-Motion Detection," *Advanced Materials Interfaces,* vol. 7, p. 1901507, 2020.
[102] S. Tsukada, H. Nakashima, and K. Torimitsu, "Conductive polymer combined silk fiber bundle for bioelectrical signal recording," *PloS one,* vol. 7, p. e33689, 2012.
[103] R. K. Pal, A. A. Farghaly, C. Wang, M. M. Collinson, S. C. Kundu, and V. K. Yadavalli, "Conducting polymer-silk biocomposites for flexible and biodegradable electrochemical sensors," *Biosensors and Bioelectronics,* vol. 81, pp. 294-302, 2016.
[104] S. T. Dubas, P. Kumlangdudsana, and P. Potiyaraj, "Layer-by-layer deposition of antimicrobial silver nanoparticles on textile fibers," *Colloids and Surfaces A: Physicochemical and Engineering Aspects,* vol. 289, pp. 105-109, 2006.
[105] X. Qin, Y. Peng, P. Li, K. Cheng, Z. Wei, P. Liu*, et al.*, "Silk fibroin and ultra-long silver nanowire based transparent, flexible and conductive composite film and its Temperature-Dependent resistance," *International Journal of Optomechatronics,* vol. 13, pp. 41-50, 2019.
[106] J. He and T. Kunitake, "Preparation and Thermal Stability of Gold Nanoparticles in Silk-Templated Porous Filaments of Titania and Zirconia," *Chemistry of Materials,* vol. 16, pp. 2656-2661, 2004.
[107] C. Guo, G. N. Hall, J. B. Addison, and J. L. Yarger, "Gold nanoparticle-doped silk film as biocompatible SERS substrate," *RSC advances,* vol. 5, pp. 1937-1942, 2015.
[108] S. K. Samal, M. Dash, T. Shelyakova, H. A. Declercq, M. Uhlarz, M. Bañobre-López*, et al.*, "Biomimetic magnetic silk scaffolds," *ACS applied materials & interfaces,* vol. 7, pp. 6282-6292, 2015.

[109] J.-T. Wang, L.-L. Li, L. Feng, J.-F. Li, L.-H. Jiang, and Q. Shen, "Directly obtaining pristine magnetic silk fibers from silkworm," *International journal of biological macromolecules,* vol. 63, pp. 205-209, 2014.
[110] X. Hu, J. Li, and Y. Bai, "Fabrication of high strength graphene/regenerated silk fibroin composite fibers by wet spinning," *Materials Letters,* vol. 194, pp. 224-226, 2017.
[111] J. Guan, C. Q. Yang, and G. Chen, "Formaldehyde-free flame retardant finishing of silk using a hydroxyl-functional organophosphorus oligomer," *Polymer Degradation and Stability,* vol. 94, pp. 450-455, 2009.
[112] T. Arai, G. Freddi, R. Innocenti, D. Kaplan, and M. Tsukada, "Acylation of silk and wool with acid anhydrides and preparation of water-repellent fibers," *Journal of Applied Polymer Science,* vol. 82, pp. 2832-2841, 2001.
[113] S. Davarpanah, N. M. Mahmoodi, M. Arami, H. Bahrami, and F. Mazaheri, "Environmentally friendly surface modification of silk fiber: Chitosan grafting and dyeing," *Applied Surface Science,* vol. 255, pp. 4171-4176, 2009.
[114] Y. Gotoh, M. Tsukada, N. Minoura, and Y. Imai, "Synthesis of poly (ethylene glycol)-silk fibroin conjugates and surface interaction between L-929 cells and the conjugates," *Biomaterials,* vol. 18, pp. 267-271, 1997.
[115] S. Manchineella, G. Thrivikraman, B. Basu, and T. Govindaraju, "Surface-functionalized silk fibroin films as a platform to guide neuron-like differentiation of human mesenchymal stem cells," *ACS applied materials & interfaces,* vol. 8, pp. 22849-22859, 2016.
[116] K. Cai, K. Yao, S. Lin, Z. Yang, X. Li, H. Xie*, et al.*, "Poly (D, L-lactic acid) surfaces modified by silk fibroin: effects on the culture of osteoblast in vitro," *Biomaterials,* vol. 23, pp. 1153-1160, 2002.
[117] A. T. Ramaprasad and V. Rao, "Chitin–polyaniline blend as humidity sensor," *Sensors and Actuators B: Chemical,* vol. 148, pp. 117-125, 2010/06/30/ 2010.
[118] S. Anandhavelu and S. Thambidurai, "Single step synthesis of chitin/chitosan-based graphene oxide–ZnO hybrid composites for better electrical conductivity and optical properties," *Electrochimica Acta,* vol. 90, pp. 194-202, 2013/02/15/ 2013.
[119] C. Chen, C. Yang, S. Li, and D. Li, "A three-dimensionally chitin nanofiber/carbon nanotube hydrogel network for foldable conductive paper," *Carbohydrate Polymers,* vol. 134, pp. 309-313, 2015/12/10/ 2015.
[120] Y. Liu, F. Wu, X. Zhao, and M. Liu, "High-Performance Strain Sensors Based on Spirally Structured Composites with Carbon Black, Chitin Nanocrystals, and Natural Rubber," *ACS Sustainable Chemistry & Engineering,* vol. 6, pp. 10595-10605, 2018/08/06 2018.
[121] E. Ohashi and I. Karube, "Development of a thin membrane glucose sensor using β-type crystalline chitin for implantable biosensor," *Journal of Biotechnology,* vol. 40, pp. 13-19, 1995/05/15/ 1995.
[122] K. Sugawara, T. Takano, H. Fukushi, S. Hoshi, K. Akatsuka, H. Kuramitz*, et al.*, "Glucose sensing by a carbon-paste electrode containing chitin modified with glucose oxidase," *Journal of Electroanalytical Chemistry,* vol. 482, pp. 81-86, 2000/02/29/ 2000.
[123] E. Ohashi and T. Koriyama, "Simple and mild preparation of an enzyme-immobilized membrane for a biosensor using β-type crystalline chitin," *Analytica Chimica Acta,* vol. 262, pp. 19-25, 1992/06/01/ 1992.
[124] C. Brysch, E. Wold, M. Patterson, R. O. Olivares, J. Eberth, and F. R. Hernandez, "Chitosan and chitosan composites reinforced with carbon nanostructures," *Journal of alloys and compounds,* vol. 615, pp. S515-S521, 2014.

[125] W. Yue, R. He, P. Yao, and Y. Wei, "Ultraviolet radiation-induced accelerated degradation of chitosan by ozone treatment," *Carbohydrate polymers,* vol. 77, pp. 639-642, 2009.
[126] V. K. Mourya and N. N. Inamdar, "Chitosan-modifications and applications: Opportunities galore," *Reactive and Functional Polymers,* vol. 68, pp. 1013-1051, 2008/06/01/ 2008.
[127] M. O. Abd El-Magied, A. A. Galhoum, A. A. Atia, A. A. Tolba, M. S. Maize, T. Vincent*, et al.*, "Cellulose and chitosan derivatives for enhanced sorption of erbium(III)," *Colloids and Surfaces A: Physicochemical and Engineering Aspects,* vol. 529, pp. 580-593, 2017/09/20/ 2017.
[128] R. Jayakumar, M. Prabaharan, R. L. Reis, and J. F. Mano, "Graft copolymerized chitosan—present status and applications," *Carbohydrate Polymers,* vol. 62, pp. 142-158, 2005/11/10/ 2005.
[129] J. Luo, X. Wang, B. Xia, and J. Wu, "Preparation and Characterization of Quaternized Chitosan Under Microwave Irradiation," *Journal of Macromolecular Science, Part A,* vol. 47, pp. 952-956, 2010/07/30 2010.
[130] X. Qu, A. Wirsén, and A. C. Albertsson, "Synthesis and characterization of pH-sensitive hydrogels based on chitosan and D, L-lactic acid," *Journal of Applied Polymer Science,* vol. 74, pp. 3193-3202, 1999.
[131] K. Kurita, M. Inoue, and M. Harata, "Graft copolymerization of methyl methacrylate onto mercaptochitin and some properties of the resulting hybrid materials," *Biomacromolecules,* vol. 3, pp. 147-152, 2002.
[132] N. E. Kurland, T. Dey, S. C. Kundu, and V. K. Yadavalli, "Precise Patterning of Silk Microstructures Using Photolithography," *Advanced Materials,* vol. 25, pp. 6207-6212, 2013/11/01/ 2013.
[133] N. E. Kurland, T. Dey, C. Wang, S. C. Kundu, and V. K. Yadavalli, "Silk Protein Lithography as a Route to Fabricate Sericin Microarchitectures," *Advanced Materials,* vol. 26, pp. 4431-4437, 2014.
[134] K. T. Tran and T. D. Nguyen, "Lithography-based methods to manufacture biomaterials at small scales," *Journal of Science: Advanced Materials and Devices,* vol. 2, pp. 1-14, 2017.
[135] M. A. Brenckle, H. Tao, S. Kim, M. Paquette, D. L. Kaplan, and F. G. Omenetto, "Protein-Protein Nanoimprinting of Silk Fibroin Films," *Advanced Materials,* vol. 25, pp. 2409-2414, 2013.
[136] B. D. Gates, Q. Xu, M. Stewart, D. Ryan, C. G. Willson, and G. M. Whitesides, "New approaches to nanofabrication: molding, printing, and other techniques," *Chemical reviews,* vol. 105, pp. 1171-1196, 2005.
[137] J. Voldman, M. L. Gray, and M. A. Schmidt, "Microfabrication in Biology and Medicine," *Annual Review of Biomedical Engineering,* vol. 1, pp. 401-425, 1999.
[138] K. Tsioris, H. Tao, M. Liu, J. A. Hopwood, D. L. Kaplan, R. D. Averitt*, et al.*, "Rapid transfer-based micropatterning and dry etching of silk microstructures," *Advanced materials (Deerfield Beach, Fla.),* vol. 23, pp. 2015-2019, 2011.
[139] R. K. Pal and V. K. Yadavalli, "Silk protein nanowires patterned using electron beam lithography," *Nanotechnology,* vol. 29, p. 335301, 2018.
[140] S. Kim, B. Marelli, M. A. Brenckle, A. N. Mitropoulos, E.-S. Gil, K. Tsioris*, et al.*, "All-water-based electron-beam lithography using silk as a resist," *Nature nanotechnology,* vol. 9, pp. 306-310, 2014.
[141] A. De Silva and C. K. Ober, "Patterning by photolithography," *Functional Polymer Films,* vol. 2, pp. 475-499, 2011.

[142] L. Rassaei, P. S. Singh, and S. G. Lemay, "Lithography-based nanoelectrochemistry," ed: ACS Publications, 2011.
[143] D. Khodagholy, T. Doublet, M. Gurfinkel, P. Quilichini, E. Ismailova, P. Leleux*, et al.*, "Highly conformable conducting polymer electrodes for in vivo recordings," *Advanced Materials,* vol. 23, pp. H268-H272, 2011.
[144] Y. Chen, Y. Zhang, Z. Liang, Y. Cao, Z. Han, and X. Feng, "Flexible inorganic bioelectronics," *npj Flexible Electronics,* vol. 4, p. 2, 2020/02/04 2020.
[145] Z. Xue, H. Song, J. A. Rogers, Y. Zhang, and Y. Huang, "Mechanically-Guided Structural Designs in Stretchable Inorganic Electronics," *Adv Mater,* vol. 32, p. e1902254, Apr 2020.
[146] Y. Jiang, X. Li, B. Liu, J. Yi, Y. Fang, F. Shi*, et al.*, "Rational design of silicon structures for optically controlled multiscale biointerfaces," *Nat Biomed Eng,* vol. 2, pp. 508-521, Jul 2018.
[147] M. H. Chiu, J. H. Li, and T. Nagao, "Optical Properties of Au-based and Pt-based Alloys for Infrared Device Applications: A Combined First Principle and Electromagnetic Simulation Study," *Micromachines (Basel),* vol. 10, Jan 20 2019.
[148] L. Yin, H. Cheng, S. Mao, R. Haasch, Y. Liu, X. Xie*, et al.*, "Dissolvable Metals for Transient Electronics," *Advanced Functional Materials,* vol. 24, pp. 645-658, 2014.
[149] M. D. Dickey, "Stretchable and Soft Electronics using Liquid Metals," *Adv Mater,* vol. 29, Jul 2017.
[150] S. K. Rastogi, A. Kalmykov, N. Johnson, and T. Cohen-Karni, "Bioelectronics with nanocarbons," *Journal of Materials Chemistry B,* vol. 6, pp. 7159-7178, 2018.
[151] E. Masvidal-Codina, X. Illa, M. Dasilva, A. B. Calia, T. Dragojević, E. E. Vidal-Rosas*, et al.*, "High-resolution mapping of infraslow cortical brain activity enabled by graphene microtransistors," *Nat Mater,* vol. 18, pp. 280-288, Mar 2019.
[152] H. Xu, Y. Xie, E. Zhu, Y. Liu, Z. Shi, C. Xiong*, et al.*, "Supertough and ultrasensitive flexible electronic skin based on nanocellulose/sulfonated carbon nanotube hydrogel films," *Journal of Materials Chemistry A,* vol. 8, pp. 6311-6318, 2020.
[153] A. Benko, A. Frączek-Szczypta, E. Menaszek, J. Wyrwa, M. Nocuń, and M. Błażewicz, "On the influence of various physicochemical properties of the CNTs based implantable devices on the fibroblasts' reaction in vitro," *Journal of Materials Science: Materials in Medicine,* vol. 26, p. 262, 2015/10/13 2015.
[154] T. Zheng, P. Pour Shahid Saeed Abadi, J. Seo, B.-H. Cha, B. Miccoli, Y.-C. Li*, et al.*, "Biocompatible Carbon Nanotube-Based Hybrid Microfiber for Implantable Electrochemical Actuator and Flexible Electronic Applications," *ACS Applied Materials & Interfaces,* vol. 11, pp. 20615-20627, 2019/06/12 2019.
[155] T.-H. Han, H. Kim, S.-J. Kwon, and T.-W. Lee, "Graphene-based flexible electronic devices," *Materials Science and Engineering: R: Reports,* vol. 118, pp. 1-43, 2017/08/01/ 2017.
[156] M. Rahaman, A. Aldalbahi, P. Govindasami, N. P. Khanam, S. Bhandari, P. Feng*, et al.*, "A new insight in determining the percolation threshold of electrical conductivity for extrinsically conducting polymer composites through different sigmoidal models," *Polymers,* vol. 9, p. 527, 2017.
[157] M. Gerard, A. Chaubey, and B. D. Malhotra, "Application of conducting polymers to biosensors," *Biosens Bioelectron,* vol. 17, pp. 345-59, May 2002.
[158] M. Berggren and A. Richter-Dahlfors, "Organic Bioelectronics," *Advanced Materials,* vol. 19, pp. 3201-3213, 2007.

[159] R. K. Pal, A. A. Farghaly, M. M. Collinson, S. C. Kundu, and V. K. Yadavalli, "Photolithographic Micropatterning of Conducting Polymers on Flexible Silk Matrices," *Advanced Materials,* vol. 28, pp. 1406-1412, 2016.
[160] S. Inal, J. Rivnay, A. O. Suiu, G. G. Malliaras, and I. McCulloch, "Conjugated Polymers in Bioelectronics," *Acc Chem Res,* vol. 51, pp. 1368-1376, Jun 19 2018.
[161] Y. Wen and J. Xu, "Scientific Importance of Water-Processable PEDOT–PSS and Preparation, Challenge and New Application in Sensors of Its Film Electrode: A Review," *Journal of Polymer Science Part A: Polymer Chemistry,* vol. 55, pp. 1121-1150, 2017.
[162] R. Po, C. Carbonera, A. Bernardi, F. Tinti, and N. Camaioni, "Polymer- and carbon-based electrodes for polymer solar cells: Toward low-cost, continuous fabrication over large area," *Solar Energy Materials and Solar Cells,* vol. 100, pp. 97-114, 2012/05/01/ 2012.
[163] V. R. Feig, H. Tran, M. Lee, and Z. Bao, "Author Correction: Mechanically tunable conductive interpenetrating network hydrogels that mimic the elastic moduli of biological tissue," *Nature Communications,* vol. 9, p. 5030, 2018/11/23 2018.
[164] X. Fan, W. Nie, H. Tsai, N. Wang, H. Huang, Y. Cheng*, et al.*, "PEDOT: PSS for flexible and stretchable electronics: modifications, strategies, and applications," *Advanced Science,* vol. 6, p. 1900813, 2019.
[165] X. Fan, B. Xu, S. Liu, C. Cui, J. Wang, and F. Yan, "Transfer-Printed PEDOT:PSS Electrodes Using Mild Acids for High Conductivity and Improved Stability with Application to Flexible Organic Solar Cells," *ACS Applied Materials & Interfaces,* vol. 8, pp. 14029-14036, 2016/06/08 2016.
[166] V. Karagkiozaki, P. G. Karagiannidis, M. Gioti, P. Kavatzikidou, D. Georgiou, E. Georgaraki*, et al.*, "Bioelectronics meets nanomedicine for cardiovascular implants: PEDOT-based nanocoatings for tissue regeneration," *Biochimica et Biophysica Acta (BBA) - General Subjects,* vol. 1830, pp. 4294-4304, 2013/09/01/ 2013.
[167] K. A. Ludwig, J. D. Uram, J. Yang, D. C. Martin, and D. R. Kipke, "Chronic neural recordings using silicon microelectrode arrays electrochemically deposited with a poly(3,4-ethylenedioxythiophene) (PEDOT) film," *J Neural Eng,* vol. 3, pp. 59-70, Mar 2006.
[168] M. H. Bolin, K. Svennersten, X. Wang, I. S. Chronakis, A. Richter-Dahlfors, E. W. H. Jager*, et al.*, "Nano-fiber scaffold electrodes based on PEDOT for cell stimulation," *Sensors and Actuators B: Chemical,* vol. 142, pp. 451-456, 2009/11/05/ 2009.
[169] L. Ghasemi-Mobarakeh, M. P. Prabhakaran, M. Morshed, M. H. Nasr-Esfahani, H. Baharvand, S. Kiani*, et al.*, "Application of conductive polymers, scaffolds and electrical stimulation for nerve tissue engineering," *Journal of Tissue Engineering and Regenerative Medicine,* vol. 5, pp. e17-e35, 2011.
[170] S.-C. Luo, E. Mohamed Ali, N. C. Tansil, H.-h. Yu, S. Gao, E. A. Kantchev*, et al.*, "Poly (3, 4-ethylenedioxythiophene)(PEDOT) nanobiointerfaces: thin, ultrasmooth, and functionalized PEDOT films with in vitro and in vivo biocompatibility," *Langmuir,* vol. 24, pp. 8071-8077, 2008.
[171] H. Zhou, X. Cheng, L. Rao, T. Li, and Y. Y. Duan, "Poly(3,4-ethylenedioxythiophene)/multiwall carbon nanotube composite coatings for improving the stability of microelectrodes in neural prostheses applications," *Acta Biomaterialia,* vol. 9, pp. 6439-6449, 2013/05/01/ 2013.
[172] M. Kiristi and A. Uygun, "Polyaniline," in *Handbook of Engineering and Specialty Thermoplastics*, ed, 2011, pp. 183-210.

[173] H. Itoi, S. Hayashi, H. Matsufusa, and Y. Ohzawa, "Electrochemical synthesis of polyaniline in the micropores of activated carbon for high-performance electrochemical capacitors," *Chem Commun (Camb),* vol. 53, pp. 3201-3204, Mar 14 2017.
[174] P. Humpolicek, V. Kasparkova, P. Saha, and J. Stejskal, "Biocompatibility of polyaniline," *Synthetic Metals,* vol. 162, pp. 722-727, 2012/05/01/ 2012.
[175] R.-S. Norouzian, M. M. Lakouraj, and E. N. Zare, "Novel conductive PANI/hydrophilic thiacalix[4]arene nanocomposites: synthesis, characterization and investigation of properties," *Chinese Journal of Polymer Science,* vol. 32, pp. 218-229, 2014/02/01 2014.
[176] A. A. R. Watt, J. P. Bothma, and P. Meredith, "The supramolecular structure of melanin," *Soft Matter,* vol. 5, p. 3754, 2009.
[177] M. Abbas, F. D'Amico, L. Morresi, N. Pinto, M. Ficcadenti, R. Natali*, et al.*, "Structural, electrical, electronic and optical properties of melanin films," *The European Physical Journal E,* vol. 28, pp. 285-291, 2009 2009.
[178] T. Ligonzo, M. Ambrico, V. Augelli, G. Perna, L. Schiavulli, M. A. Tamma*, et al.*, "Electrical and optical properties of natural and synthetic melanin biopolymer," *Journal of Non-Crystalline Solids,* vol. 355, pp. 1221-1226, 2009/07/15/ 2009.
[179] A. B. Mostert, B. J. Powell, F. L. Pratt, G. R. Hanson, T. Sarna, I. R. Gentle*, et al.*, "Role of semiconductivity and ion transport in the electrical conduction of melanin," *Proceedings of the National Academy of Sciences,* vol. 109, pp. 8943-8947, 2012/06/05/ 2012.
[180] P. Meredith, B. J. Powell, J. Riesz, S. P. Nighswander-Rempel, M. R. Pederson, and E. G. Moore, "Towards structure–property–function relationships for eumelanin," *Soft Matter,* vol. 2, pp. 37-44, 2006.
[181] D.-H. Kim and J. A. Rogers, "Stretchable Electronics: Materials Strategies and Devices," *Advanced Materials,* vol. 20, pp. 4887-4892, 2008.
[182] K. Khanafer, A. Duprey, M. Schlicht, and R. Berguer, "Effects of strain rate, mixing ratio, and stress-strain definition on the mechanical behavior of the polydimethylsiloxane (PDMS) material as related to its biological applications," *Biomed Microdevices,* vol. 11, pp. 503-8, Apr 2009.
[183] T. Someya, Y. Kato, T. Sekitani, S. Iba, Y. Noguchi, Y. Murase*, et al.*, "Conformable, flexible, large-area networks of pressure and thermal sensors with organic transistor active matrixes," *Proc Natl Acad Sci U S A,* vol. 102, pp. 12321-5, Aug 30 2005.
[184] T. Someya, Y. Kato, I. Shingo, Y. Noguchi, T. Sekitani, H. Kawaguchi*, et al.*, "Integration of organic FETs with organic photodiodes for a large area, flexible, and lightweight sheet image scanners," *IEEE Transactions on Electron Devices,* vol. 52, pp. 2502-2511, 2005.
[185] P. Baude, D. Ender, M. Haase, T. Kelley, D. Muyres, and S. Theiss, "Pentacene-based radio-frequency identification circuitry," *Applied Physics Letters,* vol. 82, pp. 3964-3966, 2003.
[186] G. Yu, J. Gao, J. C. Hummelen, F. Wudl, and A. J. Heeger, "Polymer photovoltaic cells: enhanced efficiencies via a network of internal donor-acceptor heterojunctions," *Science,* vol. 270, pp. 1789-1791, 1995.
[187] R. X. Xu, A. Zverev, A. R. Hung, C. W. Shen, L. Irie, G. Ding*, et al.*, "Kirigami-inspired, highly stretchable micro-supercapacitor patches fabricated by laser conversion and cutting," *Microsystems & Nanoengineering,* vol. 4, Dec 2018.
[188] W. Zheng, W. Huang, F. Gao, H. Yang, M. Dai, G. Liu*, et al.*, "Kirigami-Inspired Highly Stretchable Nanoscale Devices Using Multidimensional Deformation of Monolayer MoS2," *Chemistry of Materials,* vol. 30, pp. 6063-6070, 2018/09/11 2018.

[189] N.-S. Jang, K.-H. Kim, S.-H. Ha, S.-H. Jung, H. M. Lee, and J.-M. Kim, "Simple Approach to High-Performance Stretchable Heaters Based on Kirigami Patterning of Conductive Paper for Wearable Thermotherapy Applications," *ACS Applied Materials & Interfaces,* vol. 9, pp. 19612-19621, 2017/06/14 2017.
[190] M. K. Blees, A. W. Barnard, P. A. Rose, S. P. Roberts, K. L. McGill, P. Y. Huang*, et al.*, "Graphene kirigami," *Nature,* vol. 524, p. 204, 07/29/online 2015.
[191] X. Ning, X. Wang, Y. Zhang, X. Yu, D. Choi, N. Zheng*, et al.*, "Assembly of Advanced Materials into 3D Functional Structures by Methods Inspired by Origami and Kirigami: A Review," *Advanced Materials Interfaces,* vol. 5, p. 1800284, 2018.
[192] A. Lamoureux, K. Lee, M. Shlian, S. R. Forrest, and M. Shtein, "Dynamic kirigami structures for integrated solar tracking," *Nature Communications,* vol. 6, Sep 2015.
[193] J. A. Forrest and K. Dalnoki-Veress, "The glass transition in thin polymer films," *Advances in Colloid and Interface Science,* vol. 94, pp. 167-195, 2001.
[194] C. M. Stafford, C. Harrison, K. L. Beers, A. Karim, E. J. Amis, M. R. VanLandingham*, et al.*, "A buckling-based metrology for measuring the elastic moduli of polymeric thin films," *Nature materials,* vol. 3, pp. 545-550, 2004.
[195] S. Zhang, Y. Sunami, and H. Hashimoto, "Mini Review: Nanosheet Technology towards Biomedical Application," *Nanomaterials (Basel),* vol. 7, Aug 31 2017.
[196] R. R. Costa and J. F. Mano, "Polyelectrolyte multilayered assemblies in biomedical technologies," *Chemical Society Reviews,* vol. 43, pp. 3453-3479, 2014.
[197] T. Fujie, "Development of free-standing polymer nanosheets for advanced medical and health-care applications," *Polymer Journal,* vol. 48, pp. 773-780, 2016.
[198] S. J. Benight, C. Wang, J. B. H. Tok, and Z. Bao, "Stretchable and self-healing polymers and devices for electronic skin," *Progress in Polymer Science,* vol. 38, pp. 1961-1977, 2013/12/01/ 2013.
[199] L. Ricotti and T. Fujie, "Thin polymeric films for building biohybrid microrobots," *Bioinspir Biomim,* vol. 12, p. 021001, Mar 6 2017.
[200] D. Kim, N. Lu, R. Ma, Y. Kim, R. Kim, S. Wang*, et al.*, "M. 90 McCormick, P. Liu, YW Zhang, FG Omenetto, YG Huang, T. Coleman and JA Rogers," *Science,* vol. 333, pp. 838-843, 2011.
[201] J. Sugano, T. Fujie, H. Iwata, and E. Iwase, "Measurement of conformability and adhesion energy of polymeric ultrathin film to skin model," *Japanese Journal of Applied Physics,* vol. 57, p. 06HJ04, 2018.
[202] K. Ng, B. Gao, K. W. Yong, Y. Li, M. Shi, X. Zhao*, et al.*, "based cell culture platform and its emerging biomedical applications," *Materials Today,* vol. 20, pp. 32-44, 2017.
[203] J. L. Ifkovits, H. G. Sundararaghavan, and J. A. Burdick, "Electrospinning fibrous polymer scaffolds for tissue engineering and cell culture," *Journal of visualized experiments: JoVE,* 2009.
[204] X. Mo, C. Xu, M. Kotaki, and S. Ramakrishna, "Electrospun P (LLA-CL) nanofiber: a biomimetic extracellular matrix for smooth muscle cell and endothelial cell proliferation," *Biomaterials,* vol. 25, pp. 1883-1890, 2004.
[205] X. Wang, B. Ding, and B. Li, "Biomimetic electrospun nanofibrous structures for tissue engineering," *Materials today,* vol. 16, pp. 229-241, 2013.
[206] H. Cao, T. Liu, and S. Y. Chew, "The application of nanofibrous scaffolds in neural tissue engineering," *Advanced drug delivery reviews,* vol. 61, pp. 1055-1064, 2009.

[207] Q. Cheng, B. L.-P. Lee, K. Komvopoulos, and S. Li, "Engineering the microstructure of electrospun fibrous scaffolds by microtopography," *Biomacromolecules,* vol. 14, pp. 1349-1360, 2013.
[208] A. Folch, B. H. Jo, O. Hurtado, D. J. Beebe, and M. Toner, "Microfabricated elastomeric stencils for micropatterning cell cultures," *Journal of Biomedical Materials Research: An Official Journal of The Society for Biomaterials, The Japanese Society for Biomaterials, and The Australian Society for Biomaterials and the Korean Society for Biomaterials,* vol. 52, pp. 346-353, 2000.
[209] S. Halldorsson, E. Lucumi, R. Gómez-Sjöberg, and R. M. Fleming, "Advantages and challenges of microfluidic cell culture in polydimethylsiloxane devices," *Biosensors and Bioelectronics,* vol. 63, pp. 218-231, 2015.
[210] K. Kolind, K. W. Leong, F. Besenbacher, and M. Foss, "Guidance of stem cell fate on 2D patterned surfaces," *Biomaterials,* vol. 33, pp. 6626-6633, 2012.
[211] H. Tao, D. L. Kaplan, and F. G. Omenetto, "Silk Materials – A Road to Sustainable High Technology," *Advanced Materials,* vol. 24, pp. 2824-2837, 2012.
[212] N. C. Tansil, L. D. Koh, and M. Y. Han, "Functional silk: colored and luminescent," *Advanced Materials,* vol. 24, pp. 1388-1397, 2012.
[213] D.-H. Kim, J. Viventi, J. J. Amsden, J. Xiao, L. Vigeland, Y.-S. Kim*, et al.*, "Dissolvable films of silk fibroin for ultrathin conformal bio-integrated electronics," *Nature materials,* vol. 9, pp. 511-517, 2010.
[214] R. R. Costa and J. F. Mano, "Polyelectrolyte multilayered assemblies in biomedical technologies," *Chem Soc Rev,* vol. 43, pp. 3453-79, May 21 2014.
[215] A. Bucciarelli, R. K. Pal, D. Maniglio, A. Quaranta, V. Mulloni, A. Motta*, et al.*, "Fabrication of nanoscale patternable films of silk fibroin using benign solvents," *Macromolecular Materials and Engineering,* vol. 302, p. 1700110, 2017 2017.
[216] F. Zhang, Q. Lu, J. Ming, H. Dou, Z. Liu, B. Zuo*, et al.*, "Silk dissolution and regeneration at the nanofibril scale," *Journal of Materials Chemistry B,* vol. 2, p. 3879, 2014.
[217] R. Jayakumar, D. Menon, K. Manzoor, S. V. Nair, and H. Tamura, "Biomedical applications of chitin and chitosan based nanomaterials—A short review," *Carbohydrate Polymers,* vol. 82, pp. 227-232, 2010/09/05/ 2010.
[218] S. V. Madihally and H. W. Matthew, "Porous chitosan scaffolds for tissue engineering," *Biomaterials,* vol. 20, pp. 1133-42, Jun 1999.
[219] M. N. V. Ravi Kumar, "A review of chitin and chitosan applications," *Reactive and Functional Polymers,* vol. 46, pp. 1-27, 2000/11/01/ 2000.
[220] E. Khor and L. Y. Lim, "Implantable applications of chitin and chitosan," *Biomaterials,* vol. 24, pp. 2339-49, Jun 2003.
[221] D. L. Nettles, S. H. Elder, and J. A. Gilbert, "Potential use of chitosan as a cell scaffold material for cartilage tissue engineering," *Tissue Eng,* vol. 8, pp. 1009-16, Dec 2002.
[222] R. Jayakumar, M. Rajkumar, H. Freitas, N. Selvamurugan, S. V. Nair, T. Furuike*, et al.*, "Preparation, characterization, bioactive and metal uptake studies of alginate/phosphorylated chitin blend films," *Int J Biol Macromol,* vol. 44, pp. 107-11, Jan 1 2009.
[223] H. Jiankang, L. Dichen, L. Yaxiong, Y. Bo, Z. Hanxiang, L. Qin*, et al.*, "Preparation of chitosan-gelatin hybrid scaffolds with well-organized microstructures for hepatic tissue engineering," *Acta Biomater,* vol. 5, pp. 453-61, Jan 2009.

[224] K. Madhumathi, P. T. Sudheesh Kumar, K. C. Kavya, T. Furuike, H. Tamura, S. V. Nair*, et al.*, "Novel chitin/nanosilica composite scaffolds for bone tissue engineering applications," *Int J Biol Macromol,* vol. 45, pp. 289-92, Oct 1 2009.
[225] K. E. Park, S. Y. Jung, S. J. Lee, B. M. Min, and W. H. Park, "Biomimetic nanofibrous scaffolds: preparation and characterization of chitin/silk fibroin blend nanofibers," *Int J Biol Macromol,* vol. 38, pp. 165-73, May 30 2006.
[226] Z. Huang, Q. Feng, B. Yu, and S. Li, "Biomimetic properties of an injectable chitosan/nano-hydroxyapatite/collagen composite," *Materials Science and Engineering: C,* vol. 31, pp. 683-687, 2011/04/08/ 2011.
[227] J. Y. Lim and H. J. Donahue, "Cell sensing and response to micro- and nanostructured surfaces produced by chemical and topographic patterning," *Tissue Eng,* vol. 13, pp. 1879-91, Aug 2007.
[228] M. Muskovich and C. J. Bettinger, "Biomaterials-Based Electronics: Polymers and Interfaces for Biology and Medicine," *Advanced Healthcare Materials,* vol. 1, pp. 248-266, 2012.
[229] R. Chandran, K. Nowlin, and D. R. LaJeunesse, "Nanosphere Lithography of Chitin and Chitosan with Colloidal and Self-Masking Patterning," *Polymers (Basel),* vol. 10, Feb 2018.
[230] J. Jin, D. Lee, H. G. Im, Y. C. Han, E. G. Jeong, M. Rolandi*, et al.*, "Chitin Nanofiber Transparent Paper for Flexible Green Electronics," *Adv Mater,* vol. 28, pp. 5169-75, Jul 2016.
[231] J. Fukuda, A. Khademhosseini, Y. Yeo, X. Yang, J. Yeh, G. Eng*, et al.*, "Micromolding of photocrosslinkable chitosan hydrogel for spheroid microarray and co-cultures," *Biomaterials,* vol. 27, pp. 5259-67, Oct 2006.
[232] J. M. Karp, Y. Yeo, W. Geng, C. Cannizarro, K. Yan, D. S. Kohane*, et al.*, "A photolithographic method to create cellular micropatterns," *Biomaterials,* vol. 27, pp. 4755-64, Sep 2006.
[233] J. G. Fernandez, C. A. Mills, and J. Samitier, "Complex microstructured 3D surfaces using chitosan biopolymer," *Small,* vol. 5, pp. 614-20, Mar 2009.
[234] K. Tomihata and Y. Ikada, "In vitro and in vivo degradation of films of chitin and its deacetylated derivatives," *Biomaterials,* vol. 18, pp. 567-575, 1997/04/01/ 1997.
[235] Z. Cui, E. S. Beach, and P. T. Anastas, "Modification of chitosan films with environmentally benign reagents for increased water resistance," *Green Chemistry Letters and Reviews,* vol. 4, pp. 35-40, 2011/03/01 2011.
[236] J. Jin, M. Song, and D. J. Hourston, "Novel Chitosan-Based Films Cross-Linked by Genipin with Improved Physical Properties," *Biomacromolecules,* vol. 5, pp. 162-168, 2004/01/01 2004.
[237] A. Bégin and M.-R. Van Calsteren, "Antimicrobial films produced from chitosan," *International Journal of Biological Macromolecules,* vol. 26, pp. 63-67, 1999/10/01/ 1999.
[238] J. Hallmann, R. Rodríguez-Kábana, and J. W. Kloepper, "Chitin-mediated changes in bacterial communities of the soil, rhizosphere and within roots of cotton in relation to nematode control," *Soil Biology and Biochemistry,* vol. 31, pp. 551-560, 1999/04/01/ 1999.
[239] M. G. Paoletti, L. Norberto, R. Damini, and S. Musumeci, "Human gastric juice contains chitinase that can degrade chitin," *Ann Nutr Metab,* vol. 51, pp. 244-51, 2007.

[240] Y. M. Yang, W. Hu, X. D. Wang, and X. S. Gu, "The controlling biodegradation of chitosan fibers by N-acetylation in vitro and in vivo," *J Mater Sci Mater Med,* vol. 18, pp. 2117-21, Nov 2007.
[241] C. Cui, Q. Fu, L. Meng, S. Hao, R. Dai, and J. Yang, "Recent Progress in Natural Biopolymers Conductive Hydrogels for Flexible Wearable Sensors and Energy Devices: Materials, Structures, and Performance," *ACS Applied Bio Materials,* vol. 4, pp. 85-121, 2021/01/18 2021.
[242] C. Wang, T. Yokota, and T. Someya, "Natural Biopolymer-Based Biocompatible Conductors for Stretchable Bioelectronics," *Chemical Reviews,* vol. 121, pp. 2109-2146, 2021/02/24 2021.
[243] H. Li, P. Z. Toh, J. Y. Tan, M. T. Zin, C. Y. Lee, B. Li*, et al.*, "Selected Biomarkers Revealed Potential Skin Toxicity Caused by Certain Copper Compounds," *Sci Rep,* vol. 6, p. 37664, Nov 28 2016.
[244] C. Brouillard, A. C. Bursztejn, C. Latarche, J. F. Cuny, F. Truchetet, J. P. Goullé*, et al.*, "Silver absorption and toxicity evaluation of silver wound dressings in 40 patients with chronic wounds," *J Eur Acad Dermatol Venereol,* vol. 32, pp. 2295-2299, Dec 2018.
[245] I. Khansa, A. R. Schoenbrunner, C. T. Kraft, and J. E. Janis, "Silver in Wound Care—Friend or Foe?: A Comprehensive Review," *Plastic and Reconstructive Surgery – Global Open,* vol. 7, 2019.
[246] R. Ma and V. V. Tsukruk, "Seriography-Guided Reduction of Graphene Oxide Biopapers for Wearable Sensory Electronics," *Advanced Functional Materials,* vol. 27, p. 1604802, 2017.
[247] S. Ling, Q. Wang, D. Zhang, Y. Zhang, X. Mu, D. L. Kaplan*, et al.*, "Integration of stiff graphene and tough silk for the design and fabrication of versatile electronic materials," *Adv Funct Mater,* vol. 28, Feb 28 2018.
[248] L.-Y. Hsiao, L. Jing, K. Li, H. Yang, Y. Li, and P.-Y. Chen, "Carbon nanotube-integrated conductive hydrogels as multifunctional robotic skin," *Carbon,* vol. 161, pp. 784-793, 2020/05/01/ 2020.
[249] J. Thibodeau and A. Ignaszak, "Flexible Electrode Based on MWCNT Embedded in a Cross-Linked Acrylamide/Alginate Blend: Conductivity vs. Stretching," *Polymers,* vol. 12, p. 181, 2020.
[250] V. R. Feig, H. Tran, M. Lee, and Z. Bao, "Mechanically tunable conductive interpenetrating network hydrogels that mimic the elastic moduli of biological tissue," *Nature Communications,* vol. 9, p. 2740, 2018/07/16 2018.
[251] L. Han, K. Liu, M. Wang, K. Wang, L. Fang, H. Chen*, et al.*, "Mussel-Inspired Adhesive and Conductive Hydrogel with Long-Lasting Moisture and Extreme Temperature Tolerance," *Advanced Functional Materials,* vol. 28, p. 1704195, 2018.
[252] N. Aydemir, J. Malmström, and J. Travas-Sejdic, "Conducting polymer based electrochemical biosensors," *Physical Chemistry Chemical Physics,* vol. 18, pp. 8264-8277, 2016.
[253] B. D. Gates, Q. Xu, M. Stewart, D. Ryan, C. G. Willson, and G. M. Whitesides, "New Approaches to Nanofabrication: Molding, Printing, and Other Techniques," *Chemical Reviews,* vol. 105, pp. 1171-1196, 2005/04/01 2005.
[254] R. Xu, A. Gouda, M. F. Caso, F. Soavi, and C. Santato, "Melanin: A Greener Route To Enhance Energy Storage under Solar Light," *ACS Omega,* vol. 4, pp. 12244-12251, 2019/07/31/ 2019.

[255] P. Kumar, E. Di Mauro, S. Zhang, A. Pezzella, F. Soavi, C. Santato*, et al.*, "Melanin-based flexible supercapacitors," *Journal of Materials Chemistry C,* vol. 4, pp. 9516-9525, 2016 2016.
[256] Y. J. Kim, A. Khetan, W. Wu, S.-E. Chun, V. Viswanathan, J. F. Whitacre*, et al.*, "Evidence of Porphyrin-Like Structures in Natural Melanin Pigments Using Electrochemical Fingerprinting," *Advanced Materials,* vol. 28, pp. 3173-3180, 2016 2016.
[257] Y. J. Kim, W. Wu, S. E. Chun, J. F. Whitacre, and C. J. Bettinger, "Biologically derived melanin electrodes in aqueous sodium-ion energy storage devices," *Proc Natl Acad Sci U S A,* vol. 110, pp. 20912-7, Dec 24 2013.
[258] N. Bhalla, P. Jolly, N. Formisano, and P. Estrela, "Introduction to biosensors," *Essays in biochemistry,* vol. 60, pp. 1-8, 2016.
[259] N. Bhalla, P. Jolly, N. Formisano, and P. Estrela, "Introduction to biosensors," *Essays Biochem,* vol. 60, pp. 1-8, Jun 30 2016.
[260] P. Mehrotra, "Biosensors and their applications - A review," *J Oral Biol Craniofac Res,* vol. 6, pp. 153-9, May-Aug 2016.
[261] M. Pohanka, "Overview of Piezoelectric Biosensors, Immunosensors and DNA Sensors and Their Applications," *Materials (Basel),* vol. 11, Mar 19 2018.
[262] D. Rodrigues, A. I. Barbosa, R. Rebelo, I. K. Kwon, R. L. Reis, and V. M. Correlo, "Skin-Integrated Wearable Systems and Implantable Biosensors: A Comprehensive Review," *Biosensors,* vol. 10, p. 79, 2020.
[263] R. E. Fernandez, E. Lebiga, A. Koklu, A. C. Sabuncu, and A. Beskok, "Flexible Bioimpedance Sensor for Label-Free Detection of Cell Viability and Biomass," *IEEE Transactions on NanoBioscience,* vol. 14, pp. 700-706, 2015.
[264] D. Grieshaber, R. MacKenzie, J. Vörös, and E. Reimhult, "Electrochemical Biosensors - Sensor Principles and Architectures," *Sensors (Basel),* vol. 8, pp. 1400-1458, Mar 7 2008.
[265] L. A. Geddes and R. Roeder, "Criteria for the Selection of Materials for Implanted Electrodes," *Annals of Biomedical Engineering,* vol. 31, pp. 879-890, 2003/07/01 2003.
[266] N. Aydemir, J. Malmstrom, and J. Travas-Sejdic, "Conducting Polymer based Biosensors," *Phys. Chem. Chem. Phys.,* vol. 18, 02/24 2016.
[267] B. R. Eggins, *Chemical sensors and biosensors* vol. 2: John Wiley & Sons, 2002.
[268] P. B. Luppa, L. J. Sokoll, and D. W. Chan, "Immunosensors--principles and applications to clinical chemistry," *Clin Chim Acta,* vol. 314, pp. 1-26, Dec 2001.
[269] W. Cai, T. Lai, H. Du, and J. Ye, "Electrochemical determination of ascorbic acid, dopamine and uric acid based on an exfoliated graphite paper electrode: A high performance flexible sensor," *Sensors and Actuators B: Chemical,* vol. 193, pp. 492-500, 2014/03/31/ 2014.
[270] M. Marsilia and S. Susmel, "Free-standing Plastic electrodes: Formulation, electrochemical characterization and application to dopamine detection," *Sensors and Actuators B: Chemical,* vol. 255, pp. 1087-1096, 2018/02/01/ 2018.
[271] B. L. Hanssen, S. Siraj, and D. K. Y. Wong, "Recent strategies to minimise fouling in electrochemical detection systems," *Reviews in Analytical Chemistry,* vol. 35, pp. 1-28, 2016.
[272] B. A. Kuzubasoglu and S. K. Bahadir, "Flexible Temperature Sensors: A Review," *Sensors and Actuators A: Physical,* p. 112282, 2020.

[273] Q. Li, L. N. Zhang, X. M. Tao, and X. Ding, "Review of flexible temperature sensing networks for wearable physiological monitoring," *Advanced healthcare materials,* vol. 6, p. 1601371, 2017.
[274] Y. Chen, B. Lu, Y. Chen, and X. Feng, "Breathable and stretchable temperature sensors inspired by skin," *Scientific reports,* vol. 5, p. 11505, 2015.
[275] L. Dan and A. L. Elias, "Flexible and Stretchable Temperature Sensors Fabricated Using Solution-Processable Conductive Polymer Composites," *Advanced Healthcare Materials,* p. 2000380, 2020.
[276] Q. Liu, H. Tai, Z. Yuan, Y. Zhou, Y. Su, and Y. Jiang, "A High-Performances Flexible Temperature Sensor Composed of Polyethyleneimine/Reduced Graphene Oxide Bilayer for Real-Time Monitoring," *Advanced Materials Technologies,* vol. 4, p. 1800594, 2019.
[277] J. Kim, A. S. Campbell, B. E.-F. de Ávila, and J. Wang, "Wearable biosensors for healthcare monitoring," *Nature biotechnology,* vol. 37, pp. 389-406, 2019.
[278] G. A. Salvatore, J. Sülzle, F. Dalla Valle, G. Cantarella, F. Robotti, P. Jokic*, et al.*, "Biodegradable and highly deformable temperature sensors for the internet of things," *Advanced Functional Materials,* vol. 27, p. 1702390, 2017.
[279] S. Yuvaraja, A. Nawaz, Q. Liu, D. Dubal, S. G. Surya, K. N. Salama*, et al.*, "Organic field-effect transistor-based flexible sensors," *Chemical Society Reviews,* 2020.
[280] S. Jung, T. Ji, and V. K. Varadan, "Point-of-care temperature and respiration monitoring sensors for smart fabric applications," *Smart materials and structures,* vol. 15, p. 1872, 2006.
[281] M. R. R. Khan and S. Kang, "Fast, Highly Sensitive Interdigitated Capacitor Sensor to Detect Wide Range of Temperatures Using Graphene-Oxide-Containing Dielectric Membrane," *IEEE Sensors Journal,* vol. 18, pp. 2667-2674, 2018.
[282] K. Kanao, S. Harada, Y. Yamamoto, W. Honda, T. Arie, S. Akita*, et al.*, "Highly selective flexible tactile strain and temperature sensors against substrate bending for an artificial skin," *RSC Advances,* vol. 5, pp. 30170-30174, 2015.
[283] Y. Yu, S. Peng, P. Blanloeuil, S. Wu, and C. H. Wang, "Wearable Temperature Sensors with Enhanced Sensitivity by Engineering Microcrack Morphology in PEDOT: PSS–PDMS Sensors," *ACS Applied Materials & Interfaces,* vol. 12, pp. 36578-36588, 2020.
[284] T. Vuorinen, J. Niittynen, T. Kankkunen, T. M. Kraft, and M. Mäntysalo, "Inkjet-Printed Graphene/PEDOT:PSS Temperature Sensors on a Skin-Conformable Polyurethane Substrate," *Scientific Reports,* vol. 6, p. 35289, 2016/10/18 2016.
[285] L. Bießmann, L. P. Kreuzer, T. Widmann, N. Hohn, J.-F. o. Moulin, and P. Müller-Buschbaum, "Monitoring the Swelling Behavior of PEDOT: PSS electrodes under high humidity conditions," *ACS applied materials & interfaces,* vol. 10, pp. 9865-9872, 2018.
[286] Y.-F. Wang, T. Sekine, Y. Takeda, K. Yokosawa, H. Matsui, D. Kumaki*, et al.*, "Fully Printed PEDOT:PSS-based Temperature Sensor with High Humidity Stability for Wireless Healthcare Monitoring," *Scientific Reports,* vol. 10, p. 2467, 2020/02/12 2020.
[287] M. Irimia-Vladu, ""Green" electronics: biodegradable and biocompatible materials and devices for sustainable future " *Chemical Society Reviews,* vol. 43, p. 588, 2014.
[288] J. Zhang, H. Yang, G. Shen, P. Cheng, J. Zhang, and S. Guo, "Reduction of graphene oxide vial-ascorbic acid," *Chemical Communications,* vol. 46, pp. 1112-1114, 2010.
[289] M. Xu and V. K. Yadavalli, "Flexible biosensors for the impedimetric detection of protein targets using silk-conductive polymer biocomposites," *ACS Sensors,* vol. 4, pp. 1040-1047, 2019.

[290] J. Zhou, D. H. Anjum, L. Chen, X. Xu, I. A. Ventura, L. Jiang*, et al.*, "The temperature-dependent microstructure of PEDOT/PSS films: insights from morphological, mechanical and electrical analyses," *Journal of Materials Chemistry C,* vol. 2, pp. 9903-9910, 2014.
[291] E. Vitoratos, S. Sakkopoulos, E. Dalas, N. Paliatsas, D. Karageorgopoulos, F. Petraki*, et al.*, "Thermal degradation mechanisms of PEDOT: PSS," *Organic Electronics,* vol. 10, pp. 61-66, 2009.
[292] J. Liu, Q. Chen, Q. Liu, B. Zhao, S. Ling, J. Yao*, et al.*, "Intelligent Silk Fibroin Ionotronic Skin for Temperature Sensing," *Advanced Materials Technologies,* vol. 5, p. 2000430, 2020.
[293] C. Wang, K. Xia, M. Zhang, M. Jian, and Y. Zhang, "An All-Silk-Derived Dual-Mode E-skin for Simultaneous Temperature–Pressure Detection," *ACS Applied Materials & Interfaces,* vol. 9, pp. 39484-39492, 2017/11/15 2017.
[294] Q. Wang, S. Ling, X. Liang, H. Wang, H. Lu, and Y. Zhang, "Self-Healable Multifunctional Electronic Tattoos Based on Silk and Graphene," *Advanced Functional Materials,* vol. 29, p. 1808695, 2019.
[295] Y. Yu, S. Peng, P. Blanloeuil, S. Wu, and C. H. Wang, "Wearable Temperature Sensors with Enhanced Sensitivity by Engineering Microcrack Morphology in PEDOT:PSS–PDMS Sensors," *ACS Applied Materials & Interfaces,* 2020/07/15 2020.
[296] F. Zhang, H. Hu, M. Islam, S. Peng, S. Wu, S. Lim*, et al.*, "Multi-modal strain and temperature sensor by hybridizing reduced graphene oxide and PEDOT:PSS," *Composites Science and Technology,* vol. 187, p. 107959, 2020/02/08/ 2020.
[297] M. Kuş and S. Okur, "Electrical characterization of PEDOT: PSS beyond humidity saturation," *Sensors and Actuators B: Chemical,* vol. 143, pp. 177-181, 2009.
[298] K. Kawano, R. Pacios, D. Poplavskyy, J. Nelson, D. D. Bradley, and J. R. Durrant, "Degradation of organic solar cells due to air exposure," *Solar energy materials and solar cells,* vol. 90, pp. 3520-3530, 2006.
[299] J. Huang, P. F. Miller, J. S. Wilson, A. J. de Mello, J. C. de Mello, and D. D. Bradley, "Investigation of the effects of doping and post-deposition treatments on the conductivity, morphology, and work function of poly (3, 4-ethylenedioxythiophene)/poly (styrene sulfonate) films," *Advanced functional materials,* vol. 15, pp. 290-296, 2005.
[300] M. A. Brenckle, H. Cheng, S. Hwang, H. Tao, M. Paquette, D. L. Kaplan*, et al.*, "Modulated Degradation of Transient Electronic Devices through Multilayer Silk Fibroin Pockets," *ACS Applied Materials & Interfaces,* vol. 7, pp. 19870–19875, Sep 1 2015.
[301] R. L. Horan, K. Antle, A. L. Collette, Y. Z. Huang, J. Huang, J. E. Moreau*, et al.*, "In vitro degradation of silk fibroin," *Biomaterials,* vol. 26, pp. 3385-3393, Jun 2005.
[302] D.-H. Kim, R. Ghaffari, N. Lu, and J. A. Rogers, "Flexible and Stretchable Electronics for Biointegrated Devices," *Annual Review of Biomedical Engineering,* vol. 14, pp. 113-128, 2012.
[303] T. Q. Trung and N.-E. Lee, "Recent Progress on Stretchable Electronic Devices with Intrinsically Stretchable Components," *Advanced Materials,* vol. 29, p. 1603167, 2017.
[304] J.-H. Ahn and J. H. Je, "Stretchable electronics: materials, architectures and integrations," *Journal of Physics D: Applied Physics,* vol. 45, p. 103001, 2012/02/22 2012.
[305] N. Matsuhisa, X. Chen, Z. Bao, and T. Someya, "Materials and structural designs of stretchable conductors," *Chem Soc Rev,* vol. 48, pp. 2946-2966, Jun 4 2019.

[306] D. Groeger and J. Steimle, "LASEC: Instant Fabrication of Stretchable Circuits Using a Laser Cutter," in *Proceedings of the 2019 CHI Conference on Human Factors in Computing Systems*, 2019, pp. 1-14.
[307] M. K. Blees, A. W. Barnard, P. A. Rose, S. P. Roberts, K. L. McGill, P. Y. Huang*, et al.*, "Graphene kirigami," *Nature,* vol. 524, pp. 204-207, 2015.
[308] T. C. Shyu, P. F. Damasceno, P. M. Dodd, A. Lamoureux, L. Xu, M. Shlian*, et al.*, "A kirigami approach to engineering elasticity in nanocomposites through patterned defects," *Nature materials,* vol. 14, pp. 785-789, 2015.
[309] A. Lamoureux, K. Lee, M. Shlian, S. R. Forrest, and M. Shtein, "Dynamic kirigami structures for integrated solar tracking," *Nature communications,* vol. 6, pp. 1-6, 2015.
[310] M. K. Blees, A. W. Barnard, P. A. Rose, S. P. Roberts, K. L. McGill, P. Y. Huang*, et al.*, "Graphene kirigami," *Nature,* vol. 524, pp. 204-7, Aug 13 2015.
[311] K. Hu, M. K. Gupta, D. D. Kulkarni, and V. V. Tsukruk, "Ultra-robust graphene oxide-silk fibroin nanocomposite membranes," *Adv Mater,* vol. 25, pp. 2301-7, Apr 24 2013.
[312] W. Wu, "Stretchable electronics: functional materials, fabrication strategies and applications," *Science and Technology of Advanced Materials,* vol. 20, pp. 187-224, 2019/12/31 2019.
[313] C. Wang, C. Wang, Z. Huang, and S. Xu, "Materials and structures toward soft electronics," *Advanced Materials,* vol. 30, p. 1801368, 2018.
[314] M. Isobe and K. Okumura, "Initial rigid response and softening transition of highly stretchable kirigami sheet materials," *Scientific reports,* vol. 6, pp. 1-6, 2016.
[315] A. Lund, S. Darabi, S. Hultmark, J. D. Ryan, B. Andersson, A. Ström*, et al.*, "Roll-to-roll dyed conducting silk yarns: a versatile material for e-textile devices," *Advanced Materials Technologies,* vol. 3, p. 1800251, 2018.
[316] C. Müller, M. Hamedi, R. Karlsson, R. Jansson, R. Marcilla, M. Hedhammar*, et al.*, "Woven electrochemical transistors on silk fibers," *Advanced Materials,* vol. 23, pp. 898-901, 2011.
[317] M. Kapnisi, C. Mansfield, C. Marijon, A. G. Guex, F. Perbellini, I. Bardi*, et al.*, "Auxetic cardiac patches with tunable mechanical and conductive properties toward treating myocardial infarction," *Advanced functional materials,* vol. 28, p. 1800618, 2018.
[318] D. J. Lipomi and Z. Bao, "Stretchable and ultraflexible organic electronics," *MRS Bulletin,* vol. 42, pp. 93-97, 2017.
[319] M. A. Borysiewicz, "ZnO as a Functional Material, a Review," *Crystals,* vol. 9, p. 505, 2019.
[320] B. Yang, C. Yao, Y. Yu, Z. Li, and X. Wang, "Nature Degradable, Flexible, and Transparent Conductive Substrates from Green and Earth-Abundant Materials," *Scientific Reports,* vol. 7, p. 4936, 2017/07/10 2017.
[321] S. Nam and D. Mooney, "Polymeric Tissue Adhesives," *Chemical Reviews,* 2021/01/28 2021.
[322] A. Duarte, J. Coelho, J. Bordado, M. Cidade, and M. Gil, "Surgical adhesives: Systematic review of the main types and development forecast," *Progress in Polymer Science,* vol. 37, pp. 1031-1050, 2012.
[323] J.-W. Seo, H. Kim, K. Kim, S. Q. Choi, and H. J. Lee, "Calcium-Modified Silk as a Biocompatible and Strong Adhesive for Epidermal Electronics," *Advanced Functional Materials,* vol. 28, p. 1800802, 2018.

[324] X. Liu, J. Liu, J. Wang, T. Wang, Y. Jiang, J. Hu*, et al.*, "Bioinspired, Microstructured Silk Fibroin Adhesives for Flexible Skin Sensors," *ACS Applied Materials & Interfaces,* vol. 12, pp. 5601-5609, 2020/02/05 2020.
[325] E. K. Lee, M. K. Kim, and C. H. Lee, "Skin-Mountable Biosensors and Therapeutics: A Review," *Annual Review of Biomedical Engineering,* vol. 21, pp. 299-323, 2019.
[326] M. Ochoa, R. Rahimi, and B. Ziaie, "Flexible sensors for chronic wound management," *IEEE Rev Biomed Eng,* vol. 7, pp. 73-86, 2014.

Vita

Sayantan Pradhan was born on 10 September 1993 in West Bengal, India. He received his Bachelor's in Technology (B. Tech) degree in Chemical Engineering from Jawaharlal Nehru Technical University, Kakinada, India in 2016. Subsequently, he joined the Department of Chemical Engineering and Life Science at Virginia Commonwealth University in January 2017 where the doctoral work was carried out under the supervision of Dr. Vamsi Yadavalli.